Investigation and improvement of environmental stability of Al-doped ZnO transparent electrode

Samia Tabassum

Contents

ABSTRACT

Al-doped ZnO (AZO) thin film, which possess the advantages of low cost, low resistance and high transmittance, are one of the most promising candidates to replace indium tin oxide (ITO) films as the transparent electrode. However, oxidation causes a substantial increase in the sheet resistance of AZO film after exposing in air which is still a difficulty to use it for long time.

The work presented herein describes fundamental investigations of AZO thin films deposited by sol-gel method. The basic investigations include structural, optical and electrical characteristics, which were measured as functions of different conditions applied in film making procedure. Our interest in environmental stability was sparked by the desire to study, understand the behavior of degradation and improvement of stability.

The n-type conductivity of an intrinsic ZnO mainly is due to Zn interstitial and oxygen vacancy. In this experiment, conductivity increased by Al doping and heat treatment. Annealing treatments were carried out by changing its temperature, duration and atmosphere. X-ray diffraction (XRD) revealed the polycrystalline hexagonal wurtzite structure of AZO thin film. Optical transmittance which was >80%, satisfies the transparent electrodes requirement.

Firstly, several approaches were attempted by changing the annealing atmosphere (vacuum, argon + 5% hydrogen, pure hydrogen) and doping concentration (1, 2, 3 and 4 wt %) to obtain enhanced conductivity of AZO thin film,. In this experiment, pure hydrogen and 2 wt% of Al (which corresponds to doping concentration of Al/(Al+Zn) : 1.18 at%) were selected for further experiments as they

showed lower resistivity with high transparency. Hydrogen treatment in AZO films increased the conductivity by reducing the oxygen adsorbed at grain boundary when annealing was performed in vacuum atmosphere. The lowest resistivity was observed due to the increase of carrier concentration and hall mobility. The damp heat (85 °C and 85% RH) stability of AZO film was observed as function of different annealing atmosphere and doping concentration. The degradation of electrical properties was observed for all films, which indicate the possible oxygen and water molecule diffusion to the film that confines the number of free electrons. A technique has been applied to enhance the electrical stability by giving thin protective layer of Cr or Ti. In this experiment, Cr or Ti layers which oxidized in ambient condition and make a bi-layer of metal/metal oxide are found as efficient shielding layers that prevent the penetration of oxygen or moisture into the AZO film. As the sol-gel prepared AZO film is very unstable in DH environment, comparatively thick metal layer is needed to stabilize the film properly which reduces the transparency.

The effect of annealing temperature and duration on AZO film was also investigated which focused on stability in ambient and DH condition. In this case, the films were annealed under vacuum atmosphere though hydrogen atmosphere is better for conductivity, as high temperature (above 773K or 500 °C) cannot be used in hydrogen atmosphere because of surface damage. The resistivity of AZO films annealed in vacuum atmosphere at different annealing temperatures of 723, 773, 823 and 873K (450, 500, 550 and 600 °C, respectively) and durations of 1800, 3600 and 7200s (30, 60 and 120 min, respectively) was varied between 5.7 x 10^{-3} and 7.8 x 10^{-3} Ωcm. These films also showed increased resistance in air due to adsorption of oxygen and/or water molecule from atmosphere, whereas, it was found as very stable film in argon

atmosphere. Environmental stability was greatly influenced by annealing temperature. High temperature annealed film showed better stability compared to low temperature annealed film, where, annealing duration did not make any considerable changes in electrical properties and stability. Crystallite size has been estimated from XRD data using the Debye-Scherer formula. Comparatively large crystallite size and high intensity was originated in high temperature annealed film, which indicates the improved crystallinity. The healing of defects by high temperature annealing also act for improving crystallinity, which may be one of the reasons for obtaining better stability at high annealing temperature. It is well known that aluminum oxide generally acts as good moisture barrier. In this experiment, the surface oxygen and aluminium contents were relatively high for the stable film compared to the unstable film which was measured by X-ray photoelectroscopy (XPS). This higher concentration and presence of Al^{3+} at the topmost surface of stable film indicate the presence of ultrathin Al_2O_3 layer, though not detected by x-ray diffractometry, which formed during annealing at high temperature. This layer may act as a protective layer that can repel atmospheric oxygen to enter the film.

Highly improved environmental stability was found in AZO film prepared by RF sputtering. In this manner, a comparative study was employed between sol-gel and sputtered film which includes structural, optical, electrical properties and environmental stability also. Results are therefore presented regarding the change in crystal orientation, smooth surface, increased band gap energy and carrier concentration, improved stability etc., which was found in sputtered film. High quality (110) crystal orientation was observed in this film, whereas, (002) plane with large intensity originated in sol-gel prepared film. In order to clarify the role of crystal orientation, AZO thin film was

prepared by a combination of two methods. It ensured the presence of (110) plane in film and it also improved the environmental stability. In this manner it can say that smooth surface and (110) plane present in AZO film by sputtering, which can play an important role for increasing the stability compared to sol-gel prepared film. AZO thin film prepared by sputtering showed very stable electrical properties in ambient condition. But in DH condition, it increased slightly with low increasing rate compare to the sol-gel prepared film. To minimize this problem, sample was annealed at high temperature in vacuum atmosphere and found very stable film in DH condition. Here, vacuum atmosphere was chosen, though hydrogen atmosphere showed better electrical properties, as high temperature may damage the surface of film during hydrogen annealing. This film has relatively high resistance of 60 Ω/□, but showed very high stability in DH condition.

In this experiment, through an analysis on structural, optical and electrical properties, AZO films were investigated in terms of various parameters. Degradation of these properties under ambient and harsh environment was studied and several approaches are suggested to improve the electrical stability such as increased thickness, preferrable deposition method, improved crystallinity, surface smoothness, changing crystal orientation etc.

Acknowledgement

The present thesis has been carried out at the Dept. of socio-environmental energy science, graduate school of energy science, Kyoto University from October 2011 to September 2014. I am indebted to many people for their assistance and encouragement during this time in the graduate school. First of all, I would like to express my sincere gratitude to my supervisor, Professor Keiichi N Ishihara, for his advice, guidance, patience and tremendous help to complete the work properly. His constant encouragement and freedom to work made my study much enjoyable and it helped me to work more efficiently. I would also like to thank Prof. Hideyuki Okumura for his interest and many fruitful discussions. I am also very grateful to Professor Eiji Yamasue, for his detailed and constructive comments, and all time support throughout this work.

I am really very grateful to all of my lab mates who helped me a lot for learning the instrumental uses and also attended many helpful discussions. The knowledge and experience of the staff technician in our group, Mr. Shoji Fujimoto, for his kind support and instructions about various experimental techniques also helped me. In addition, I want to thank Dr. Tsutomu Shinagawa of Osaka Municipal Technical Research Institute for the support of thickness and Hall Effect measurement. Also, I greatly appreciate Mr. Sasaki for his help in performing the XPS measurement.

I would like to express my appreciation from the Global Center of Excellence (GCOE) program, Kyoto University, and the Monbukagakusho Scholarship, Japan.

Special thanks to my husband for his help, sacrifice and continuous support during this work. My sweet little child also did a lot for me. I would also like to express my heartiest thanks to my parents for their encouragement and support also, and so that, I would like to dedicate this thesis to all of my family members. Finally, all praises to almighty Allah for the strengths and His blessings in completing this thesis.

Chapter 1

Introduction

1.1 Research backgrounds

For the realization of information-oriented, low-carbon consumption, safe and secure society; the development of high-reliability and high-performance electronic devices is required. In order to realize these devices, it is essential to develop innovative new electronic materials as well as various types of electronic components and devices utilizing these materials. In recent time, transparent conductive oxide (TCOs) with high transparency and good electrical conductivity have a lot of interest in research field due to the use in photovoltaic cells, low emissivity windows, electro-chromic devices, sensors, touch-screen technology and flat panel displays: including, liquid crystal displays (LCD), organic light emitting displays (OLED) and plasma screen displays [1-3].

Fig. 1-1 gives an idea of the function of TCO on photovoltaic cell. In photovoltaic applications, TCO mounted at the top of the cell which act as a window for light to pass through to the active layer (where carrier generation occurs), as an ohmic contact for carrier transport of the photovoltaic, and can also act as transparent carrier for surface mount devices used between laminated glass or light transmissible composites. As TCO is transparent, sunlight passes through it and when photon of light hits the active material, it generates an electron-hole pair, called an "exciton". Exciton can a) recombine, b) migrate or c) separate into free charges. Charge separation tends to occur at a donor-acceptor (D-A) interface, then free electron and hole can head to opposite electrodes and electric current generates.

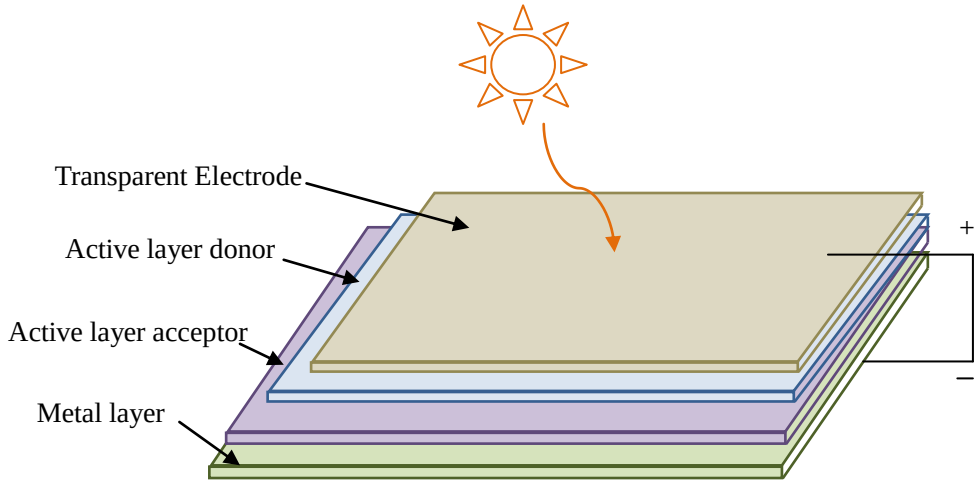

Fig. 1-1 Basic function of transparent electrode in solar cell

Two of the most important parameters for measuring the properties of transparent conductive films are total light transmittance (%T) and film surface electric conductivity. Higher light transmittance allows clear picture quality for display applications, higher efficiency for lighting and solar energy conversion applications. Lower resistivity (ρ) is most desirable for transparent conductive films applications in which power consumption can be minimized. Therefore, the higher the T/ρ ratio of the transparent conductive films is, the better transparent conductive films are. For practical applications in devices, a TCO must have a resistivity of less than 10^{-3} Ωcm and over 80% transmittance in the visible region. Transparent materials possess band gaps with energies corresponding to wavelengths which are shorter than the visible range of 380 nm to 750 nm. As such, photons with energies below the band gap are not collected by these materials and thus visible light passes through. Low resistivity is achieved through very high levels of carrier concentrations in excess of 1 x 10^{20} cm^{-3}. This can then result in high free carrier absorption and high plasma resonance reflectivity,

resulting in poor transmission. So, TCO material chosen is very important. The first TCO material was reported in 1907 by K. Badeker who has developed cadmium oxide thin film by using sputtering [4]. This film showed a relatively high electrical resistance compared to metals and was unstable over time because of full oxidation. In the next, several researches have been adopted to introduce new material with improved conductivity, transparency and stability.

Traditionally, doped metal oxides have the most widespread use for various applications requiring a transparent conductor. These materials have been well researched and refined for over fifty years. The dominant material used today is tin doped indium oxides (ITO) which have been studied enough, and as a result, the material offers many beneficial properties that have made it the material of choice. ITO serves as anode in OLED and organic solar cells. However, the large use of ITO in the flat panel industry, combined with the shortage of indium resources globally, has made the price of ITO increase significantly in the past few years. The cost of indium tin oxide in 2006 reached more than 10 times its price in 2003 due to the explosion of the flat panel display market [5, 6]. In addition, ITO also has other eternal drawbacks due to the material properties: such as lack of flexibility, chemical stability, fragility and toxicity of indium element. All of the above mentioned problems urge us to explore alternatives to the ITO anode. Some alternative TCO films have been investigated by scientists, among them are:

1) Conductive polymer thin film such as Poly (3, 4-ethylenedioxythiophene):Poly (styrene sulfonate) has potentiality to fulfill the requirement of transparent electrode. The conductivity and transparency of PEDOT:PSS makes it competitive to other commercialized transparent conducting oxide materials. In

fact, PEDOT:PSS was the key technology in an antistatic layer used in motion picture films, which resulted in the 2004 Scientific and Engineering Academy Award. Careful exploration by H.C. Starck led to PEDOT:PSS formulations which could yield 500-1000 S/cm conductivity, becoming competitive to transparent conducting oxides on plastic substrates [7]. But, it is known that these electrodes can decrease conductivity upon exposure to high temperatures, humidity or UV light.

2) Several emerging nano-scale materials are showing great promise as transparent electrodes. These include nano-scale forms of carbon such as Carbon nanotube (CNT) and graphene, as well as nano-structured metals, which includes metal grids, thin metal films, and metallic nanowires [8] The utility of these materials as transparent electrodes stems largely from their intrinsically high dc conductivity, which enable ultrathin, optically transparent films of the order of 1-100 nm thick to have appropriate conductance.

In order to maximize the CNT film's potentiality for use as a transparent conductor; typically it is desirable to have a low sheet resistance and a high optical transmission. Since CNT films in the technologically relevant range have thickness less than 50 nm, and an index of refraction of about 1.5 – 1.6, they have very low reflection when on a plastic or glass substrate [7]. Therefore, the CNT film optical transmission at a given film thickness is dominated by absorption. Typically a value of 200 S/cm is used for the optical conductivity, which was measured by Ruzicka et al. on potassium doped single-walled CNT films [9].

The two-dimensional allotrope of carbon graphene is an emerging material currently being researched both for its fundamental science and application potential [10 - 12]. Graphene, as a two-dimensional single atomic layer of crystalline carbon, is a

zero-band gap semiconductor [13]. The high electrical conductivity and low optical absorption of graphene sheets make them an excellent candidate for next generation transparent electrodes.

Metal films can be used as transparent electrodes when they are sufficiently thin, usually less than 10 nm, at which point they become transparent to visible light. There is a tradeoff between making the films thin enough to transmit sufficient light without becoming so thin that the films become discontinuous and begin to suffer from poor electrical conductivity. Various metals can be used to make these transparent films including metal alloys, thin noble metals, alkaline earth metals protected from oxidation by noble metal layers, multi-component metals and single-component metals such as chromium and nickel. Metals such as chromium and nickel are relatively inexpensive (compared with ITO) and are compatible with most organic and semiconductor materials. To get increased optical transmittance, multi-layer films of metal oxide/metal layer/ metal oxide film may be used as well [14].

Transparent electrodes consisting of a random network of metal nanowires have recently been realized and explored. Metal nanowires networks maintain the advantages of patterned metal films and combine that with the low cost manufacturing available with solution deposited roll to roll techniques. The key to this technology is in the growth of small diameter, long, smooth, highly pure metallic nanowires AgNWs have great potential for use as transparent conductors due to the intrinsic high conductivity of silver. AgNWs can be grown at diameters of ~40-200 nm and lengths of ~1-20 μm.

3) Doped metal oxide: Doped metal oxide transparent electrodes are typically n-type semiconductors, though p-type TCOs have been studied. Although there are several types of conductive metal oxides, the most widely used material is ITO

which is already discussed in previous section. Because of several drawbacks of ITO, a number of alternative metal doped oxides to ITO are currently being studied. These include efforts to fabricate reduced indium TCO materials such as ZnO-In_2O_3, In_2O_3-SnO_2, and Zn-In-Sn-O as well as indium free materials such as Al and Ga doped ZnO (AZO and GZO), and Fluorine doped tin oxide (FTO). These materials tend to have inferior opt-electronic properties to ITO. Traditionally, doped metal oxides have the most widespread use for various applications requiring a transparent conductor. Additionally, one of the major concerns for materials such as AZO is the electrical stability of the film upon exposure to humid environment. As there are number of reports which have explained the alternative of ITO, it is difficult to understand the present situation of these materials. In this manner, a comparison of TCO materials current status is summarized in Table 1-1. Among all of these materials, doped ZnO is the most important candidates to combine electrical and optical properties. From the table, it is clear that doped ZnO has high capability to fulfill the requirements of transparent electrode. It has very low sheet resistance, high transparency and low cost also. But it is unstable in air or humid atmosphere which can be a suitable work to locate the doped ZnO as alter of ITO.

Table 1-1 Comparison of TCO materials

Properties of TCO materials	ITO	AZO	CNT	Metal nanowires	Conductive Polymers	Graphene
Sheet resistance	10 Ω/□	14 Ω/□	180 Ω/□	9.7 Ω/□	42 Ω/□	30 Ω/□
Transparency	90%	>85%	85%	89%	82%	90%
Stability	Good	Poor	Excellent	Medium	Medium	Excellent
Flexibility	Poor	Poor	Flexible	Flexible	Highly flexible	Highly flexible
Material cost	High	Low	Low	Medium	Low	Low
Reference	[14]	[15-16]	[17-18]	[19-20]	[21-22]	[23]

1.2 Structural, Electrical and Optical Properties of Zinc Oxide

Zinc oxide (ZnO) is II-VI binary compound semiconductor which exhibits a direct and wide band gap of 3.36 eV and a large free exciton binding energy of 60 meV at room temperature [24]. This large exciton binding energy indicates that efficient exciton emission in ZnO can persist at room temperature and higher. The basic properties of ZnO are shown in Table 1-2.

ZnO has a stable hexagonal wurtzite structure cell with two lattice parameters a = 0.325 nm and c = 0.521 nm. A schematic representation of the wurtzite ZnO structure is shown in Fig. 1-2. The wurtzite ZnO structure consists of alternating zinc (Zn) and

oxygen (O) atoms. The ZnO structure has polar surface (0001), which is either Zn or O terminated and non-polar surfaces (1120) and (1010) possessing an equal number of both atoms. The polar surface of ZnO is responsible for several unique and astonishing properties including piezoelectric properties; it also plays a key role in column growth, favorable for etching due to higher energy. The polar surface is also known to possess different physical and chemical properties [25].

Table 1-2 Key properties of bulk wurtzite ZnO

Property	**Value**	**Reference**
Density (kg/m^3)	5,600	[26]
Melting point (K)	2248	[27]
Exciton binding energy	60 meV	[28-29]
Thermal conductivity (W/cm.K)	0.46-1.67 (Bulk)	[30]
Band gap	3.37 eV	[31]
Refractive index	2.0041	
Lattice parameters at 300 K		[32]
a (nm)	0.32495	
c (nm)	0.52069	
c/a	1.602	
Stable phase at 300 K	Wurtzite	[33]

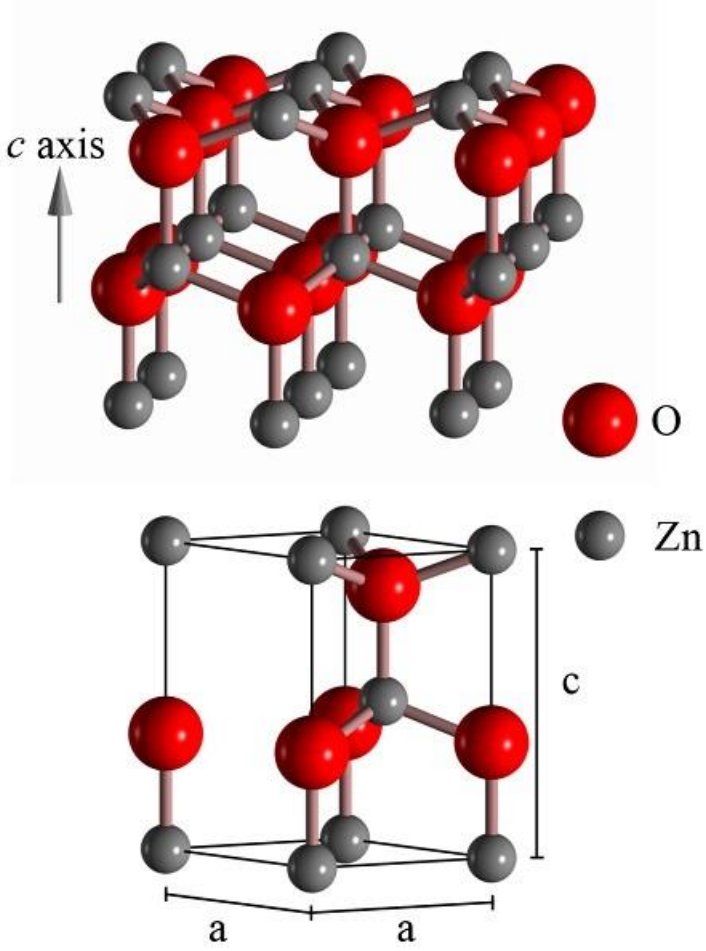

Fig. 1-2 Top: A section of a wurtzite ZnO crystal lattice. Bottom: The unit cell lattice parameters for wurtzite ZnO (Copyright: Slade Joseph Jokela)

Stoichiometric single crystal ZnO is undoped, and practically insulator at room temperature, with a carrier concentration of the order of 10^{13} – 10^{14} cm^{-3}. Creation of intrinsic donors by defects within the crystal structure or doping with other materials can increase the conductivity by increasing the free carrier density enough to move the Fermi level into the conduction band. The resistivity values of ZnO films may be adjusted between 10^{-4} Ωcm and 10^{12} Ωcm, by changing the annealing condition and doping concentration [34]. ZnO with a wurtzite structure is intrinsically n-type

semiconductor because of deviation from the stoichiometry of the ZnO crystal structure. This deviation can lead to oxygen vacancies (V_o) and zinc interstitial (Zn_i), with both having shallow energetic donor positions below the conduction band. The extrinsic doping of ZnO is realized by introducing foreign atoms to the crystal structure. For ZnO, n-doping is easier compared to p-doping due to its high conduction band, while a p-type doping is facilitated for a low band gap material. For the n-type doped metal oxides, native donor or extrinsic dopant-induced charges (electrons) form a level just below the bottom of the conduction band which is empty in the intrinsic semiconductors. With the increase of doping density, these impurity levels eventually merge and form a continuous band, as is illustrated in Fig. 1-3 (middle). Beyond a certain critical concentration n_c, the donor band overlaps with the conduction band and electrons behave like free charge carriers. So, the carrier concentration influences the band gap, as further detailed in next section.

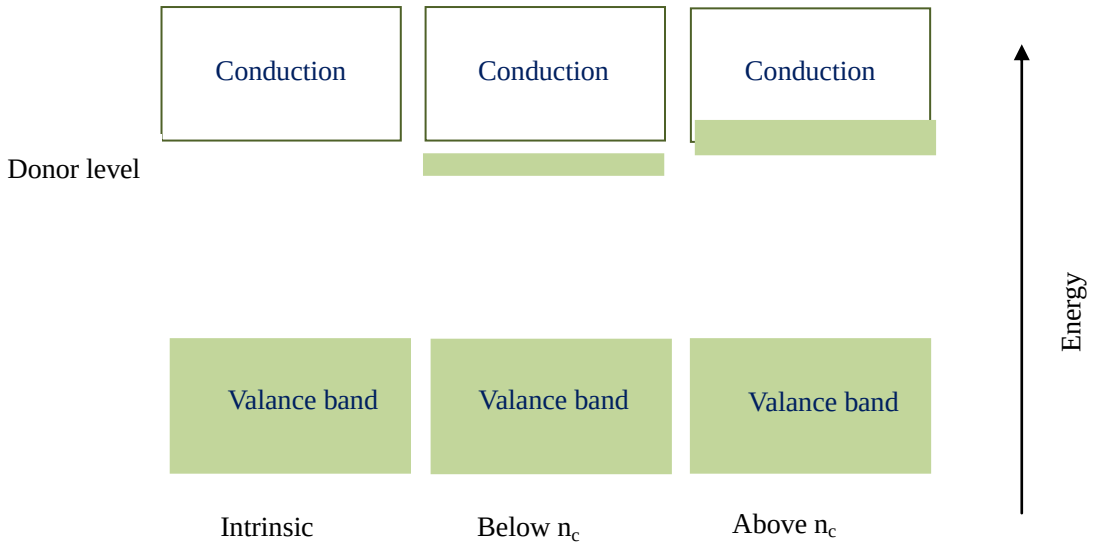

Fig. 1-3 Schematic diagram of n-type doping

In the doped wide band gap metal oxides, carrier concentration and mobility cannot be increased simultaneously. High charge carrier concentration can be achieved from intrinsic or extrinsic doping, however, the presence of native donors and impurity ions induce scattering [35] (electron-electron scattering, electron-impurity scattering, doping modified lattice scattering) for the movement of charge carriers, hence, the charge mobility decreases. At a certain doping concentration, the conductivity reaches a limit and does not increase anymore. On the other hand, the continually growing doping concentration decreases the optical transmission and makes the optical window narrower, according to the Drude model. For example, for indium tin oxide, electron concentration should be less than 2.6 x 10^{21} cm^{-3} in order to achieve efficient transmission in the whole visible range. Therefore, we can see that the charge carrier concentration and transport mobility are the fundamental factors influencing the properties of TCO materials. The fundamental requirement for the band gap energy of a metal oxide concerns the photon absorption induced transmittance loss in the visible spectrum. Generally, a small band gap is advantageous for the electron excitation from valence band to conduction band, resulting in high conductivity. However, this decreases the optical transparency, since photons with energy corresponding to the visible light spectrum (wavelength from 350 nm to 750 nm) can be absorbed. When the band gap energy is above 3 eV, the photons lying in the visible range are not absorbed and thus the optical transparency remains high. The electrical and optical properties of ZnO may be changed by doping with a group III impurity, such as Al, In or Ga. The magnitude of band gap shift due to moderate or heavy doping level is determined by two competing mechanisms: band gap narrowing (BGN) which is a consequence of many body effects on the conduction and valence bands and the band gap widening

(BGW) which is referred to the (well-known) Burstein-Moss effect. Figure 1-4 depicts the band gap change based on heavily doped metal oxide, where, actual band gap change which is due to Burstein Moss shift.

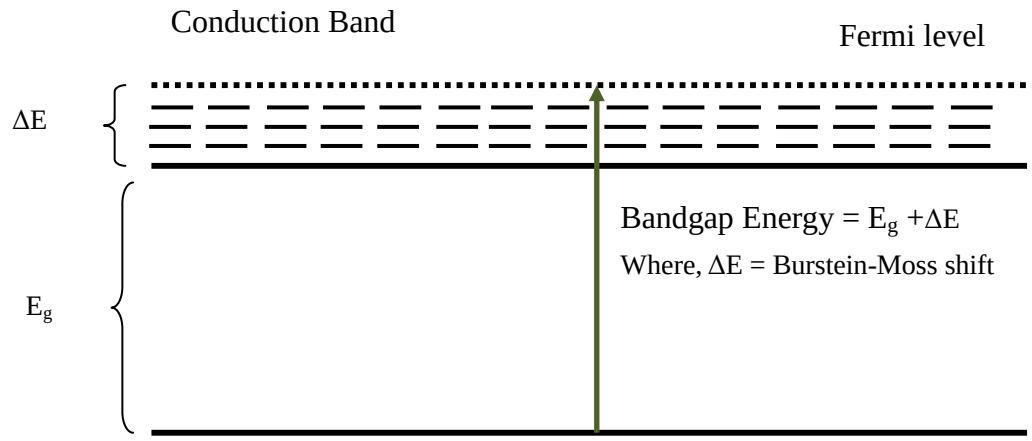

Fig. 1-4 Band gap changes based on Burstein-Moss effect

1.3 Thin film deposition techniques

Thin films of semiconductor material can be deposited by different techniques which can be put into three distinct groups: wet chemical, physical vapor deposition (PVD) and chemical vapor deposition (CVD). Each methodology has some parameters which influence film properties such as crystallinity, microstructure, optical, electrical and adhesion [36-40].

Wet Chemical

Chemical bath and Sol-gel methods are wet chemical routes to thin films. These usually involve the use of chemical precursors which react and form a colloidal solution which forms the basis of the network of the desired material. When the solution is left to age and the solvent is evaporated, a continuous solid network forms. Thin films

can be formed from these solutions in relatively simple ways. The two most common forms are:

- Dip coating, where a substrate is dipped into a precursor solution and the solvent is driven off by heating and forming a solid film.
- Spin coating, where the precursor solution is dropped onto a spinning substrate, which results in the formation of thin layer of material on substrate.

Physical Vapor Deposition

PVD techniques involve expensive high vacuum equipment as the desired material is vaporized and then condenses onto a substrate. PVD techniques encapsulate:

- Evaporative deposition: The material is heated and condenses onto the substrate where it forms a solid layer.
- Electron beam vapor deposition: Electrons impinge on the desired material which results in vaporization and film formation is achieved by condensation.
- Sputtering: Plasma is the form of energy used to vaporize the desired material.
- Pulsed laser deposition (PLD): A high energy laser pulse impinges on the material to achieve vaporization.

Chemical Vapor Deposition

CVD involves the formation of a thin solid film on a substrate via chemical reactions of precursors in the vapor phase. It is the chemical reaction, which distinguishes CVD from PVD processes. The chemical reactions occur homogeneously in the gas phase and/or heterogeneously on the substrate.

1.4 Doping material and concentration

Generally, the group III elements (e.g. Al, Ga, B) are used as doping material in ZnO, as they assist to increase the number of carriers and therefore the conductivity. Among them, Al is most preferred because of its low cost and availability. P.C. Yao have deposited AZO thin film by sol-gel route and obtained minimum resistivity of 9.90 x 10^{-3} Ωcm with optical transmittance of ~90% [41]. M. Zhu improved the conductivity of sol-gel prepared AZO thin film by annealing treatment. He obtained the minimum resistivity of 5.97 x 10^{-3} Ωcm with the transmission in visible light region above 85% after vacuum annealing. He suggested that desorption of oxygen, which is chemisorbed on the surface and at the grain boundary is responsible for the observed improvement [42]. A. Suzuki et al. deposited Al-doped ZnO (AZO) using pulsed laser deposition (PLD), having resistivity of 1.43 x 10^{-4} Ωcm and average transmittance of 90% [43]. Another report explained the effect of Al content in the AZO film, where, lowest resistivity of 8.54 x 10^{-4} Ωcm and average transmittance of >88% was obtained for the best film [44]. Radio Frequency (RF) magnetron sputtering is very popular film deposition method and so that, there are many reports based on sputtering have explained AZO film in different aspects. W.J. Lee has developed AZO film by sputtering and found the minimum resistivity of 2.2 x 10^{-4} Ωcm in his experiment [45]. An optimal doping concentration can contribute for giving better electrical properties. P.C. Yao varied Al concentration from 2 to 2.75 at% and found an optimal concentration of Al/Zn is 2.25 at% with minimum resistivity of 9.9 x 10^{-3} Ωcm [46]. In another report, C.O. Kim et al. reported the structural, electrical and optical properties of AZO films in different doping concentration from 0 to 5 wt% by sputtering. The best film was observed for 2 wt% [47]. H.M. Zhou used sol-gel method to prepare AZO film, where,

Al concentration was varied from 1 to 3 at% and the best conductor was obtained at 1 at% of Al [48].

For practical uses, the environmental stability of transparent electrode should be considered, which still a problem in Al-doped ZnO (AZO) film. This is because the conductivity of AZO decreases in harsh environment, such as annealing in air or high humid condition, preventing AZO films to use for longer duration [49]. Miyata et al. reported that adsorption of oxygen at grain boundaries and thus grain boundary scattering is the main reason for degradation of electrical properties in air [50]. A. Illiberi ascribed the increase in resistivity due to degradation of the structural properties of films, resulting in a higher level of tensile stress. Al_2O_3 thin (25 – 75 nm) films grown by spatial-ALD were used as moisture barrier to effectively enhance the stability of the electrical and structural properties of the films [51]. T. Minami has studied the stability of AZO and GZO thin films prepared with a thickness in the range from approximately 20 to 300 nm. They found that the thickness affects to the resistivity stability. The stability improved as the thickness was increased; in particular, AZO thin films prepared with a thickness below approximately 100 nm were very unstable, whereas films with a thickness above approximately 100 nm were relatively stable [52]. Metal capping layer can be used to enhance the physical properties of thin film. T.L. Chen has used an oxidized Ni capping layer (2.5 nm) on AZO films to enhance the stability of AZO in harsh environment. The capping layer inhibits the penetration of oxygen and water into the films grain boundaries thus significantly increases the stability in damp heat condition (95 ^{o}C and 95% humidity). As Ni layered film losses its transparency, they used O_2 plasma and recovered transparency and work function also through the Ni oxide formation [49]. Though there are some reports which relate to

stability of AZO film and some of them already discussed above, the electrical stability of AZO thin film combined with high transparency and conductivity is still a difficulty compared to ITO. Moreover, deposition method is very important for maintaining high efficiency and low cost. Some reports ascribed the stability of AZO film prepared by sputtering and PLD method. But the study of stability of sol-gel prepared AZO films is not reported yet, though this method has many advantages like large production capability, low cost etc.

The purpose of the following doctoral work is to investigate the structural, optical, electrical properties and electrical stability of Al-doped ZnO (AZO) thin film prepared by using different deposition parameters, such as: annealing temperature, duration and atmosphere of sol-gel prepared film; annealing condition and RF power effect of sputtered AZO film etc. The objective is to improve the properties of AZO films with respect to application as a transparent conducting electrode where improvement of electrical stability under ambient and harsh environment was major concern of this work.

1.5 Research objectives

There have been several studies on Al-doped ZnO film, from a viewpoint of structural, optical and electrical properties. The high transparency (>80%) in the visible wave range and low resistivity (10^{-3} to 10^{-4} Ωcm) of these films make it as a candidate of transparent electrode for applications of different optoelectronic devices. Environmental stability of transparent electrode is very important, which is still a problem for AZO thin films. So, many reports have explored within the last few years with different aspects or mechanisms about the cause of degradation and way for

improvement. To approach these issues, the various experimental and theoretical methods for AZO have been examined intensively. There have been some reports concerning influences of the film thickness, the deposition method, the capping layer, co-doping on the stability of AZO film [52-53]. However, the environmental stability of AZO film prepared by sol-gel method is not reported yet. In this work, the effect of doping concentration, annealing condition such as: temperature, duration, and atmosphere is investigated, with the set of these parameters for sol-gel prepared AZO films. The different deposition technique: RF sputtering was also studied and compared with sol-gel prepared film. Structural, optical, electrical properties and the environmental stability were studied for all films. Also, to identify the reason of instability and improved stability in some preferred conditions; detailed analysis is performed, such as crystallinity, bonding states analysis at the nano-scale or atomic-scale outermost surface in addition to the bulk properties of the film. Beside this, surface smoothness, crystal orientation are also analyzed and finally, AZO thin film with high transparency, low resistivity and improved stability is suggested, and discuss the role of different film preparing parameters on stability.

1.6 Structure of the thesis

The following chapters are structured in six different chapters:

Chapter 2 describes the experimental set up developed in this work to produce the Al-doped ZnO film as well as detail of the experiments undertaken. An overview of the characterization techniques is also presented here. **Chapter 3** reports a preparation of the AZO films using sol-gel method in different annealing atmospheres and doping concentrations. This chapter investigates the structural, optical, electrical properties and

electrical stability of films under damp heat condition. As the electrical stability is not satisfactory, the reason of instability is mentioned here and also describes the effect of thin metallic protective layer on AZO film to improve the stability. **Chapter 4** improves the electrical stability of AZO films using high annealing temperature and discusses the reason of improvement through different aspects, especially the change of elemental concentration at the outermost surface of film. **Chapter 5** reports a comparative study between AZO films prepared by using two different deposition techniques: sol-gel and RF sputtering. Improved environmental stability in sputtered film was also discussed by surface smoothness and crystal orientation. **Chapter 6** describes the further possible mechanism and factors for improving the stability of AZO film. The role of RF power on AZO film properties and improvement of sputtered film stability will also discuss in this chapter. The thesis concludes with **Chapter 7**, which summarizes the main conclusions and provides general considerations on how to improve the electrical properties and environmental stability of AZO film. Some future work topics are also suggested, which may play an important role in today's TCO materials research, and could be worthy of further investigations.

References

[1] D. S. Ginley and C. Bright, MRS Bulletin, **25** (2000) 15-18

[2] I. Hamberg and C. G. Granqvist, Journal of Applied Physics, **60** (1986) R 123

[3] M. Batzill and U. Diebold, Progress in Surface Science, **79** (2005) 47

[4] K. Baedeker, Annals of Physics, **22** (1907) 749-766

[5] T. Jansseune, Compound semiconductor, **11** (2005) 34

[6] C.A. DiFrancesco, M.W. George, J.F. Carlin Jr and A.C. Tolcin, USGS Indium Report, (2007)

[7] D. S. Hecht, L. Hu and G. Irvin, Advanced Materials, **23** (2011) 1482-1513

[8] A. Kumar and C.W. Zhou, ACS Nano, **4** (2010) 11

[9] B. Ruzicka, L. Degiorgi, R. Gaal, L. Thien-Nga, R. Bacsa, J. -P. Salvetat and L. Forro, Physical Review B, **61** (2000) R2468

[10] K.S. Novoselov, A.K. Geim, S.V. Morozow, D. Jiang, M.I. Katsnelson, I.V. Grigorieva, S.V. Dubonos and A.A. Firsov, Nature, **438** (2005) 197

[11] A.K. Geim and K.S. Novoselov, Nature Materials, **6** (2007) 183

[12] A.H. Castro Neto, F. Guinea, N.M.R. Peres, K.S. Novoselov and A.K. Geim, Reviews of Modern Physics, **81** (2009) 109

[13] S. Somiya, "Handbook of advanced ceramics: materials, Applications, Processing, and properties" 2nd edition, Elsevier, (2013), P.77, ISBN: 978-0-12-385469-8

[14] K. Ellmer, Nature Photonics, **6** (2012) 809-817

[15] H. Kong, P. Yang and J. Chu, Journal of Physics: Conference Series, **276** (2011) 012170

[16] T. Yang, S. Song, Y. Li, Y. Xin, G. Du, M. Lv and S. Han, Physica B:

Condensed Matter, **407** (2012) 4518-4522

[17] Z. Yu, X. Niu, Z. Liu and Q. Pei, Advanced Materials, **23** (2011) 3989-3994

[18] Y.A. Kim, H. Muramatsu, T. Hayashi, M. Endo, M. Terrones and M.S. Dresselhaus, Chemical Physics Letters, **398** (2004) 87-92

[19] J. Liang, L. Li, X. Niu, Z. Yu and Q. Pei, Nature Photonics, **7** (2013) 817-824

[20] T. B. Song, Y. Chen, C.H. Chung, Y. Yang, B. Bob, H. S. Duan, G. Li, K.N. Tu and Y. Huang, ACS Nano, **8** (2014) 2804-2811

[21] M. Vosgueritchian, D. J. Lipomi and Z. Bao, Advanced Functional Materials, **22** (2012) 421-428

[22] Y. Xia, K. Sun and J. Ouyang, Advanced Materials, **24** (2012) 2436-2440

[23] S. Bae, H. Kim, Y. Lee, X. F. Xu, J.S. Park, Y. Zheng, J. Balakrishnan, T. Lei, H.R. Kim and Y.I. Song, Nature Nanotechnology, **5** (2010) 574-578

[24] L. Cui, H. Zhang, G. Wang, F. Yang, X. Kuang, R. Sun and J. Han, Applied Surface Science, **258** (2012) 2479-2485

[25] http://www.edn.com/design/led/4391796/2/White-LEDs-Printed-on-Paper-A-Doctoral-Thesis-Part-I

[26] J.P. Reithmaier et al., "Nanostructured materials for advanced technological applications", Springer, (2009), 204, ISBN: 978-1-4020-9915-1

[27] K. Takahashi, A. Yoshikawa and A. Sandhu, "Wide Bandgap Semiconductors-Fundamental Properties and Modern Photonic and Electronic Devices", Springer, (2007), 357, ISBN: 3-540-47234-7

[28] D.C. Reynolds, D.C. Look and B. Jogai, Solid State Communications, **99** (1996) 873

[29] D.M. Bagnall, Y.F. Chen, Z. Zhu, T. Yao, S. Koyama, M.Y. Shen and T. Goto,

Applied Physics Letters, **70** (1997) 2230

[30] PhD thesis of Hajime Wagata, Tokyo Institute of Technology (2011)

[31] A. Mang, K. Reimann and S. Rubenacke, Solid State Communications, **94** (1995) 251

[32] U. Rossler and L. Bornstein, New Series, Group III. 17B, **22** and 41B (1999), Springer

[33] J. L. G Fierro, "Metal Oxides: Chemistry & Applications" CRC Press, (2006), P. 182, ISBN 0824723716

[34] H.A. Mohamed, Optoelectronics and Advanced Materials-Rapid Communications, **6** (2012) 389-393

[35] K.L. Chopra, S. Major and D.K. Pandya, Thin Solid Films, **102** (1983) 1-46

[36] T. Maruyama and J. Shionoya, Journal of material Science letters, **11** (1992) 170-172

[37] C.M. Mahajan, A.G. Godbole, S.P. Gumfekar, S.H. Sonawane and M.G. Takwale, Advanced Materials Research, **67** (2009) 103-108

[38] X. Lv, Y. Dou and J. Wang, Advanced Materials Research, **152-153** (2011) 868-873

[39] H. Agura, H. Okinaka, S. Hoki, T. Aoki, A. Suzuki, T. Matsushita and M. Okuda, Electrical Engineering in Japan, **151** 2 **(**2005)

[40] J. Nomoto, T. Hirano, T. Miyata and T. Minami, Thin Solid Films, **520** (2011) 1400–1406

[41] P.C. Yao, S.T. Hang, Y. S. Lin, W.T. Yen and Y.C. Lin, Applied surface science, **257** (2010) 1441-1448

[42] M. Zhu, H. Huang, J. Gong and C. Sun, Journal of Applied Physics, **102** (2007)

043106

[43] A. Suzuki, T. Matsushita, N. Wada, Y. Sakamoto and M. Okuda, Japanese Journal of Applied Physics, **35** (1996) 56 – 59

[44] H. Agura, A. Suzuki, T. Matsushita, T. Aoki and M. Okuda, Thin solid Films, **445** (2003)263

[45] W. Lee et al., Journal of the Korean Physical Society, **47 (**2005) S296~S299

[46] P.C. Yao, S.T. Hang, Y.S. Lin, W.T. Yen and Y.C. Lin, Applied Surface Science, **257** (2010) 1441-1448

[47] C.O. Kim, D.H. Shin, S. Kim and S.H. Choi, Journal of the Korean Physical Society, **61** (2012) 599-602

[48] H.M. Zhou, D.Q. Yi, Z.M. Yu, L.R. Xiao and J. Li, Thin solid films, **515** (2007) 6900-6914

[49] T.L. Chen, D.S. Ghosh, D. Krautz, S. Cheylan, and V. Pruneri, Applied Physics Letters, **99** (2011) 093302

[50] T. Miyata, Y. Ohtani, T. Kuboi and T. Minami, Thin Solid Films, **516** (2008) 1354

[51] A. illiberi et al. Journal of Vacuum Science & Technology A, **31** 6 (2013)

[52] T. Minami, Thin Solid Films, **516** (2008) 1314–1321

[53] D. Kang, J. Kwon, D. Lee, and M. Han, Journal of the Electrochemical Society, **159** (2012) H61-H65

Chapter 2

Growth and Characterization techniques of AZO thin films

2.1 Introduction

Chapter one illustrated the role of transparent conducting oxides (TCOs) in optoelectronic devices. The following chapter describes the experimental methodology performed in order to prepare Al-doped ZnO thin film by two different deposition techniques: sol-gel and RF sputtering. It will also highlight the characteristic measurement instrument and analytical technologies used in this thesis to investigate the thin film properties.

2.2 Film preparation method

2.2.1 Sol-gel

In general, the sol-gel process involves the transition of a solution system from a liquid "sol" (mostly colloidal) into a solid "gel" phase [1]. Thin film preparation by using sol-gel method can be divided into three parts: (i) preparation of the precursor solution; (ii) deposit of the prepared sol on the substrate by the chosen technique: dip coating or spin coating; and (iii) heat treatment of the gel film. Fig. 2-1 shows the overall view of thin film preparation by sol-gel method using dip coating method [2].

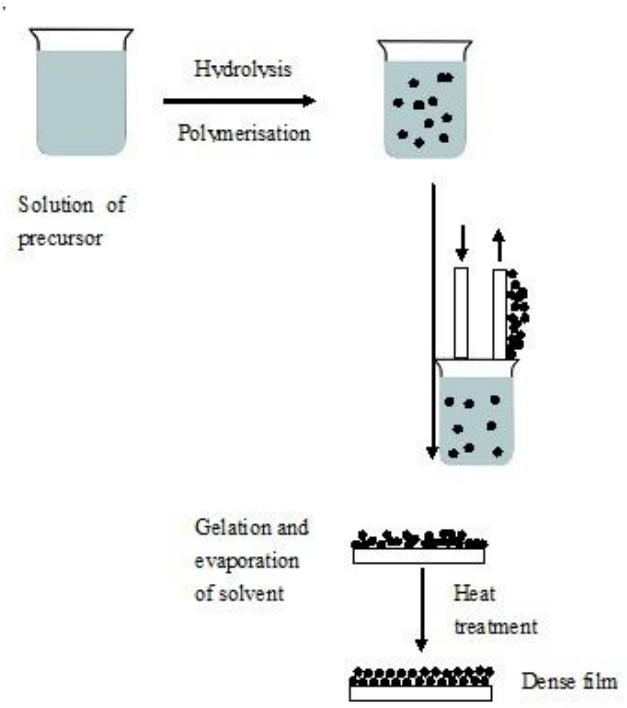

Fig. 2-1 Overview of sol-gel method

In this research, as a starting material, zinc acetate dihydrate ($Zn(CH_3COO)_2.2H_2O$) was dissolved into 2 Methoxyethanol which acts as solvent. Monoethanolamine (MEA) was added to the solution as stabilizer. Aluminum nitrate nonahydrate ($Al(NO_3)_3.9H_2O$) was used as doping material. The solution was stirred at 333 K (60 °C) for 7200 s (2 h) by magnetic stirrer to obtain clear and homogeneous solution. The solution was then kept at room temperature for several hours before coating. The soda-lime glass substrates (48 x 28 mm) were cleaned by acetone in ultrasonic cleaner for 900 s (15 min) and dried in air. Then the substrate was dip-coated into the AZO precursor sol and pulled out at a uniform withdrawal speed of 0.5 mm/s. The dip coating was repeated several times to obtain the required film thickness. The coated glass slide was each time dried (pre heated) in air at 723 K

(450 °C) for 300 s (5 min) to evaporate the solvent and to remove the organic residue. The prepared film was annealed (post heat) in different annealing condition according to experimental requirement. The pre-heat treatment assists to enhance the crystal growth, while the post-heat treatment in specific condition increases the concentration of oxygen vacancy and thus the conductivity of the films [3].

2.2.2 Sputtering

The other deposition method was also performed using Radio Frequency (RF) magnetron sputtering. This is the most widely used method for thin film preparation and is advantageous for producing uniform, well-crystallized, and large-area films. The film thickness, crystal structure, composition, microstructure and defect structure depend on many factors such as sputtering power, substrate temperature, partial pressures of sputtering gas, sputtering time, and distance from target to substrate. [4-7]

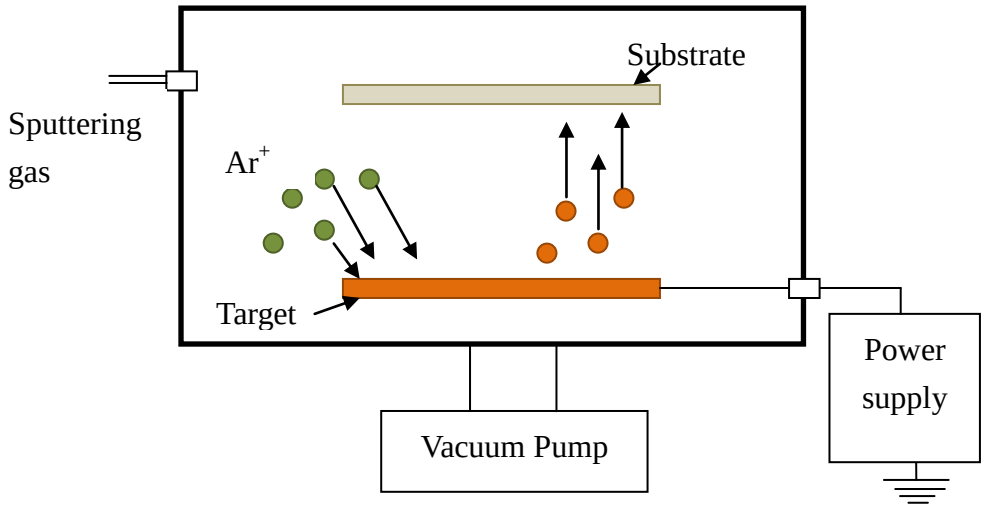

Fig. 2-2 Schematic diagram of sputtering method

In its simplest representation, the phenomenon of sputtering consists of material erosion from a target on an atomic scale, and the formation of a thin layer of the extracted material on a suitable substrate. The process is initiated in a glow discharge produced in a vacuum chamber under pressure-controlled gas flow. Target erosion occurs due to energetic particle bombardment by either reactive or non-reactive ions produced in the discharge. A sputtering system consists of an evacuated chamber, a target (cathode) and a substrate plate (anode). The glow discharge is initiated by applying RF power to the target in a controlled gas atmosphere, and is constituted of a partially ionized gas of ions, electrons, and neutral species. The ejected material diffuses until it reaches and nucleates on the substrate. The duration of this process controls the thin film thickness [8].

In this dissertation, zinc, titanium and chromium disk (99.9% purity) of 75 mm diameter and 5 mm thick was used as a target to develop thin film as the requirement of different experiment. A soda-lime silica glass (24x48x1 mm) was used as a substrate which was cleaned ultrasonically in acetone followed by drying in air. The sputtering procedure is commenced by evacuating the chamber to pressures lower than 10^{-3} Pa. Argon, being an inert gas which does not react with the target, is then introduced into the chamber at a specified pressure. The RF supply is then switched on and stabilized to the required power and induced power levels. During this time the substrate is shielded by the top shutter for 600 s (10 min) in order to remove oxide layer and contaminant on the surface of the target.

2.2.3 Post heat treatment

The as-deposited AZO thin films were heat-treated under different annealing conditions according to experimental requirement, which will explain specifically at the introduction section of each chapter. Overall, the films were heat-treated for 1800, 3600 and 7200 s (30, 60 and 120 min respectively) at a set temperature of 723, 773, 823 and 873 K (450, 500, 550 and 600 ºC respectively). Three different atmospheres were investigated for the thermal annealing process: vacuum (by using mechanical pump at a pressure of 5 Pa), argon + 5% hydrogen and pure hydrogen. Samples were placed in a quartz tube on ceramic boat in different atmosphere and heated in furnace. After heat treatment, this system was kept out from furnace and cooled down until it comes to room temperature. The prepared sample then characterized using following appliances.

2.3 Physical characterization

2.3.1 Film Thickness Measurement by surface profilometer

Profilometry is a simple, accurate and non-destructive measurement technique, frequently used for the determination of the thickness of thin films. Film thickness in this work was measured by surface profilometer with stylus (Surf coder ET 3000). A diamond stylus or probe in contact with the surface is moved laterally to detect and measure small vertical variations.

2.3.2 Structural properties by X-ray Diffraction

The crystal structure of the films was evaluated by X-ray diffraction (XRD) with Cu Ka radiation at 40 kV and 30 mA working in the Θ-2Θ mode (RINT 2100, Rigaku). XRD is an efficient non-destructive analytic technique to identify the crystalline phase and preferred orientations of the films [9-11]. In XRD, the crystals are bombarded with monochromatic X-rays with wavelength (~ 1-10 Å) in the order of

inter-atomic spacing of the atoms. The incoming X-ray photons interact with the electron densities of the atoms and are scattered in all directions. These scattered X-rays interfere with each other constructively or destructively upon reaching the detector, depending on the phase differences of all the X-rays scattered by the different atoms of the crystal lattice. These interference patterns give information on the atomic structure of the crystals. Constructive interference produces diffracted beam where, the condition for constructive interference is given by the Bragg's law: $n\lambda=2d\sin\Theta$, where, n is an integer, λ is the wavelength, d is the inter-atomic spacing, and Θ is the diffraction angle. The diffracted beam intensity will depend on several factors such as the chemical composition of the film and the local arrangement of the atoms.

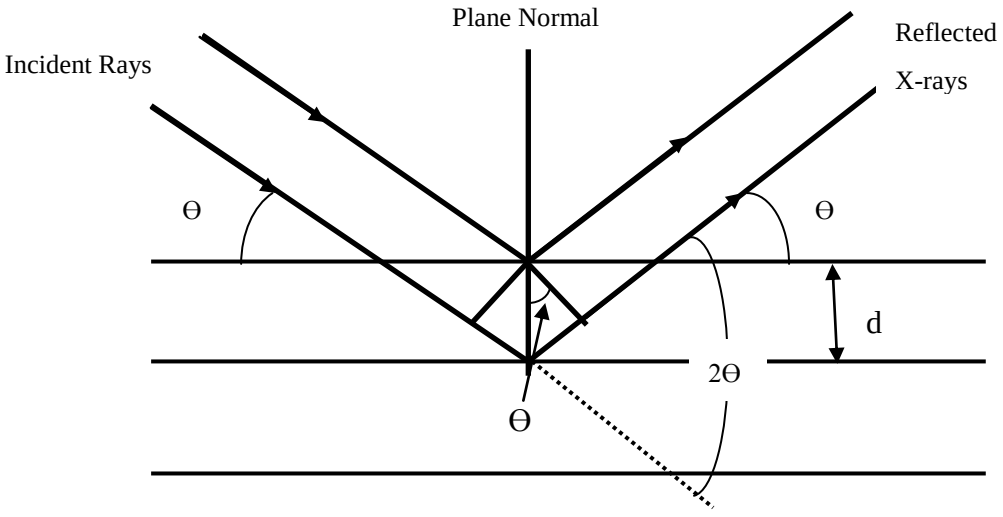

Fig. 2-3 Scheme of the diffraction geometry

In this work, crystallite size was estimated from the full-width at half-maximum (FWHM) of different peaks by Scherrer's equation:

$$D = \frac{0.9\lambda}{ß \cos\Theta}$$

Where, D is the crystallite size, λ (=1.5405 Å) the wavelength of X-rays used, ß the broadening of diffraction line measured at half its maximum intensity in radians and Θ is the angle of diffraction [12].

2.3.3 Optical properties by UV-Vis spectrophotometer

A UV-Vis spectrophotometry is an instrument designed to measure the transmittance or absorbance of a sample as a function of the wavelength of the incident light. It uses light in the visible and adjacent (near UV and near infrared (NIR)) ranges. In the case of thin films, the optical constants, viz., the absorption coefficient and band gap of the material can be determined from the absorption or transmission spectrum. The absorption of light by a sample in the ultraviolet region or visible region is accompanied by a change in the electronic state of the atoms in the sample. Thin films of a semiconductor only absorb light if the incident photons have energy equal to or greater than the band gap. As a result, the absorption spectra of semiconductor thin films are characterized by a sudden sharp increase in absorption at the band gap energy. The absorption edge or band edge is defined as the transition between the strong short-wavelength and the weak long-wavelength absorption in the spectrum. In the case of transparent solids, the absorption edge can be measured using transmittance techniques [13].

The UV-visible spectrometer consists of source, sample, spectrometer and detector. The light source can emit light of wavelength 200-1100 nm. After passing through the sample, the transmitted light is passed through a spectrometer, which disperses the light onto the photodiode detector. In this work, A UV/Vis/NIR spectrometer (Lambda 750s, PerkinElmer) was used to determine the transmission spectra from 300 nm to 800 nm.

The absorption coefficient data were used to determine optical band gap, E_g using the relation [14]:

$$\alpha h\nu \sim A(h\nu - E_g)^{m/2}$$

where, A is a constant, hν is the photon energy (eV) and m=1 for direct transition, m=4 for indirect transition. It is well known that ZnO is a direct band gap material. The absorption coefficient (α) was obtained from the transmittance data by using the relation $\alpha = (1/d)\ln(1/T)$, where, d and T are the thickness and the transmittance of the films. Accordingly, the optical band gap E_g can be obtained by extrapolating downwards the corresponding straight lines till the photon energy axis in the Tauc plot [15]. Tauc's plot gives the relationship between $(\alpha h\nu)^2$ and photon energy hν.

2.3.4 Surface properties by X-ray photoelectron spectroscopy

X-ray photoelectron spectroscope (XPS) is the most widely used surface analysis technique because of its relative simplicity in use and data interpretation. It works by irradiating a sample with an x-ray beam and then quantifying the kinetic energy and number of electrons that are ejected from the material. Fig. 2-4 below illustrates the steps that occur during the XPS process. This technique works by having a high energy X-ray beam and using it to excite the surface of the desired sample. XPS

measure the kinetic energy and number of electrons that escape from the top 0 to 10 nm of the material being analyzed. If the incoming X-ray has enough energy and is absorbed by an atom in the surface, then innermost electron will be ejected. This phenomenon is known as the photoelectric effect. Because the energy of an X-ray with a particular wavelength is known, the ejected photoelectron has a kinetic energy that can be calculated to be equal to the energy of the incident X-ray minus the binding energy and the work function of the element. By detecting and measuring the energy of this electron that is unique for each element, one is able to determine the composition of the sample. XPS can be considered as a surface analysis technique, and depth profiling analysis (measure of the elemental composition as a function of depth) of a material is also feasible by ion beam etching [16].

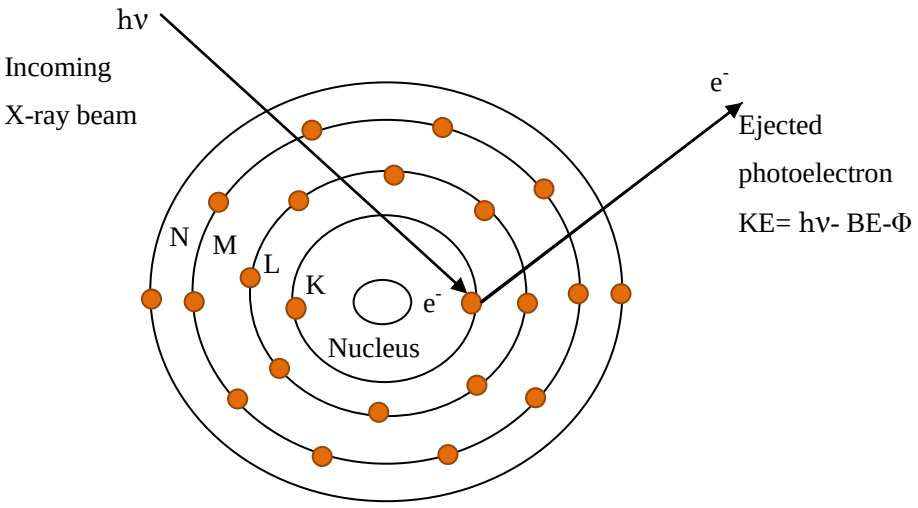

Fig. 2-4 Basic of X-ray photoelectron spectroscopy

2.3.5 Electrical properties by four point probe and Hall effect measurement system

The electrical properties of AZO thin films are a key point in this dissertation. The resistivity should be as small as possible to minimize ohmic losses for the transport of the carrier. The electrical sheet resistance of the deposited films was determined with four point probe (Fig. 2-5). The probe consists of four point contacts, which were pressed toward a film using adequate pressure. The two contacts in the centre were connected to a voltmeter and the outermost contacts were connected to a current generator in series with an ammeter [17]. For good accuracy, the diameter of the point contact tip should be much smaller than the tip spacing, the electrical resistance, R, of a rectangular shaped sample is given by

$$R = \rho . (l/bd) \qquad \text{……...……} \quad (2.1)$$

Where, ρ is the electrical resistivity of the sample and l, b and d are the length, the width and the thickness of the film, respectively. If l=b, equation 2.1 becomes

$$R = \rho/d = R_s$$

Where, R_s is the sheet resistance.

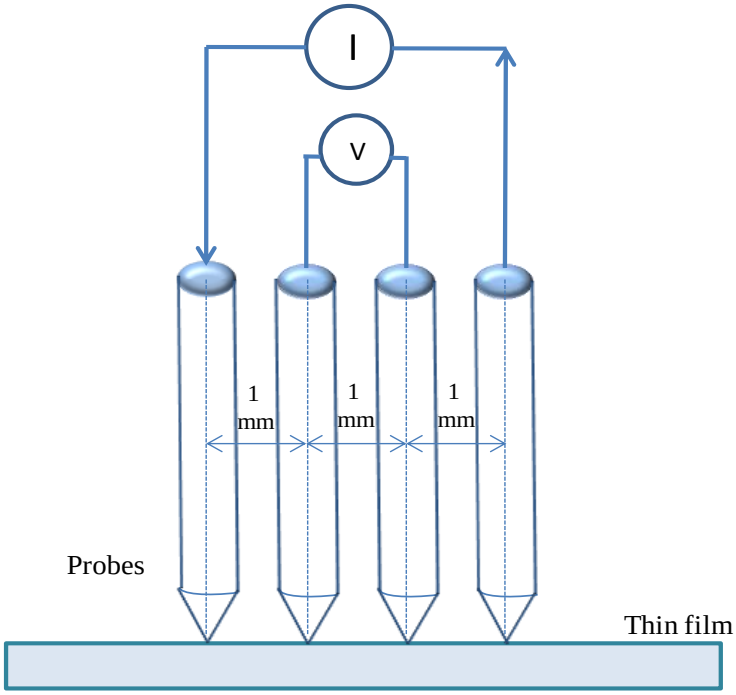

Fig. 2-5 Configuration of Four Point Probe

In 1879, E. H. Hall observed that when an electrical current passes through a sample placed in a magnetic field, a potential proportional to the current and to the magnetic field is developed across the material in a direction perpendicular to both the current and to the magnetic field [18]. This effect is known as the Hall effect which is a useful technique for characterizing the electrical transport properties of metals and semiconductors. It also allows determining the charge carrier density and mobility. The Hall effect occurs when a current is passed through a sample in the presence of a transverse magnetic field and a small potential difference, the Hall voltage is developed between two opposite faces of the sample, in a direction perpendicular to both the current and applied magnetic field. In this work, Hall effect measurement system (Hall resist 3300) was used, whereas, four point probe meter was also used when only sheet resistance was considered as the focusing point.

The Hall effect refers to the voltage difference V_H resulting from the deflection of the charged carriers by the Lorentz force as shown in Fig. 2-6. Due to the Lorentz force, charged particles moving in the x-direction will be deflected in the ±z direction depending on their charge. This causes a buildup of charge on one side of the film, which leads to an electric filed in the z-direction, measurable as the Hall voltage (V_H) across the film. The Lorentz force is

$$F_L = -ev \times H \qquad \text{……....……} \quad (2.2)$$

Where, v is the drift velocity, e is the electronic charge and H is the magnetic field.

Equation 2.2 proves the charge carrier density n from the measurement of the Hall voltage by the input of the current I:

$$n = \frac{IH}{eV_H d} \qquad \text{…….……..} \quad (2.3)$$

where, d is the thickness of film.

The Hall effect measurement system measures the sheet resistance by van der Pauw method. In this method, four small contacts are considered at the periphery of a square shaped (10 x 10 mm) two dimensional sample. To measure R_s, a current is passed from one contact to adjacent contact, while the corresponding voltage difference is measured across the two contacts on the opposite side.

From the Hall measurements associated to the van der Pauw sheet resistance determination, the resistivity and the Hall mobility (μ_H) are deduced with following equation:

$$\rho = R_{sh} \times d \qquad \text{……} \quad (2.4)$$

$$\mu_H = (en\rho)^{-1} \qquad \text{……} \quad (2.5)$$

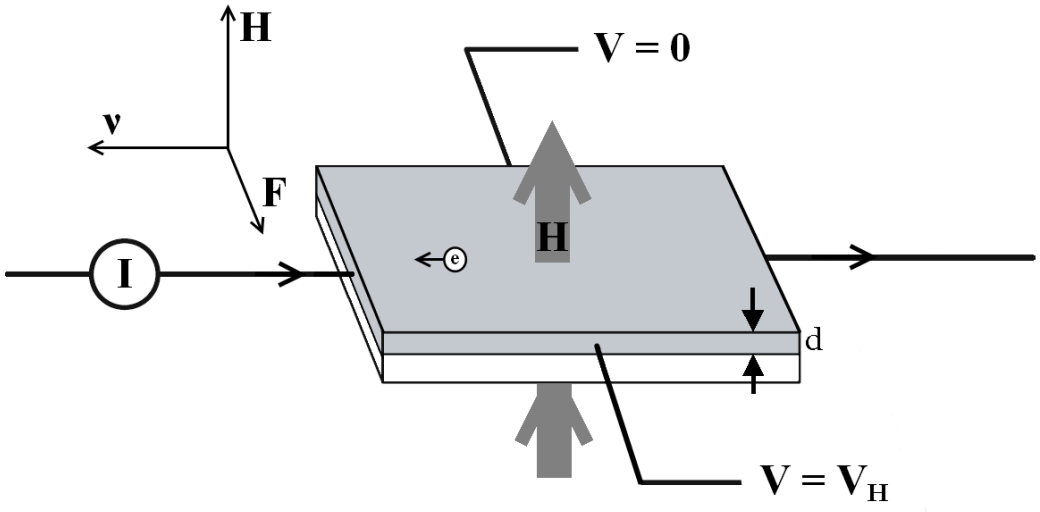

Fig. 2-6 Schematic representation of the Hall effect

2.3.6 Scanning Electron Microscope (SEM)

The scanning electron microscope (SEM) uses a focused beam of high-energy electrons which generates a variety of signals at the surface of the samples. The signals that derive from electron-sample interactions are collected over a selected area of the surface of the sample, and a 2-dimensional image is generated [19]. The signals generated by the interaction of the accelerated electrons with the samples include secondary electrons, backscattered electrons, diffracted backscattered electrons, photons, visible light and heat. Secondary electrons and backscattered electrons are commonly used for imaging samples: secondary electrons are most valuable for showing morphology and topography on samples and backscattered electrons are most valuable for illustrating contrasts in composition in multiphase samples. In this work, the SEM analysis was done by a field emission scanning electron microscopy (FESEM) HITACHI SU6600.

2.4 Summery

In this chapter, the growth and characterization techniques of AZO thin film deposited by sol-gel and RF sputtering have been discussed in detail. The post-deposition treatments have been exposed by parameters of temperature, duration and atmosphere. These different steps have a strong influence on the properties of the thin films. Many characterization techniques have been used in this work to have a large and detailed view of the material properties. Structural attributes have been studied by X-ray diffraction measurements. The optoelectronic properties are studied by UV/Vis/NIR spectroscopy, Hall effect and four point probe measurements. SEM techniques allow investigating the morphological characteristics of the films.

References

[1] T. Schneller, R. Waser, M. Kosec and D. Payne, “Chemical solution deposition of functional oxide thin films”, (2013), (ISBN 978-3-211-993310-1)

[2] C.J. Brinker, G.C. Frye, A.J. Hurd and C. S. Ashley, Thin Solid Films, **201** (1991) 97-108

[3] G.M. Wu, Y.F. Chen and H.C. Lu, Proceedings of the VIII International Conference ION 2010, Kazimierz Dolny, Poland, June 14–17, (2010)

[4] P. Zeman and S. Takabayashi, Surface and Coatings Technology, **153** (2002) 93

[5] H. Wang, T. Wang and P. Xu, Journal of Materials Science: Materials in Electronics, **9** (1998) 327

[6] M. Yamagishi, S. Kuriki, P.K. Song and Y. Shigesato, Thin Solid Films, **442** (2003) 227

[7] M.C. Barnes, A. R. Gerson, S. Kumar and N.M. Hwang, Thin Solid Films, **446** (2004) 29

[8] K. Wasa, I. Kanno and H. Kotera, “Handbook of sputtering technology”, (2012), (ISBN 978-1-4377-3483-6)

[9] L.G. Parratt, Physical Review, **95** (1954) 359

[10] M. Birkholz, “Thin film analysis by X-ray scattering”, (2006), ISBN: 3-527-31052-5

[11] P. F Fewster, Reports on Progress in Physics, **59** (1996) 1339

[12] M.C. Jun and J.H. Koh, Journal of Electrical Engineering & Technology, **8** (2013) 163-167

[13] H.-H. Perkampus, ‘Encyclopedia of Spectroscopy’, VCH, (1995), ISBN: 3-527-29281

[14] J.W. Kim and H.B. Kim, Journal of the Korean physical society, **59** (2011) 2349-2353

[15] J.H. Shin and D.K. Choi, "Journal of the Korean physical society, **53** (2008) 2019

[16] J. F. Watts, J. Wolstenholme, "An Introduction to surface analysis by XPS and AES", (2003), ISBN: 978-0470867938

[17] J.C. Li, Y. Wang and D.C. Ba, Physics Procedia, **32** (2012) 347-355

[18] E. H. Hall, American Journal of Mathematics, **2** (1879) 287-292

[19] R.F. Egerton, "Physical Principles of Electron Microscopy: An introduction to TEM, SEM, and AEM", 1st edition, Springer, (2005), ISBN: 978-0387258003

Chapter 3

Damp heat stability of Al-doped ZnO (AZO) transparent electrode and influence of thin metal film for enhancing the stability

3.1 Introduction

Many studies have been focused on the Al-doped ZnO (AZO) developed by various routs to make efficient transparent conducting oxides. These reports have explained the heat treatment effect, doping effect, different film development procedures etc. shedding light on various characteristics of AZO [1-6]. The optoelectronic properties are generally dependent on the deposition and post deposition conditions [7], where, deposition techniques such as sputtering [8-14], spray pyrolysis [15], sol-gel [3-5], pulsed layer deposition (PLD) [16], chemical vapor deposition (CVD) [17] are well known.

Meanwhile, in terms of the electrical stability, the AZO thin films have a critical problem in that the resistivity of the film largely increases in air, unlike the ITO film, that shows high stability in moisture environment [18]. There have been some reports concerning influences of the film thickness, the deposition method, the capping layer, co-doping on the stability of AZO film [19-21], however, sol-gel prepared film and the annealing effect on the film stability has not been extensively studied. The purpose of this work is to investigate the environmental stability of AZO film prepared by sol-gel method as function of different doping concentration and annealing atmosphere. Structural, optical and electrical stability in damp heat condition was

observed for several days. The effect of sputtered thin metal film (Ti and Cr) encapsulation for enhancing the electrical stability of AZO films has also been investigated in this chapter.

AZO thin film was prepared by using sol-gel dip-coated method. As this experiment explained the effect of doping concentration and annealing atmosphere, different pre-cursor solution was made with different Al concentration at first. Here, 1, 2 3 and 4 % (Al/(Zn+Al) atomic ratio : 0.58, 1.18, 1.77 and 2.3 at%, respectively) of aluminum nitrate nonahydrate was mixed to the starting material zinc acetate dihydrate. These films were annealed in pure hydrogen atmosphere at 450 °C for 30 min. On the other hand, different atmospheres: vacuum, argon + 5% hydrogen and pure hydrogen atmosphere was settled during annealing for investigating annealing atmosphere effect on AZO film.

3.2 Results and Discussion

Fig. 3-1(a) shows the effect of dip coating number on thickness of thin film. It shows that the thickness increases linearly when the coating number increases. The sheet resistance of thin film measured by four point probe meter decreases with increasing of film thickness as shown in Fig. 3-1(b). Very high resistance (10^5 Ω/□) was observed for one time coating. It decreases to ~ 300 Ω/□ for 5 times coating. For thin layered film, stress may happen on AZO film which leads lots of defects. So, free electrons may trapped by this defects. Another reason can be formation of islands of materials with lot of insulating gaps for very thin layers. This gaps can be minimized in increased thickness of film and for that conductivity improved.

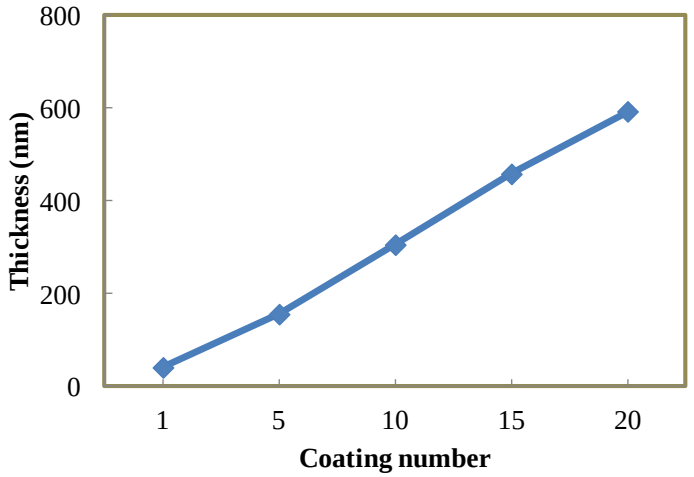

(a)

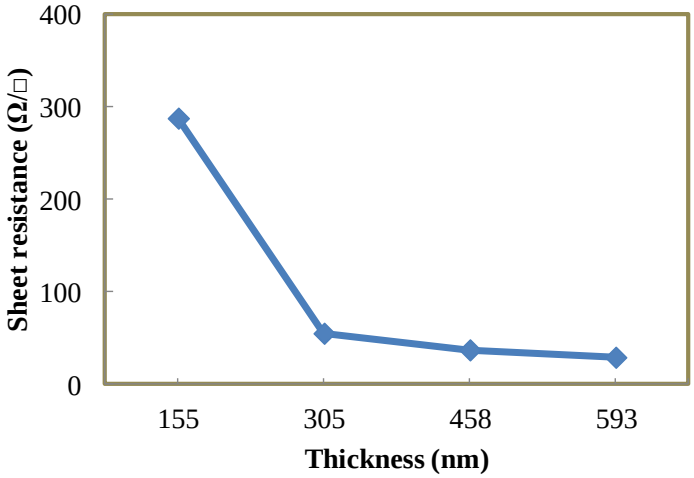

(b)

Fig. 3-1 (a) Thickness of thin film dependency on coating number and **(b)** sheet resistance vs. thickness of AZO thin film

Fig. 3-2 shows the micrographs of sol-gel prepared AZO film at different number of coating. It shows that no grain formed when it was only one time coated. Spherical shaped grains can be observed after 5 times coating, which became densed with increasing coating number to 10 times. After annealing, grains coalescence and clearly showed the larger grain size.

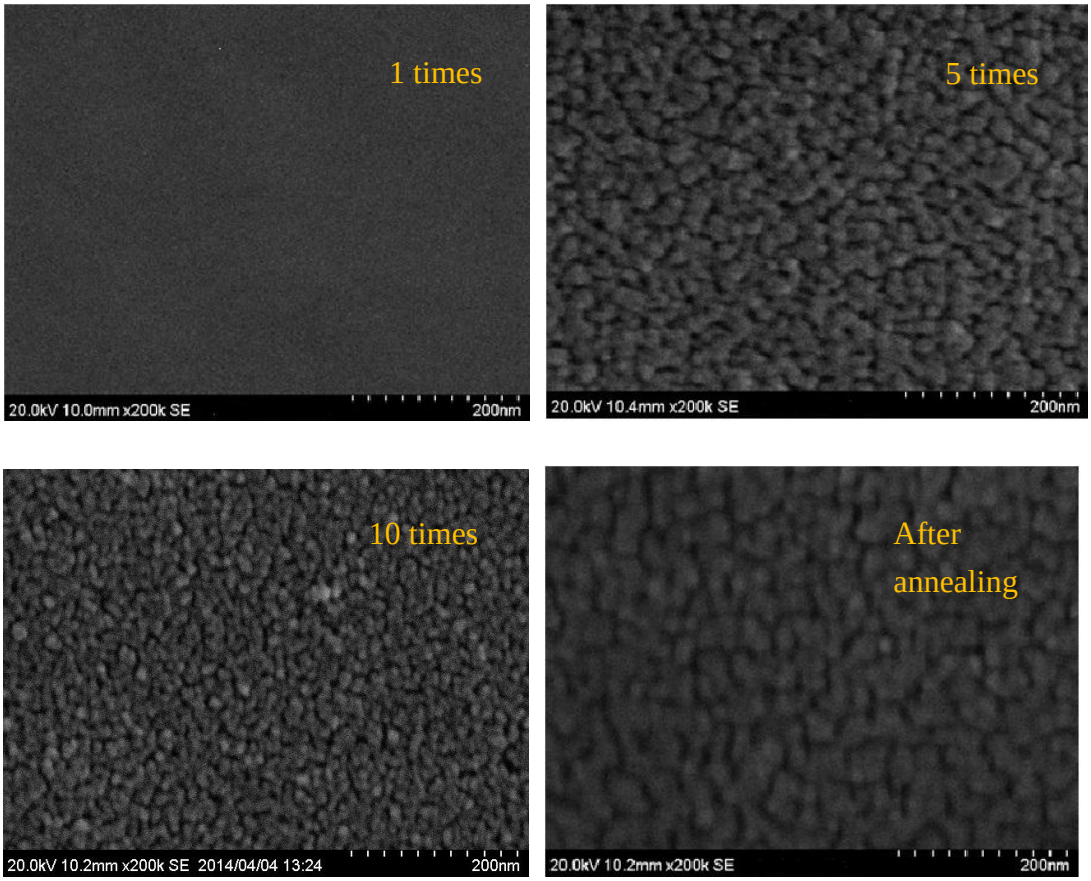

Fig. 3-2 SEM pictures of sol-gel prepared AZO thin films at different coating number

3.2.1 Effect of annealing atmosphere

The resistivity was calculated by measuring sheet resistance and thickness of film, since the sheet resistance (R_s) is proportional to resistivity (ρ) as written as $\rho = R_s t$, where, t is the film thickness. The resistivity of AZO thin films (approx. 300 nm) annealed under different atmosphere (vacuum, argon + 5% hydrogen and pure hydrogen) and duration (30, 60 and 90 min) was measured and depicted in Fig. 3-3. It shows that annealing duration did not make any considerable changes on the film resistivity. But it showed a remarkable change that is the resistivity decreased sharply when the atmosphere changes from vacuum to argon + 5% hydrogen and then slightly

decreased for pure hydrogen.

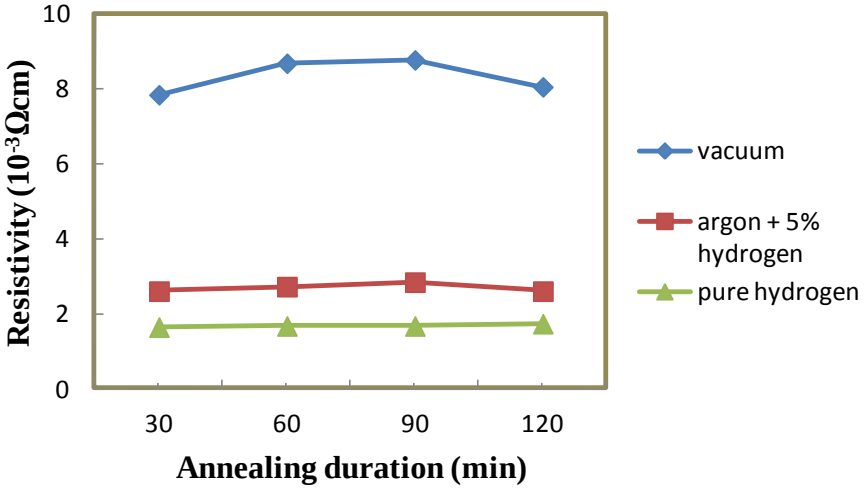

Fig. 3-3 Effect of annealing duration on resistivity of AZO film prepared in different annealing atmosphere

Table 3-1 Electrical properties of 2 wt% Al doped ZnO thin film annealed at 450 °C for 30 min in different atmosphere

Annealing atmosphere	**Resistivity (Ωcm)**	**Carrier concentration (cm^{-3})**	**Hall Mobility (cm^2/Vs)**
Vacuum	0.00786	5.95×10^{19}	13.3
argon + 5% hydrogen	0.00261	2.18×10^{20}	13.9
pure hydrogen	0.00165	2.18×10^{20}	17.3

As shown in Table 3-1, a resistivity value of 7.8×10^{-3} Ωcm was obtained in the vacuum annealed AZO film, which was decreased very sharply for argon + 5% hydrogen annealing and it reached to the lowest value of 1.6×10^{-3} Ωcm for pure

hydrogen annealing film. The number of oxygen vacancies is one of the major causes of variation of resistivity in AZO thin films. Annealing in hydrogen atmosphere can make oxygen annihilation and formed oxygen vacancies which act as carrier and so that, with the increase of carrier concentration resistivity decreases [22]. In our experiment, carrier concentration increases from 5.95 x 10^{19} to 2.18 x 10^{20} cm^{-3}, when the atmosphere changes from vacuum to argon + 5% hydrogen and keep constant for pure hydrogen annealing. On the other hand, some adsorbed oxygen in grain boundaries of vacuum annealed film may increase the barrier height which act as trap for the motion of carriers, resulting the lower mobility. The mobility increases slightly (13.3 to 13.9 cm^2/Vs) for vacuum to argon + 5% hydrogen and then sharply increased to 17.3 cm^2/Vs for pure hydrogen annealing. This is probably due to the desorption of adsorbed oxygen from the grain boundaries and during the decrease of barrier height, mobility increases. So carrier concentration and hall mobility both helps to increase the conductivity, which was also reported by H. Tong [23]. Since a minimum resistivity (1.65 x 10^{-3} Ωcm) is obtained under pure hydrogen atmosphere annealing and duration did not cause any major effect on resistivity in this experiment, pure hydrogen atmosphere and 30 min duration is chosen for further study.

3.2.2 Effect of doping concentration

Fig. 3-4 shows the electrical properties of AZO thin films prepared using different Al concentration of 1, 2, 3 and 4 wt%, which corresponds to Al/(Zn+Al) atomic ratio of 0.58, 1.18, 1.77 and 2.3 at%, respectively, by adding aluminum nitrate nonahydrate ($Al(NO_3)_3.9H_2O$) to the starting material zinc acetate dihydrate. The

resistivity is initially decreased with increasing Al content from 1 to 2 wt%, where, a minimum value of 1.65 x 10^{-3} Ωcm is obtained. However, the resistivity increased for 3 and 4 wt% Al concentration.

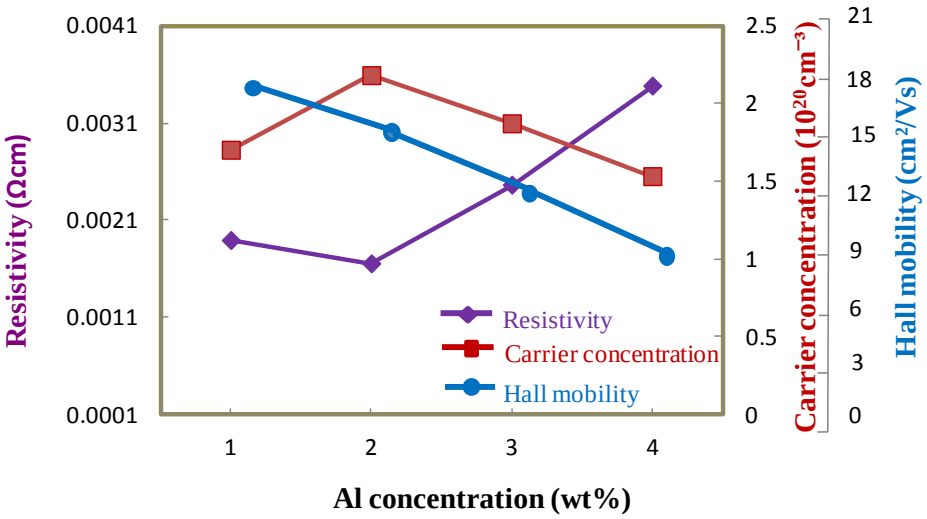

Fig. 3-4 Electrical properties of AZO film in different doping concentration

The highest carrier concentration (2.18 x 10^{20} cm^{-3}) was found in 2 wt% Al concentration. The increasing and decreasing tendency of carrier concentration was differing with resistivity, whereas, mobility decreased with increasing Al concentration. Generally, resistivity of films is mainly affected by carrier concentration and mobility. Since mobility showed decreasing tendency in everywhere, the optimal resistivity at 2 wt% is mainly due to the increase of carrier concentration here. Hu and Gordon [24] reported that excess Al doping forms non-conducting Al_2O_3 clusters in the films causing crystal disorder, which act as carrier traps rather than electron donors. In this experiment, the excess Al doping which was observed for 3 and 4 wt%, decreases the carrier concentration in the film and consequently increases the resistivity. On the other hand, the low crystallinity of the AZO films in high Al concentration was found from the

XRD curve which is shown in Fig. 3-5. The crystallite size was determined by Scherer's formula and which was 22 nm for 1 and 2 wt% Al doping and then decreased to 21 and 19 nm for 3 and 4 wt% Al doping, respectively. It is reasonable to say that the scattering by the impurities, the defects in the crystal and the grain boundaries increase as the aluminum concentration becomes higher, and results in lower mobility.

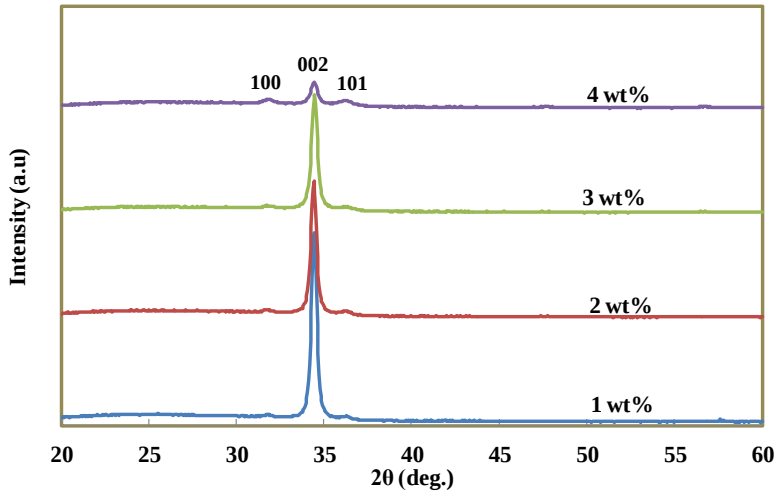

(a)

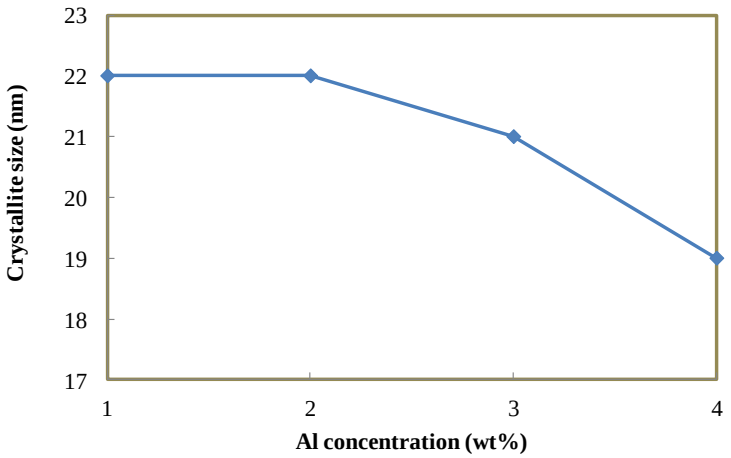

(b)

Fig. 3-5 (a) XRD spectra and **(b)** crystallite size of AZO films with different doping concentration

3.2.3 Damp heat stability

The damp heat stability was investigated for AZO thin films under DH condition for 7 days which is shown in Fig. 3-6. Degradation of electrical properties was found in all films. Fig. 3-6(a) shows the stability of film prepared in different annealing atmosphere. As the films were exposed to humidity, the increased resistivity indicates the possible oxygen and water molecule diffusion to the film that confines the number of free electrons. Beside the diffusion of O_2 and/or H_2O molecule, some adsorbed oxygen present at grain boundary also insists to decrease the carrier. Very fast oxidation was observed in films within one day, especially for vacuum annealed film, probably due to both adsorbed molecule. On the other hand, the increasing rate was slightly low for hydrogen annealed film, because, during hydrogen annealing, oxygen at grain boundary desorbed and thus O_2/H_2O diffusion seems the only reason for increasing resistivity, resulting the low degradation rate. In addition, the energetic oxygen bombardment disturbs the grain growth, which results in an increase of the proportion of grain boundaries in ZnO thin film. This induces the scattering at the boundaries and decreases the carrier mobility [25], thus changing the conductivity of AZO film. The decreasing trend of carrier concentration and mobility for pure hydrogen annealed film is shown in Fig. 3-6(b), where, carrier concentration sharply decreased within first 12 h from 2.18 x 10^{20} to 1.92 x 10^{19} cm^{-3} and then 1.25 x 10^{19} cm^{-3} in next 12 h, where mobility decreased from 17.34 to 6.24 cm^2/Vs in 12 h and it showed very low value of 1.96 cm^2/Vs after 24 h.

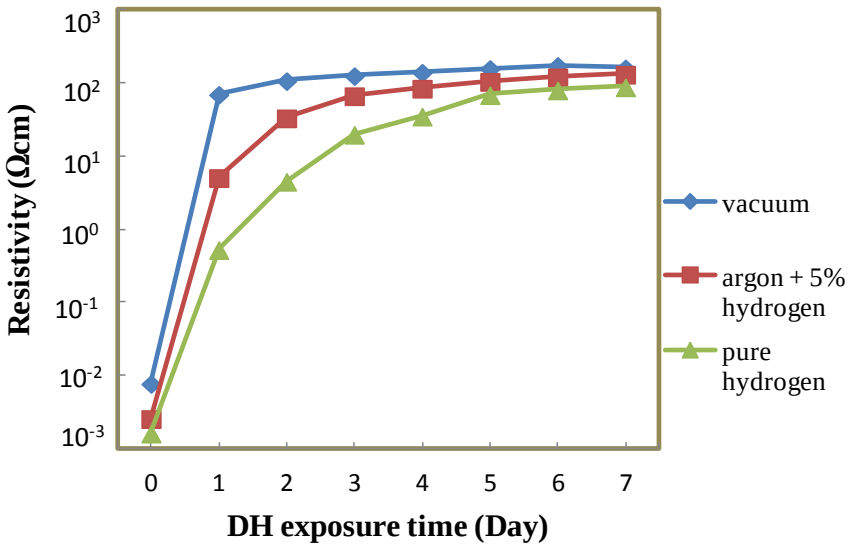
Resistivity (Ωcm)
10^3
10^2
10^1
10^0
10^-1
10^-2
10^-3
0
1
2
3
4
5
6
7
DH exposure time (Day)
vacuum
argon + 5% hydrogen
pure hydrogen

(a)

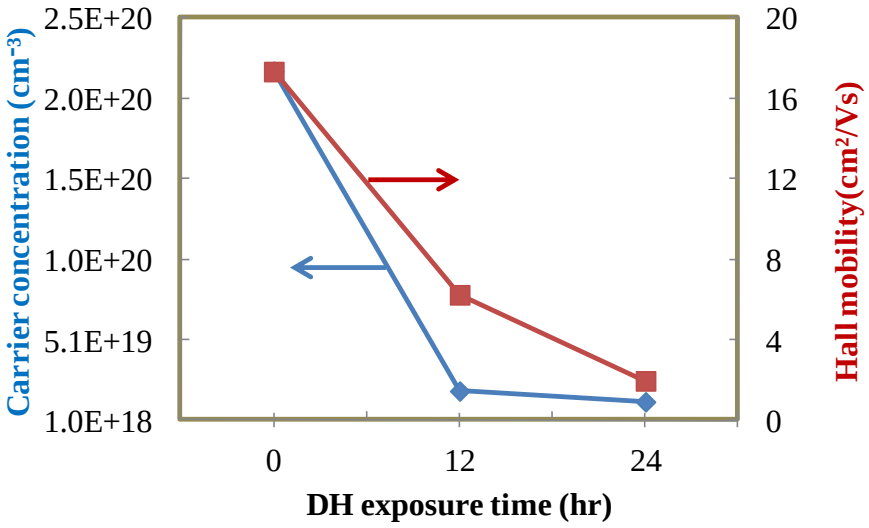
Carrier concentration (cm^-3)
2.5E+20
2.0E+20
1.5E+20
1.0E+20
5.1E+19
1.0E+18
Hall mobility(cm²/Vs)
20
16
12
8
4
0
0
12
24
DH exposure time (hr)

(b)

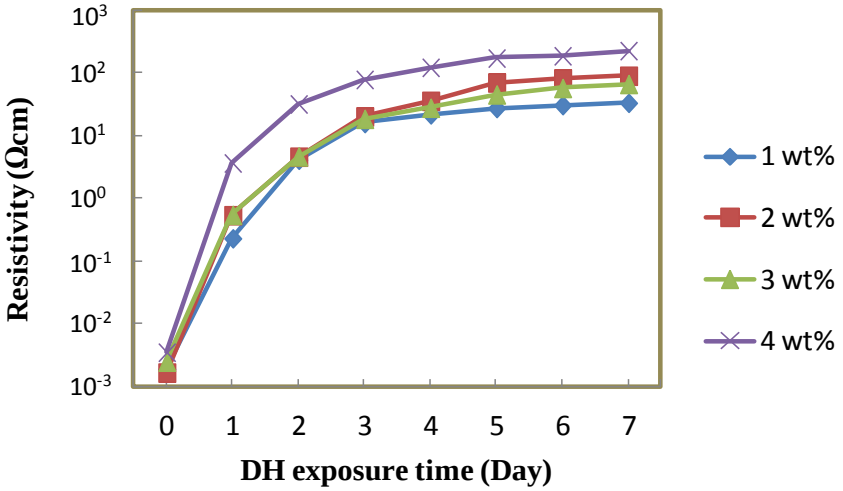

(c)

Fig. 3-6 (a) Electrical stability of 2 wt% Al doped ZnO thin film in DH condition as function of annealing atmosphere, **(b)** carrier concentration and Hall mobility of the film annealed in pure hydrogen and **(c)** DH test for film in different Al concentration

The resulting electrical stability was also dependent on the Al concentration (Fig. 3-6(c)). AZO film with 4 wt% Al showed highest instability compared to others, which was probably due to the decrease of crystallite size in this film which is shown in Fig. 3-5(b). Small crystallite size enhances the grain boundary area, which is the preferable path for oxygen to diffuse to the film and thus the resistivity increases intensively. But degradation rate of resistivity is very high for other films also due to possible diffusion of O_2 and/or H_2O molecule to the film. The possibility of the diffusion was investigated by keeping the films in air and argon atmosphere for 30 days at room temperature. It was observed that the resistivity of AZO film stored in air environment increased by approximately 62%, whereas, it was only 3% for film stored in argon atmosphere. This slight change may be due to the presence of small quantity of H_2O molecules in the argon environment or strain relief of film.

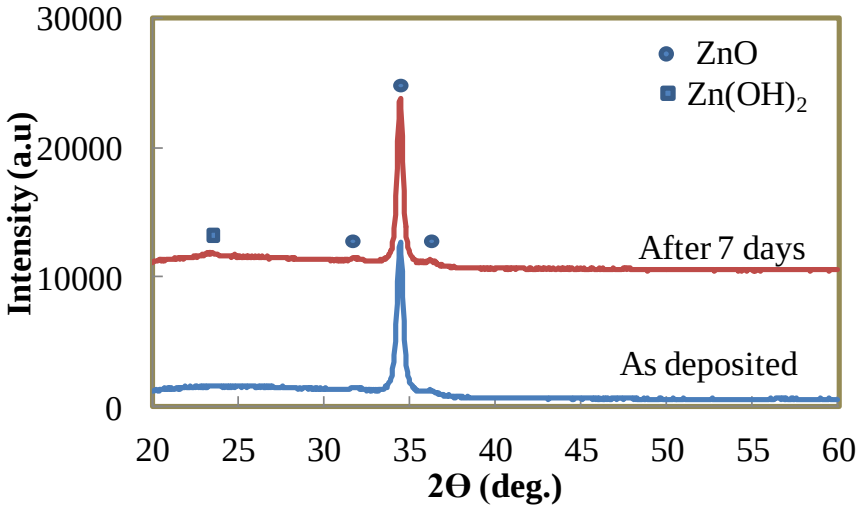

(a)

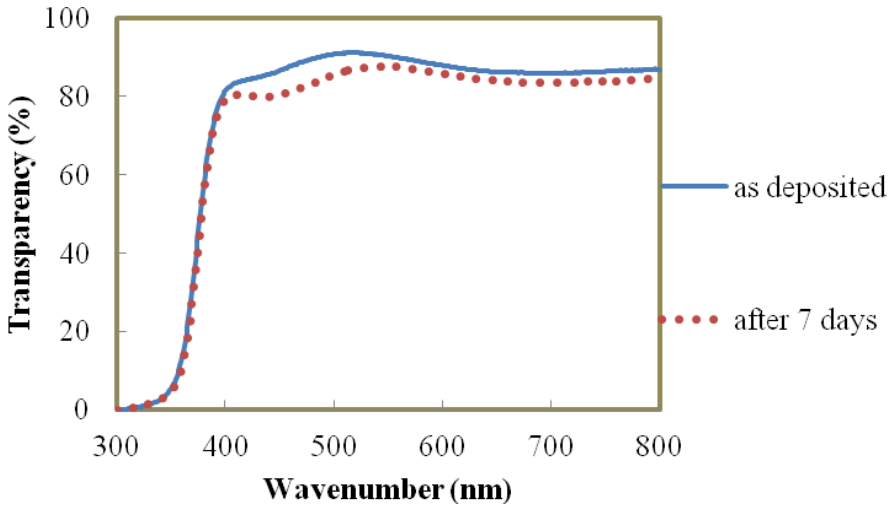

(b)

Fig. 3-7 (a) Structural and **(b)** optical changes of AZO film in damp heat condition

Fig. 3-7 shows the structural and optical changes of AZO film (1.18 at% Al doped and pure hydrogen annealed) for as prepared and after exposing in DH for 7 days. XRD measurement shown in Fig. 3-7(a) indicates that all films were polycrystalline and exhibited a preferred wurtzite c-axis orientation. A strong diffraction peak was observed

at 34.45 deg., corresponding to the (002) plane of ZnO, which was not changed after 7 day stored in DH condition. c-axis length (5.2028 Å) calculated using the Bragg equation and crystallite size (22 nm) of strong peak evaluated by using Scherer's formula was also unchanged after DH test. A very weak peak of $Zn(OH)_2$ peak at 23.35 deg. was observed after DH exposure because of water molecule diffusion to the film. The transmission spectra of AZO thin films were observed in visible wavelength. An average transmittance of above 87% was obtained in films before DH treatment which was slightly decreased after damp heat treatment. Similar observations were found for almost all films.

3.2.4 Effect of metal layer on AZO

Some efforts have been applied to enhance the electrical stability by giving thin protective layer through Cr and Ti. In this experiment, Cr or Ti layers which oxidized at ambient condition are found as efficient shielding layers that prevent the penetration of oxygen or moisture into the AZO film. The Cr or Ti thin layer was deposited on the AZO thin films by sputtering method. Cr or Ti disk (99.9% purity) of 75 mm in diameter was used as target and glass plate coated with AZO with thickness approx. 300 nm was used as a substrate. Argon flow was supplied which act as the sputtering gas.

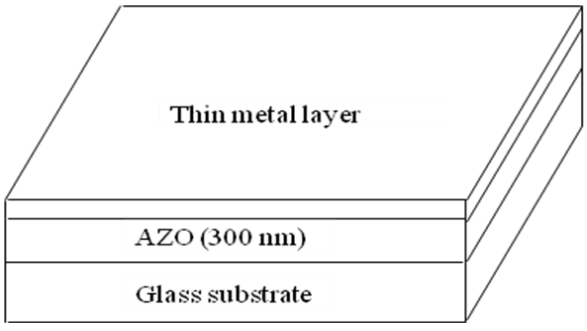

Fig. 3-8 Schematic diagram of AZO thin film covered by thin metal layer

The RF input power and substrate temperature were fixed at 150 W and 423 K (150 °C), respectively. After deposition of Cr (4, 8 and 15 nm) or Ti (10, 13 and 30 nm) layer on AZO, it transformed into a bi-layer of Cr/CrO_x or Ti/TiO_2, when it comes to air at room temperature. This can be explained by x-ray photoelectron spectroscopy analysis which is shown in Fig. 3-9.

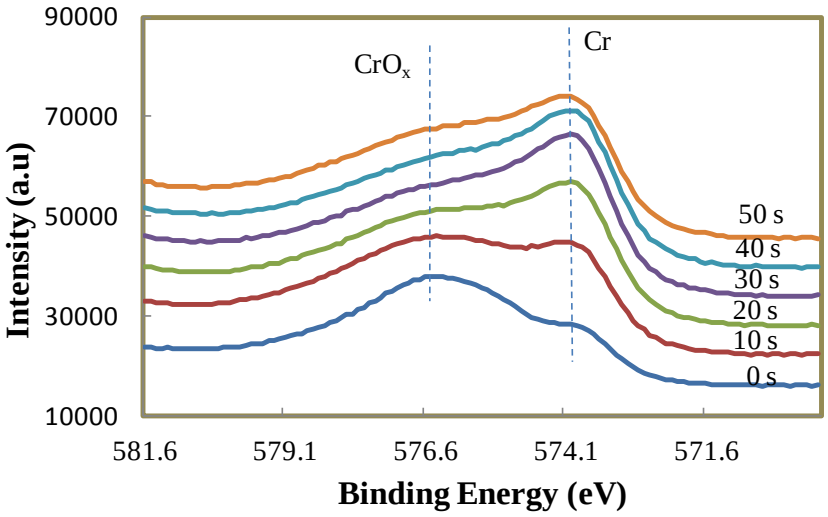

(a)

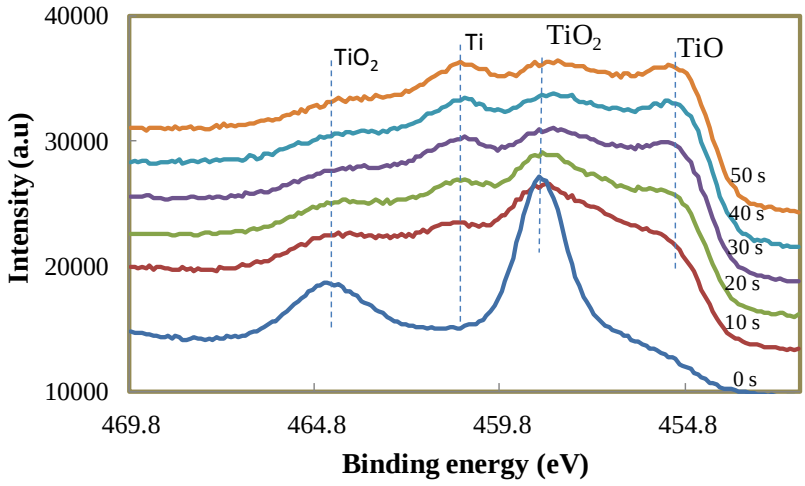

(b)

Fig. 3-9 Binding energy of different etched parts of film **(a)** AZO-Cr (4 nm) and **(b)** AZO-Ti (10 nm)

Fig. 3-9 shows the binding energy of surface and different etched parts of both Cr (4 nm) and Ti (10 nm) covered AZO film. It clearly indicates the surface oxidation of metals which formed in air at room temperature. In Fig. 3-9(a), the film surface contains CrO_x peak at binding energy 576.5 eV [26] with high intensity which gradually decreases with etching time. On the other hand, metallic Cr at 574.2 eV [27] has very weak peak on surface and relatively strong peak at etched parts. The same observation was found in Fig. 3-9(b) which show the XPS depth profiles of titanium covered AZO film. Before etching of film, Ti2p and $Ti2p_{1/2}$ XPS peak at 458.8 and 464.6 eV was observed, which could be identified as that of Ti^{4++} from TiO_2 [28-29]. Intensity of these peaks decreased with an increase of etching time. On the other hand, the XPS peak due to Ti^{2++} and metallic Ti at 455.4 and 461 eV, respectively, appeared in the sample etched for 10 – 50 s with low intensity [30-31].

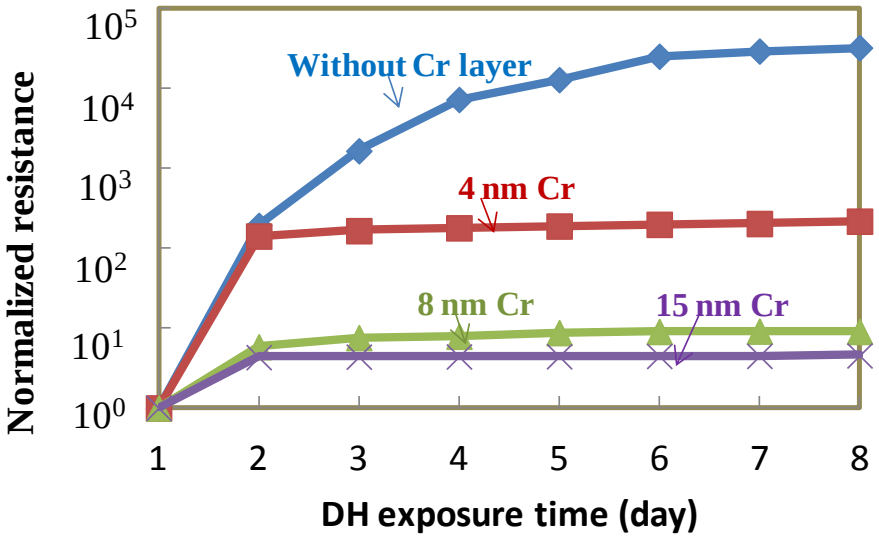

(a)

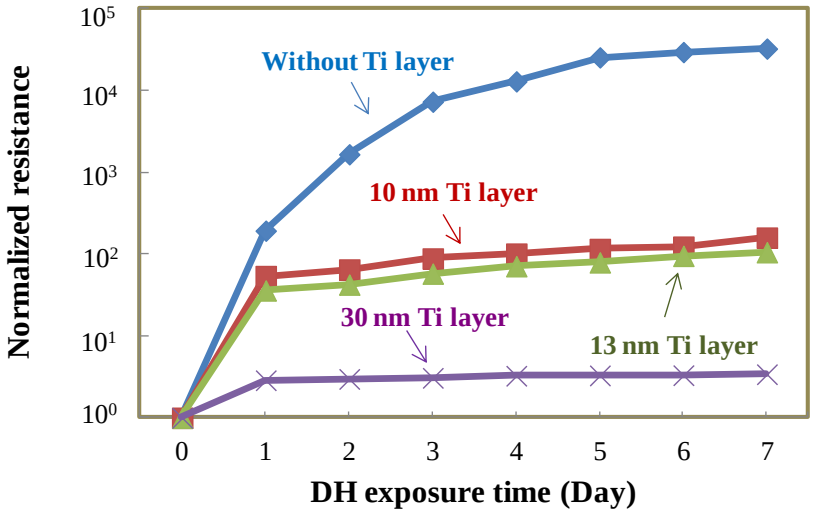

(b)

Fig. 3-10 Damp heat stability of AZO and **(a)** AZO-Cr **(b)** AZO-Ti film

After deposition of the metallic thin layer, AZO films resistivity did not show any significant change, probably, these material acts as an electron transport material due to its metallic characteristic. Slight increase of resistivity (0.00015 Ωcm) may be due to short duration of presence in air and oxygen diffusion to film before sputtering the metal layer. The damp heat test result is shown in Fig. 3-10, which states the improved stability by the formation of bilayer of Cr/CrO_x or Ti/TiO_2 on AZO. This bilayer, especially oxide layer on very top surface serves as a protective layer to prevent the penetration of oxygen and water into the AZO film and reduce the degradation rate of conductivity. With the increase of thickness of metallic layer, stability improved. But at a time, the transparency also decreased and found as 70% for 4 nm Cr and 67% for 10 nm Ti layered film. The effect of thickness of Cr layer on electrical stability and transparency was also investigated in Fig. 3-11, where normalized resistivity after 7

day in DH exposure was considered for understanding the improved stability. It showed that, with increasing Cr layer thickness on AZO, stability improves immensely but at the same time, it loses its transparency. Since the degradation rate of conductivity is very high for AZO film prepared by sol-gel method, it is still a big challenge to get both transparency and stability in a film by using thin metallic layer.

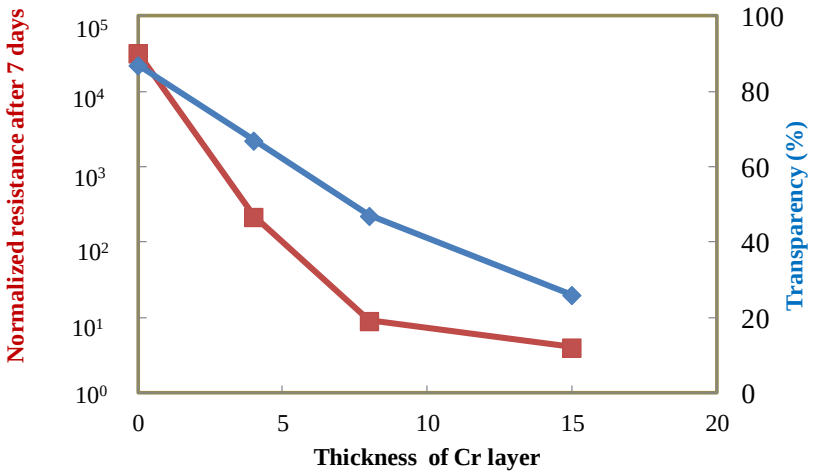

Fig. 3-11 Effect of Cr layer thickness on stability and transparency

3.3 Conclusion

In summary, the AZO thin films were successfully prepared by sol-gel method using different annealing atmosphere and different Al concentration. Electrical properties were enhanced in pure hydrogen annealing and 2 wt% Al doping due to the increase of carrier concentration in both cases. The high degradation of the resistivity was observed under damp heat (85 °C and 85% RH) condition for all films. Oxygen and water molecule diffuse to the film and increase the resistivity. This is assumed as very stable resistivity was found after keeping the film in argon atmosphere. Very thin Cr or

Ti layer was deposited by sputtering on AZO for protecting them against O_2/H_2O absorption. These films obtained without any significant enhancement of resistivity due to their metallic character. Electrical stability enhancement was due to the formation of oxide layer of these thin metals at room temperature. This thin oxide layer protects further oxidation and improves stability.

References

[1] G. J.Fang, D. Li and B. Yao, Thin Solid Films, **418** (2002) 156–162

[2] C.M. Mahajan, A.G. Godbole, S.P. Gumfekar, S.H. Sonawane and M.G. Takwale, Advanced Materials Research, **67** (2009) 103-108

[3] X. Lv, Y. Dou, J. Wang and Y. Xu, Advanced Materials Research, **152-153** (2011) 868-873

[4] C. JianLin, C. Ding and C. ZhenHua, Science in China Series E: Technological Science, **52** (2009) 88-94

[5] J. Lin and J. Wu, Applied Physics Letters, **92** (2008) 134103

[6] P. C. Yao, S. T. Hang, Y.S. Lin, W.T. Yen and Y.C. Lin, Applied Surface Science, **257** (2010) 1441–1448

[7] P. Nunes, E. Fortunato and R. Martins, Thin Solid Films, **383** (2001) 277-280

[8] K. Hummer, Physica Status Solidi (b), **56** (1973) 249

[9] J. Nomoto, T. Hirano, T. Miyata and T. Minami, Thin Solid Films, **520** (2011) 1400–1406

[10] S.T. Hwang and C. B. Park, Transactions on Electrical and Electronic Materials, **11** (2010) 81

[11] C. Lennon, R.B. Tapia, R. Kodama, Y. Chang, S. Sivananthan and M. Deshpande, Journal of Electronic Materials, **38** (2009) 1568-1573

[12] C. G. Huang, M.L. Wang, Z.H. Deng, Y.G. Cao, Q.L. Liu, Z. Huang, Y. Liu, W. Guo and Q. Huang, Journal of Materials Science: Materials in Electronics, **21** (2010) 1221–1227

[13] J.F. Chang, W.C. Lin and M.H. Hon, Applied surface Science, **183** (2001) 18-25

[14] H. Kong, P. Yang and J. Chu, Journal of Physics: Conference Series, **276** (2011) 012170

[15] V. Rakhesh and V.K. Vaidyan, Journal of Optoelectronics and Biomedical Materials, **1 (**2009) 281 – 290

[16] H. Agura, H. Okinaka, S. Hoki, T. Aoki, A. Suzuki, T. Matsushita and M. Okuda, Electrical Engineering in Japan, **151** 2 (2005)

[17] T. Maruyama and J. Shionoya, Journal of Materials Science Letters, **11** (1992) 170-172

[18] C. Guillén and J. Herrero, Surface and Coatings Technology, **201** (2006) 309–312

[19] T. Minami, Thin Solid Films, **516** (2008) 1314–1321

[20] T.L. Chen, D.S. Ghosh, D. Krautz, S. Cheylan, and V. Pruneri, Applied Physics Letters, **99** (2011) 093302

[21] D. Kang, J. Kwon, D. Lee, and M. Han, Journal of the Electrochemical Society, **159** (2011) H61-H65

[22] C. Huang, M. Wang, Z. Deng, Y. Cao, Q. Liu, Z. Huang, Y. Liu, W. Guo and Q. Huang, Journal of Materials Science: Materials in Electronics, **21** (2010) 1221

[23] H. Tong, Z. Deng, Z. Lie, C. Huang, J. Huang, H. Lan, C. Wang and Y. Cao, Applied Surface Science, **257** (2011) 4906-4911

[24] J. Hu and R.G. Gordon, Journal of Applied Physics, **71** (1992) 880-890

[25] K. Wasa, I. Kanno, H. Kotera, "Handbook of Sputter Deposition Technology: Fundamentals and Applications for functional thin films, nanomaterials and MEMS", 2nd edition, Elsevier, (2012) 395

[26] P. Dolle, M. Alnot, J.J. Ehrhardt and A. Cassuto, Journal of Electron

Spectroscopy and Related Phenomena, **17** (1979) 299-321

[27] G.C. Allen, P.M. Tucker and R.K. Wild, Journal of the Chemical Society, Faraday Transactions II, **74** (1978) 1126

[28] A.R. Burke, C.R. Brown, W.C. Bowling, J.E. Glaub, D. Kapsch, C.M. Love, R.B. Whitaker and W.E. Moddeman, Surface and Interface Analysis, **11** (1988) 353-358

[29] D. Gonbeau, C. Guimon, G. Pfister-Guillouzo, A. Levasseur, G. Meunier and R. Dormoy, Surface Science, **254** (1991) 81-89

[30] D. Simon, C. Perrin and J. Bardolle, Journal of Electron Microscopy, **1** (1976) 175

[31] A. Lebugle, U. Axelsson, R. Nyholm and N. Martensson, Physica Scripta, **23** (1981) 825-827

Chapter 4

Investigation and improvement of the environmental stability of Al-doped ZnO (AZO) thin film prepared by sol-gel method

4.1 Introduction

In the previous section, AZO thin films were developed by sol-gel method using different annealing atmosphere: vacuum, argon + 5% hydrogen, pure hydrogen; and different annealing duration: 30, 60 and 90 min. The doping concentration effect also investigated in that part. Enhanced electrical properties were observed in 1.18 at% of Al doped film, which was annealed in pure hydrogen due to the increase of carrier concentration. These films were environmentally unstable in damp-heat condition, which was improved by using ultrathin metal layer (Cr or Ti) on AZO film. As sol-gel prepared film is very unstable in DH condition, comparatively larger thickness of metallic layer needed for getting better stability which reduced transparency. The results indicate that more detailed analysis is required to get the film which will fulfill the optoelectronic properties as transparent electrode with improved stability.

This chapter describes the improvement of resistivity stability without using of protective layer. Here, AZO thin films were prepared by sol-gel method in different annealing temperature and duration. AZO films were deposited, where, doping concentration i.e., Al/(Zn+Al) atomic ratio was fixed at 1.18 at%. The soda lime glass substrate was dip coated into precursor solution for 10 times by drying each time at 723 K (450 °C) for 300 s (5 min) in air, subsequently annealed at different temperatures and

durations under vacuum atmosphere. It can be noted that, the film was annealed under vacuum atmosphere though pure hydrogen showed better electrical properties in previous chapter. In this experiment, sheet resistance increased sharply when AZO film was annealed in hydrogen with a temperature higher than 500 ℃. H. Tong has explained this increasing tendency and he found that surface of film may damage at high temperature annealing [1]. Here, for vacuum annealing, temperature was selected as 450, 500, 550, or 600 °C, and the duration was 30, 60, or 120 min, for each temperature. The investigated samples will be labeled in the following parts as s-x-y, where x, y are annealing temperature and duration respectively.

4.2 Results

The estimated film thickness was 300 ± 40 nm. The variation of thickness along with sheet resistance was observed in different positions of film (Fig. 3-1(a)). Lower thickness corresponding to high resistance was observed around the vertical edges of film.

.

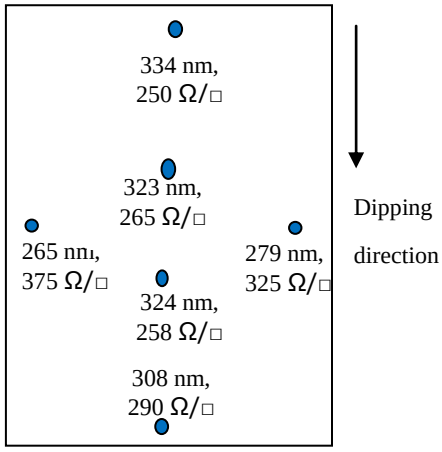

(a)

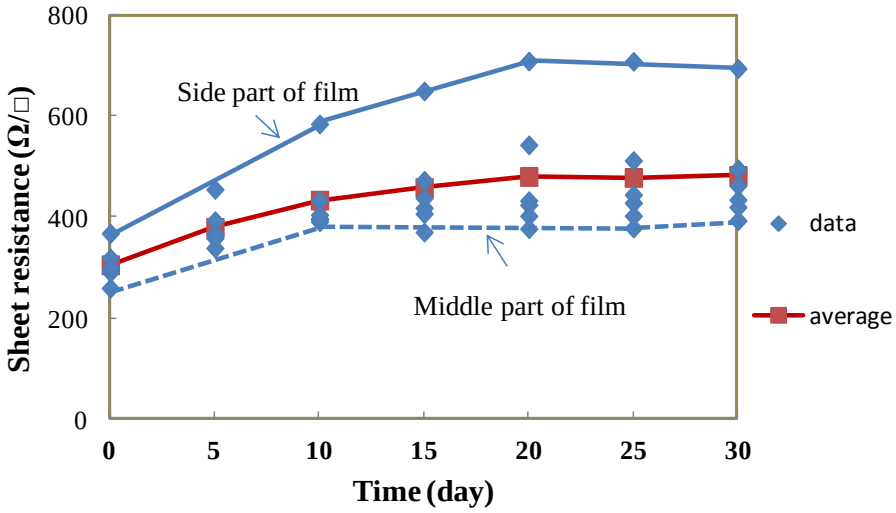

(b)

Fig. 4-1 (a) Position dependent thickness variation of thin film. **(b)** Investigation of electrical stability in ambient condition of film annealed at 450 °C for 30 min. Resistance value was taken from different random positions of film.

Fig. 4-1(b) shows the stability of sheet resistance for film s-450-30 with all value taken at different positions. The lower thickness part of film (approx. 260 nm), which has high resistance (375 Ω/□) and also very unstable in further days. For that, we selected the middle part only for stability measurement and further investigation.

In general, the n type conductivity of an intrinsic ZnO mainly is due to Zn interstitial and oxygen vacancy [2-5]. The electrical properties of doped ZnO films strongly depend on carrier concentration, which depends on contributions from Al^{3+} on substitutional sites of Zn^{2+} ions, Al and Zn interstitial atoms, and oxygen vacancies. In this experiment, the intrinsic ZnO film (after vacuum annealing at 500 °C for 30 min) showed the resistivity of 8.0 x 10^{-2} Ωcm. After doping with 1.18 at% Al, the electrical resistivity was found to decrease of 5.7 x 10^{-3}Ωcm. This is due to increased carrier concentration as a result of substitution of Zn^{2+} by Al^{3+} and formation of one extra free

electron from each Al atom which act as carrier.

Resistivity of AZO films were measured as function of different annealing temperatures and durations which is shown in Table 4-1. As shown in this table, film annealed at low temperature (450 °C) in different durations have higher resistivity (7.53 x 10^{-3} - 7.86 x 10^{-3} Ωcm), which is slightly decreased to the range of 5.73 x 10^{-3} – 6.09 x 10^{-3} Ωcm, when the temperature was 500 °C. It increased again for 550 °C and 600 °C in duration of 30 to 120 min. In general, by increasing the annealing temperature, the resistivity of AZO films decreases since the grain boundaries and crystal deficiencies of the film were decreased. On the other hand, increased resistance may be attributed from decreased mobility of carriers caused by further formation of aluminum compounds at the grain boundaries [6]. It also shows that annealing duration did not cause any major effect on resistivity. The minimum resistivity value obtained in this work is very close to the reported in the literature [7], although it can be further improved through introduction of ensuring controlled atmosphere during annealing.

Table 4-1 Resistivity of AZO thin film in different annealing temperature and duration

Annealing duration (min)	Resistivity (x 10^{-3} Ωcm) annealing temperature			
	450 °C	500 °C	550 °C	600 °C
30	7.74	5.73	6.18	6.16
60	7.86	6.09	6.54	6.27
120	7.53	5.8	6.78	6.66

The resistivity stability of these films in ambient condition which is the focusing point in this experiment are shown in Fig. 4-2(a) – (d). It clearly indicates that annealing temperature plays an important role on environmental stability. In this experiment, high temperature annealed film showed better stability compared to low temperature annealed film. As an example, the resistivity of the film annealed at 450 °C for 30 min is gradually increased by 62% after 30 days. The increasing tendency reduced to 35%, 27% and 9% for 500, 550 and 600 °C, respectively, in film, which was annealed for 30 min. The fast increasing rate in first few days was observed, which will be explained in the following part through DH test. The lowest increased resistivity was found (only 4%) for the film developed by using high temperature (600 °C) with longer duration (120 min). To further investigate the mechanism of stability improvement, detailed experiments were carried out for two samples : s-450-30 and s-600-120. These films showed the highest (62%) and lowest (4%) increasing tendency of resistivity in this experiment.

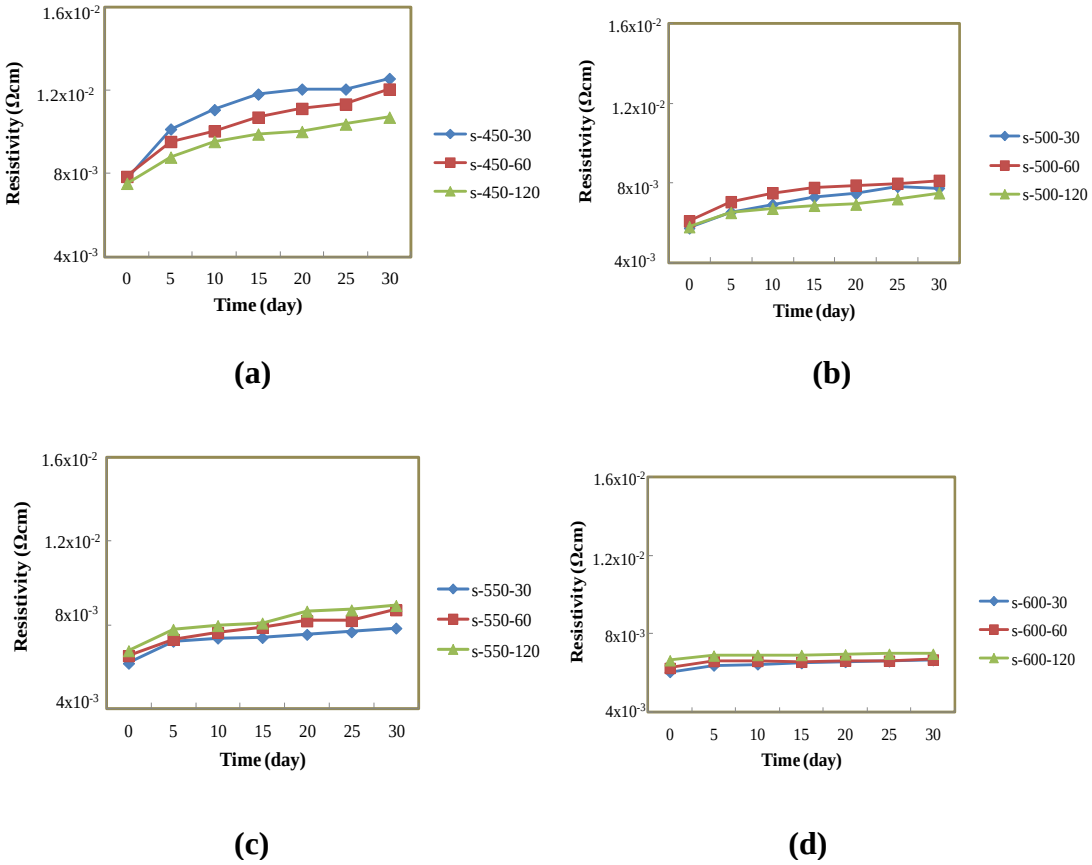

Fig. 4-2 Investigation of electrical stability in ambient condition of AZO film annealed at **a)** 450 °C **b)** 500 °C **c)** 550 °C and **d)** 600 °C in different duration.

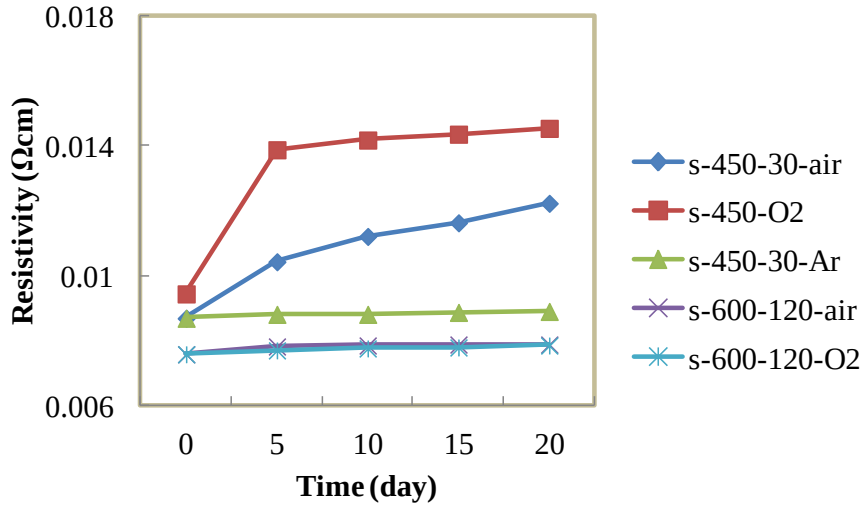

Fig.4-3 Investigation of resistivity of AZO films stored in different atmosphere

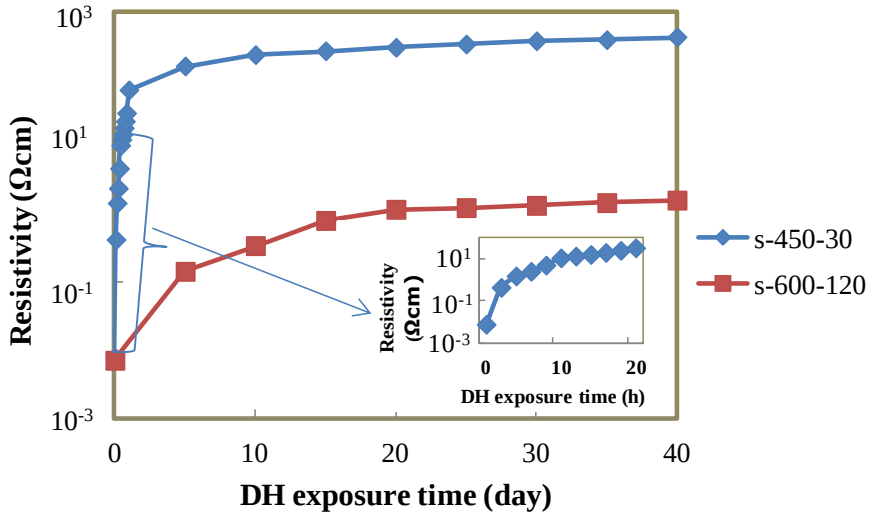

Fig. 4-4 Investigation of degradation rate of resistivity under damp heat condition (85 °C and 85% RH).

The degradation behavior of AZO films under different storage atmosphere at room temperature is shown in Fig. 4-3. s-450-30 film has high increasing rate of resistivity, when it was stored in oxygen and air atmosphere. But in argon atmosphere, where, oxygen and water molecule are deficient, this film showed very stable resistivity. On the other hand, the film annealed at high temperature did not increase its resistivity

in air and even in the oxygen atmosphere.

The damp heat stability of selected AZO films of s-450-30 and s-600-120 was also investigated in this work. The variation of resistivity with exposure time to the DH treatment is shown in Fig. 4-4. The degradation on the DH test appears the same nature as that for the ambient condition i.e. the film annealed at high temperature showed better stability compared to the film annealed at low temperature. The topmost surface oxidation appears fast, within a few hours of air exposure, while the whole film is affected after a longer period due to possible diffusion of oxygen.

The structural properties of as-deposited films (s-450-30 and s-600-120) were studied by X-ray diffractometry as revealed in Fig. 4-5. Both films were polycrystalline in nature having hexagonal wurtzite structure with a preferred orientation along c-axis (002) plane. The other orientations along (100) and (101) planes were also observed, however, their intensities were very weak compared to that of the (002) peak. Scherer's formula was employed to estimate the crystallite size of the films from (002) peak, which was found to be 18 and 21 nm for s-450-30 and s-600-120, respectively. The increased intensity of (002) peak and increase of crystallite size for s-600-120 thin film can be attributed to the high temperature annealing along with longer duration, which indicates improvement of crystallinity of the AZO film.

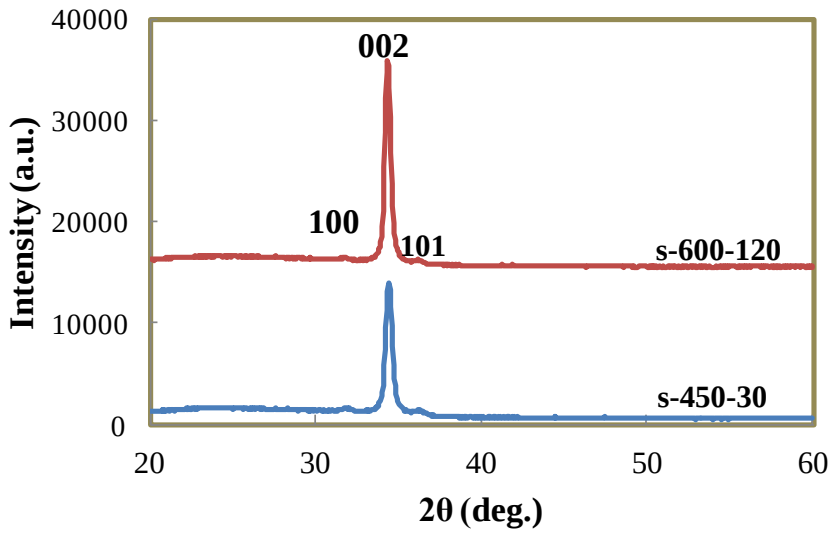

Fig. 4-5 XRD diffraction patterns of s-450-30 and s-600-120 films

Field emission scanning electron micrographs (FESEMs) as given in Fig. 4-6 show the microstructure of the AZO films. It shows that both films are consisting of many spherical shaped crystalline particles. The grains more or less cover the substrate surface uniformity. The film s-450-30 have relatively smooth surface, whereas, s-600-120 film shows the granular structure. Thus, high temperature annealing seems to have modified the surface morphology. It also shows that, after high temperature annealing, the surface cluster size of AZO film was increased and diameter value of s-450-30 and s-600-120 is estimated as the value of 28 and 35 nm respectively. This can be considered as the coalescence process induced at high temperature thermal treatment.

On the other hand, point or dislocation defect and Al interstitial may form on the film annealed at low temperature which may reduce the stability. The healing of defects by high temperature annealing also reduces these trap states thereby the grain size increases and improving the crystallinity of the film which coincides with the XRD result [8].

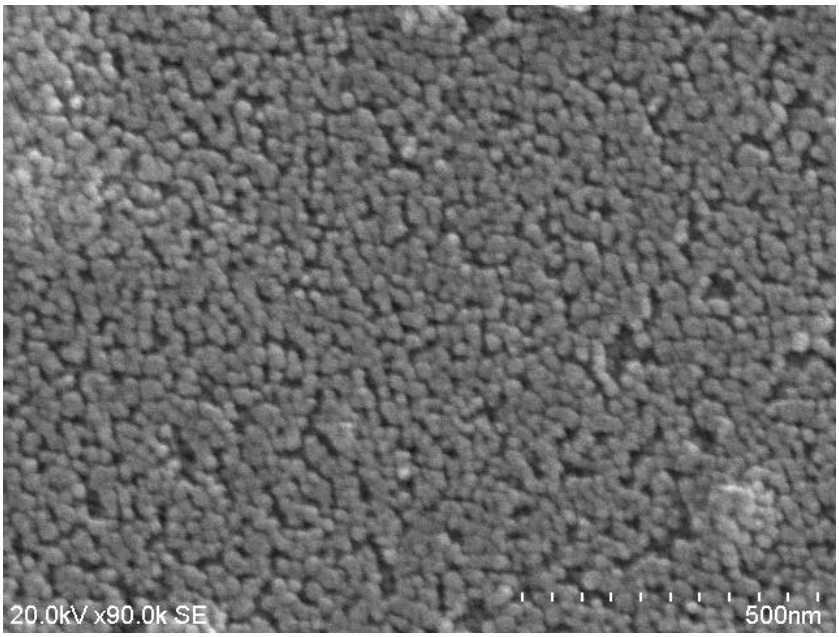

(a)

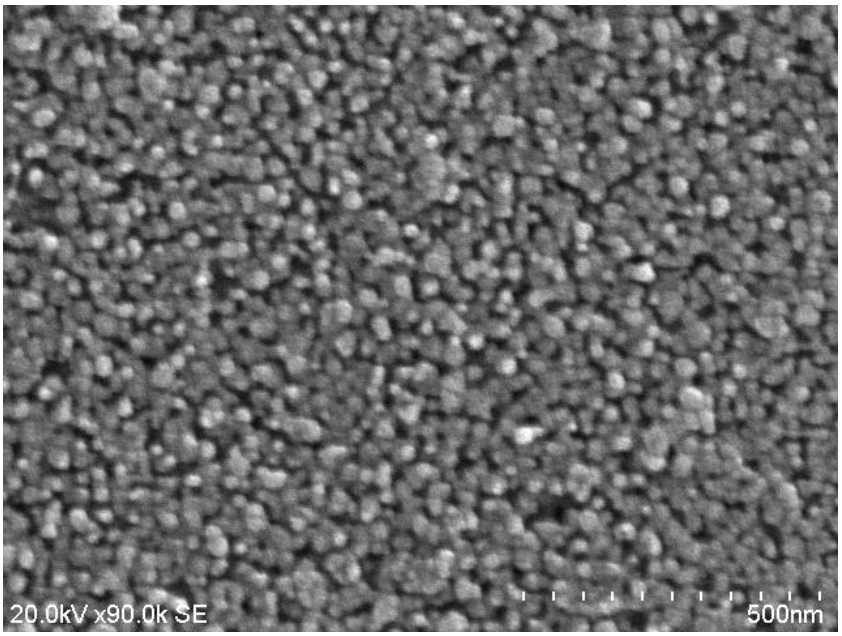

(b)

Fig. 4-6 Surface morphology of **(a)** s-450-30 and **(b)** s-600-120

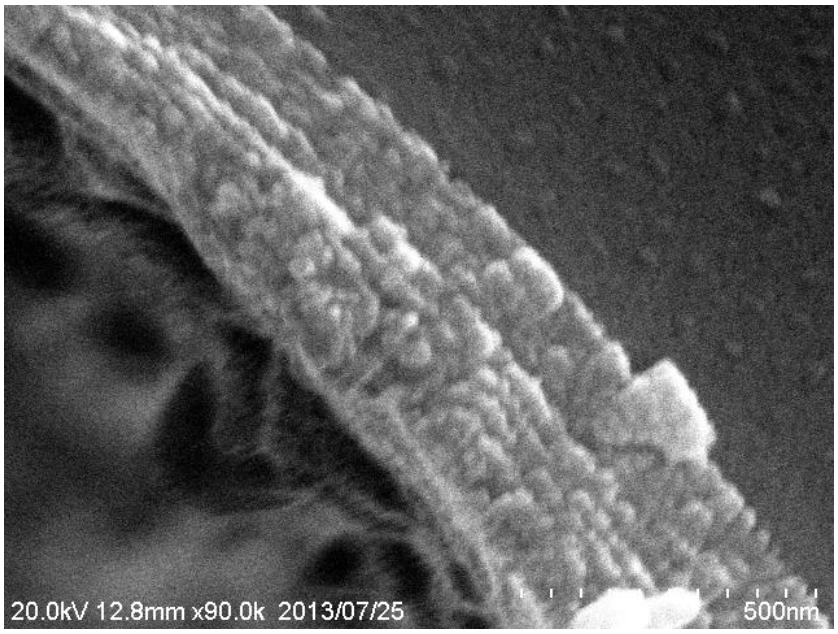

Fig. 4-7 Cross sectional view of AZO thin film

Fig. 4-7 shows the cross sectional view of AZO thin film, where, different layers are clearly observed. As the film developed by dip coating method using 10 times coating, it makes different layers of film with granular structure.

As shown in Fig. 4-8, the average transmittance in the visible light wavelength range of 300 – 800 nm is approximately 85 - 90% for both s-450-30 and s-600-120 films. The absorption edge was shifted towards shorter wavelength at increased annealing temperature and duration. It indicates the increase of carrier concentration of the thin film after annealing at high temperature with longer duration. The absorption coefficient data was used to determine optical band gap, E_g. The band gap energy measured by Tauc plot (inset of Fig. 4-8) increases from 3.37 for s-450-30 to 3.48 eV for s-600-120, respectively. Typically the blue shift of the absorption edge of the AZO films is associated with an increase of the carrier concentration blocking the lowest states in the conduction band, known as the Burstein-Moss effect [9-10].

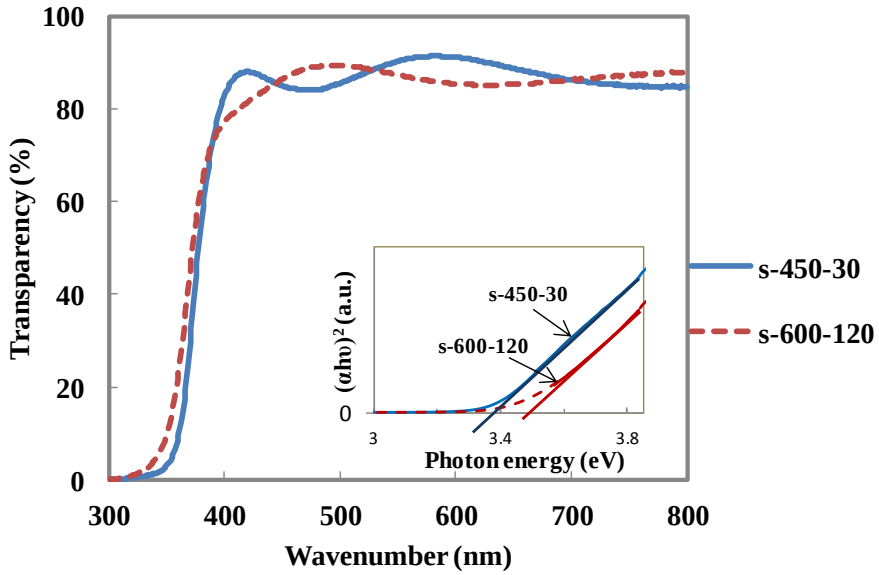

Fig. 4-8 Optical transmission spectra of s-450-30 and s-600-120 along with Tauc plot (inset) for measurement of band gap energy.

4.3 Discussion

The reduction of the resistivity of AZO thin film after doping and heat treatment can be ascribed thorough creation of free electron by doping and formation of oxygen vacancies by annealing in vacuum atmosphere. The degradation of resistivity in air was observed which is mainly due to the adsorption of oxygen and/or water molecule to the film. This is considered due to the result of investigation of film stored in different atmosphere. The resistivity did not change significantly in oxygen or water molecule deficient atmosphere (argon). It is also reported that adsorbed oxygen or water molecule reduce the carrier concentration and increase the resistivity [11]. In this experiment, the electrical stability is improved when the film was annealed at high temperature. Improved electrical stability in ambient or damp heat conditions can be explained from different viewpoints such as through variation on structural, surface

morphological and elemental concentration on surface of the film.

Generally, for the thin film with good crystallinity and large crystallite sizes, the total area of grain boundaries per volume is relatively small. So, the total diffusion area of oxygen to enter the film is reduced, which may one of the reasons of weaker oxidation on the film and so that enhancement of stability may take place. During high temperature annealing, crystallites gain enough diffusion/activation energy and small crystallites migrate to relatively equilibrium sites in the crystal lattice and coalescences of grains results larger crystallite size. In this experiment, slightly larger crystallite size and higher intensity of (002) peak was found in film annealed at high temperature, which indicates the improvement of crystallinity. Beside this, point or dislocation defect and Al interstitial may be remained on the film annealed at low temperature, which may influence on stability. The healing of defects by high temperature annealing also reduces these trap states thereby improving the crystallinity [8]. The result implies that beside the film crystallinity, other basis may cause to improve the stability. Another possibility is that the chemisorbed-oxygen permeation into film through surface of film. The film which contains small grains with cracks or voids on surface can easily adsorb oxygen and/or water molecule from atmosphere. Reduction of these voids can be one of the solutions to improve the stability. It is reported that by increasing the post-heating temperature, the grains become denser and larger which can be considered the coalescence process induced from thermal treatment [12]. Our FESEM result also showed the increased grain size in film at high temperature annealed film, which may reduce the rate of oxygen and/or water molecule diffusion to the film.

Third possibility may come from the formation of self passivation layer on AZO film. To clarify this, chemical states and atomic concentrations were determined

by XPS. Fig. 4-9(a) and (b) represents the total measured depth profiles, where the sharp change around 1200 s indicates the end of thin film (apprx. 300 nm observed by surface profilometer). The surface state of AZO films for Zn $2p_{3/2}$, O1s and Al2s are indicated in Fig. 4-10. Although no significant differences are observed between s-450-30 and s-600-120, either in Zn $2p_{3/2}$ or O1s, there is a slight shift (~ 0.1 eV for Zn $2p_{3/2}$) toward lower binding energy for higher annealing temperatures, probably due to the variation of chemical environments of Zn elements [13]. The binding energy of O1s of two samples is shown in Fig. 4-10 (b) and (c). The broadening of oxygen spectrum is found to be composed of two components located around 530 eV and 531.5 eV, respectively, from fitting results of these spectra. The low BE component is ascribed to covalently bonded oxygen in ZnO structure (lattice oxygen) binding with Zn or substitutional Al, while the high BE is attributed to the adsorbed oxygen. The higher binding energy is usually attributed to chemisorbed or dissociated oxygen or OH species on the surface of the AZO thin film, such as adsorbed H_2O or O_2 [14]. The vacuum annealing was performed by mechanical pump (5 Pa). So, in this condition, a part of adsorbed oxygen may still exist on the surface of film. Fig. 4-10(d) shows the Al2s state on surface for two samples. The Al 2s for s-450-30 shows very low intensity, whereas, comparatively strong peak with high intensity was observed in film s-600-120. The binding energy for s-600-120 was 118.9 eV which assures the presence of comparatively large amount of Al^{3+} on surface.

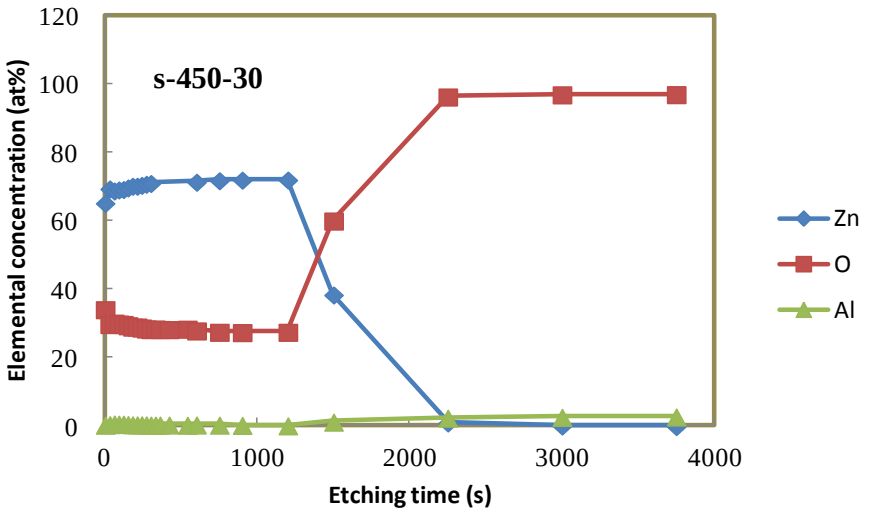

(a)

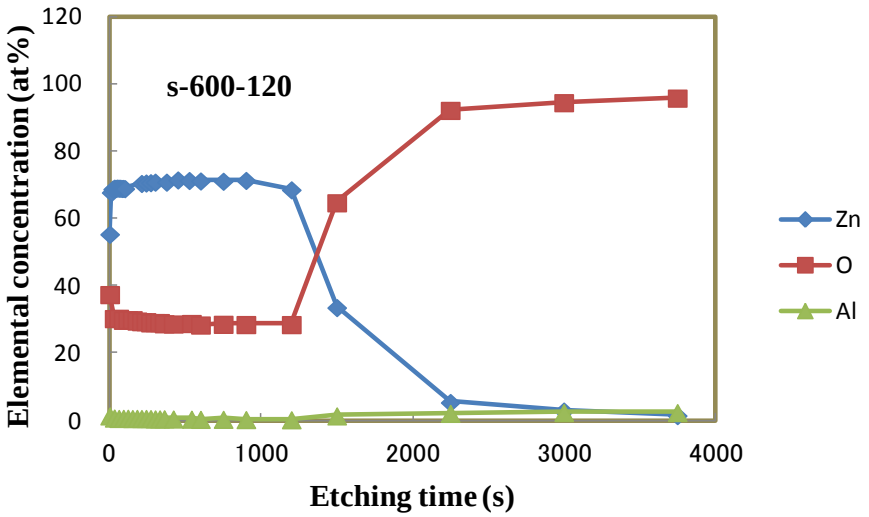

(b)

Fig. 4-9 Total depth profile of **(a)** s-450-30 and **(b)** s-600-120

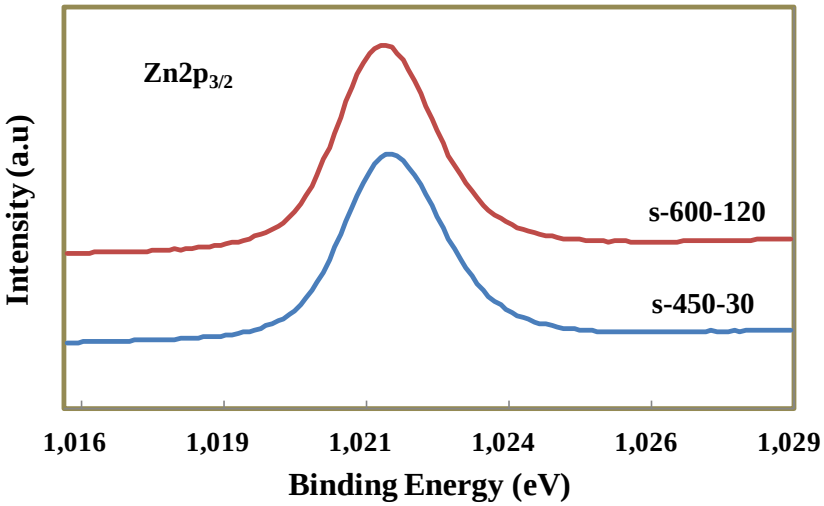
Zn2p3/2
s-600-120
s-450-30
Intensity (a.u)
1,016
1,019
1,021
1,024
1,026
1,029
Binding Energy (eV)

(a)

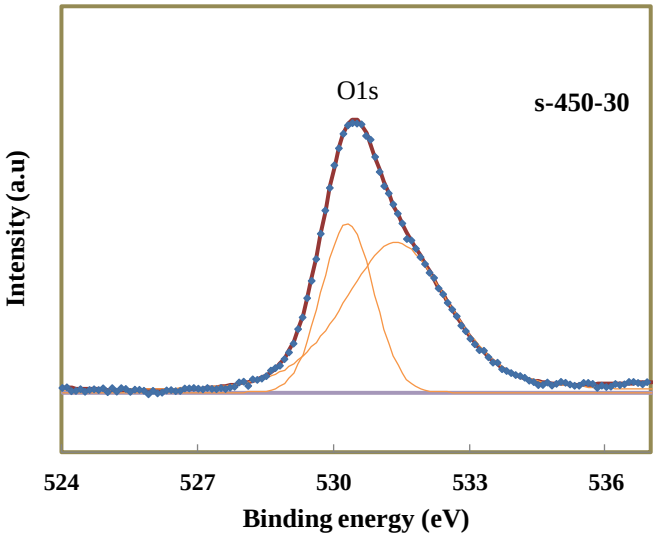
O1s
s-450-30
Intensity (a.u)
524
527
530
533
536
Binding energy (eV)

(b)

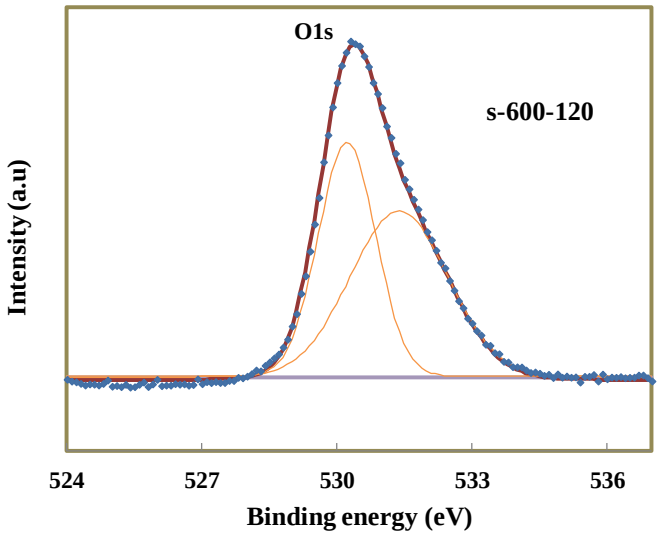

(c)

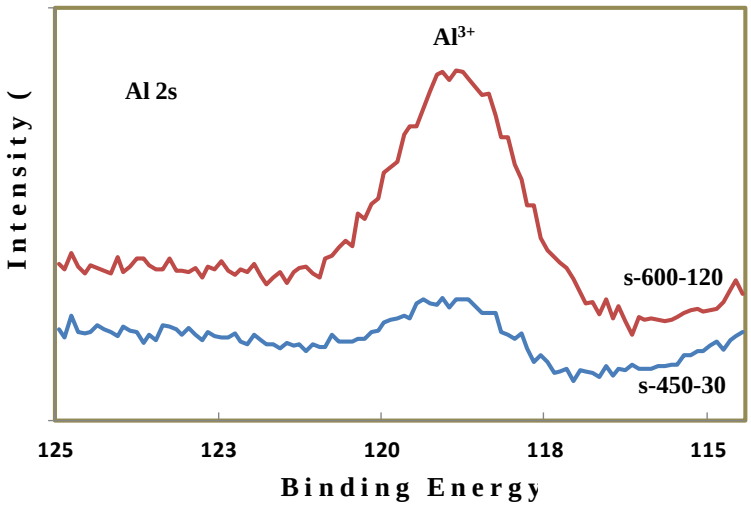

(d)

Fig. 4-10 Surface states of AZO films: **(a)** Zn $2p_{3/2}$ **(b)** O 1s for s-450-30, **(c)** O 1s for s-600-120 and **(d)** Al2s

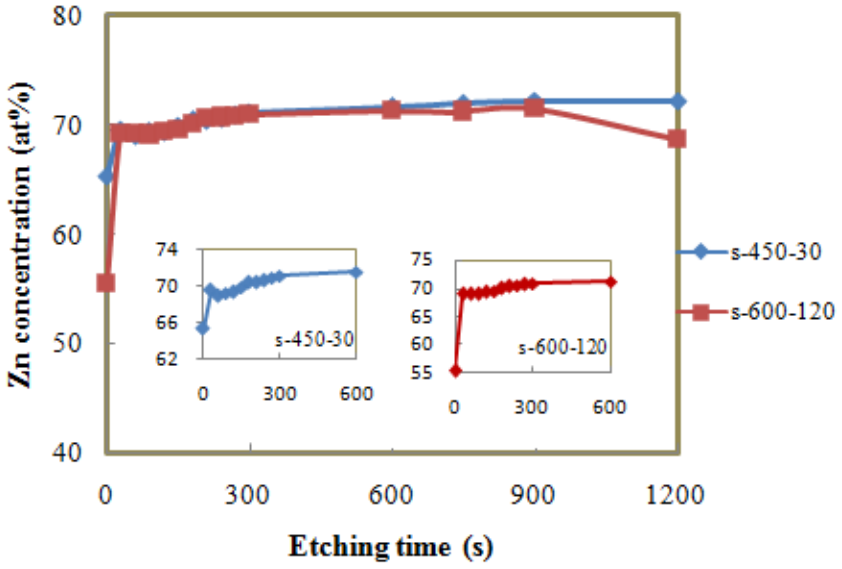
Zn concentration (at%)
Etching time (s)
s-450-30
s-600-120
s-450-30
s-600-120

(a)

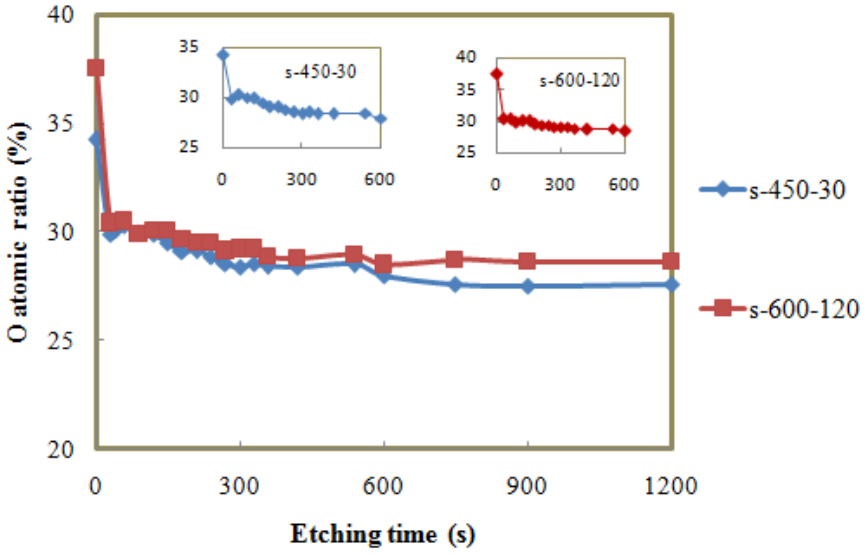
O atomic ratio (%)
Etching time (s)
s-450-30
s-600-120
s-450-30
s-600-120

(b)

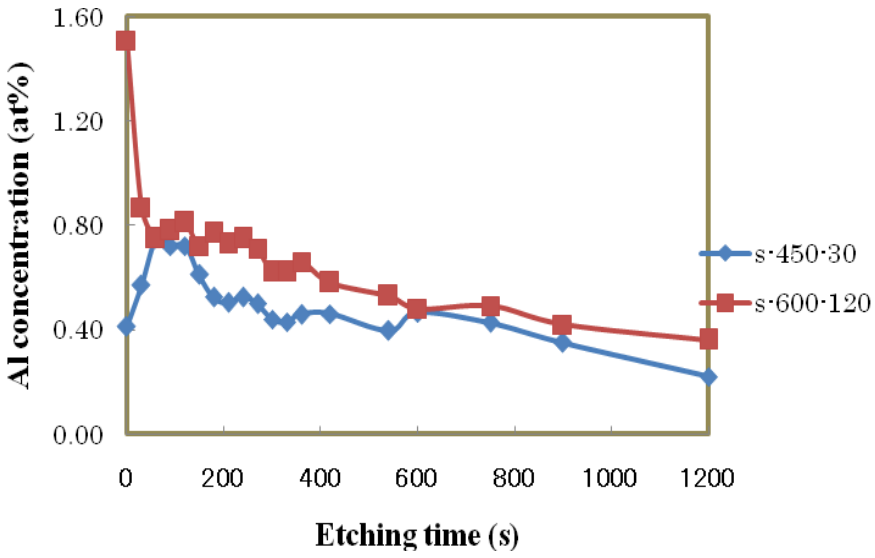

(c)

Fig. 4-11 XPS depth profile of AZO film for **(a)** Zn **(b)** O and **(c)** Al

Elemental concentrations were determined from Zn $2p_{3/2}$, O1s and Al2s XPS peak areas using Savitzky-Golay smoothing, background removal by Shirley method and sensitivity factors provided by spectrometer manufacturer. Fig. 4-11 summarizes the quantitative XPS analysis of the spectra of Zn $2p_{3/2}$, O 1s and Al 2s for two films as a function of the sputtering time. It has two different phases: outer surface and bulk film. There appeared in Fig. 4-11(a), the sharp decrease of Zn concentration (65.3 to 55.4 at%) at the outermost surface for the s-600-120 film, compared to modest decrease for the s-450-30 film. On the other hand, O concentration was comparatively high on surface of s-600-120 film (4-11(b)). Al concentration was also high on surface in s-600-120 film, whereas, it showed very low value on the surface of s-450-30 (4-11(c)). These two values of O and Al are also explained in the surface state graph in Fig. 4-10(d), where, it clearly indicated that the film s-600-120 consists more Al^{3+} on surface. By considering this, formation of ultrathin Al_2O_3 and/or $ZnAl_2O_4$ layer or islands is

considered at the topmost surface of film s-600-120, though not detected by x-ray diffractometry. It is well known that aluminum oxide generally acts as good moisture barrier and may form at high temperature [15-16]. There has been much research into the development of protective alumina layer. P. Poodt and co-workers have deposited Al_2O_3 films by atomic-layer deposition (ALD) for solar cell passivation [17]. A. Illiberi et al. have also used ALD technique for deposition of thin (25-75 nm) Al_2O_3 layer on indium-doped ZnO film as moisture barrier and effectively enhanced the stability of the electrical and structural properties of the films in harsh environment (85 °C and 85% RH) [16]. On the other hand, self formation of protective Al_2O_3 scales on alloys at high temperature has explained in several reports. Wood et al. have described the formation of γ-Al_2O_3 on Ni-Al alloys at 600 °C. The γ-Al_2O_3 was formed as a healing layer beneath the outer reaction products NiO and $NiAl_2O_4$ [18-19]. γ-Al_2O_3 has also been reported on Fe-based alumina-forming alloys in the temperature range 700-900 °C. Above 900 °C, the oxide contains more α-Al_2O_3 than γ-Al_2O_3. As, in this experiment, we used high temperature (600 °C) for annealing, it is considered the formation of Al_2O_3 layer or islands on surface that can repel atmospheric oxygen to enter the film.

An oscillating variation of Zn, O and Al were observed in near surface of films in Fig. 4-11. The concave/convex curve in Zn was opposite to those in Al and O. This suggests formation of different phases of Al such as Al_2O_3 and/or $ZnAl_2O_4$. The degradation of atomic concentration of O and Al in bulk film may the effect of film preparing method of sol-gel. The film was made by 10 different layers each time dried at 450 °C for 5 min in air. Though drying time was for very short duration, it can make different layers of AZO film which has already shown by FESEM picture in the previous section which influence to concentrate elements more towards surface. Beside

this, the film may feel tensile stress against the glass substrate during annealing as the thermal expansion coefficient is about twice larger for the latter. It is thus possible that the film feels position-dependent stress according to the distance from the substrate interface and the topmost surface, which could exhibit oscillating tendency. The strain-induced precipitates should ripen during annealing via atomic diffusion. As a result, the phase stability may be affected by the aluminum oxides and/or zinc aluminate precipitates near the surface.

4.4 Conclusion

AZO film was prepared by sol-gel method followed by vacuum annealing as function of different temperature and duration. The electrical stability of these films was investigated in air over time. The films annealed at low temperature showed large increase of the resistance, whereas, those at high temperature remained stable. The damp heat test also assured the same increasing tendency of films. Improved crystallinity and surface morphology with large grain size of film may assist to obtain better environmental stability in ambient or damp heat condition for film prepared by using high annealing temperature and longer duration. Beside this, the formation of an ultrathin Al_2O_3 layer or islands was considered due to the presence of Al^{3+} on surface with high intensity, which may protect the AZO film from oxidation and enhance the stability.

References

[1] H. Tong, Z. Deng, Z. Liu, C. Huang, J. Huang, H. Lan, C. Wang and Y. Cao, Applied surface science, **257** (2011) 4906-4911

[2] W. Yang et al., Thin Solid Films, **519** (2010) 31–36

[3] T.S. Biorheim and E.A. Kotomin, Journal of Physical Chemistry Letters, **5** (2014) 4238-4242

[4] A. Kushwaha, H. Tyagi and M. Aslam, AIP advances, **3** (2013) 042110

[5] B.N. Pawar, S.R. Jadkar and M.G. Takwale, Journal of physics and chemistry of solids, **66** (2005) 1779-1782

[6] Y.M. Hu, C.W. Lin and J.C.A. Huang, Thin Solid Films, **497** (2006) 130-134

[7] M. Zhu, H. Huang, J. Gong, C. Sun and X. Jiang, Journal of Applied Physics, **102** (2007) 043106

[8] S.Y. Choi, K. Chow and S.J. Kim, International Journal of Advanced Research in Electrical Electronics and Instrumentation Engineering, **2** (12) (2013)

[9] E. Burstein, Physical Review, **93** (1954) 632

[10] T.S. Moss, Proceedings of the Physical Society of London, **67** (1954) 775

[11] T. Miyata, Y. Ohtani, T. Kuboi and T. Minami, Thin Solid Films, **516** (2008) 1354 - 1358

[12] M. C. Jun and J.H. Koh, Journal of Electrical Engineering & Technology, **8 (**2013) 163-167

[13] W. Yang et al. Thin Solid Films, **519** (2010) 31–36

[14] T.P. Rao and M.C.S. Kumar, Journal of Crystallization process and technology, **2** (2012) 72-79

[15] S.K. Sampath and J.F. Cordaro, Journal of the American Ceramic Society, **81**

(1998) 649-654

[16] A. Illiberi, R. Scherpenborg, M. Theelen, P. Poodt and F. Roozeboom, Journal of Vacuum Science & Technology A, **31** (2013) 061504

[17] P. Poodt, A. Lankhorst, F. Roozeboom, K. Spee, D. Maas and A. Vermeer, Advanced Materials, **22** (2010) 3564-3567

[18] G.C. Wood and B. Chattopadhay, Corrosion Science, **10** (1970) 471-480

[19] G.C. Wood and B. Chattopadhay, Oxidation of Metals, **2** (1970) 373-399

Chapter 5

Sol-gel and RF sputtered AZO thin films: Analysis of oxidation kinetics in harsh environment

5.1 Introduction

The structural, optical and electrical properties of Al-doped ZnO (AZO) thin film prepared by sol-gel method was explained by many factors such as doping concentration and different annealing condition: temperature, duration, atmosphere. The experimental results indicate that environmental stability is not satisfactory of sol-gel prepared AZO film. Some steps were approached for improving the stability by using high temperature and using thin metal film as protective layer.

There are many reports have been published related to the damp heat stability of doped ZnO thin film prepared by sputtering method and improvement was considered by different approaches: increasing thickness or giving protective layer [1-5]. But the increasing rate of resistivity in reported sputtered film was much smaller compared to film prepared by sol-gel method found in our experiment. However, very few reports involved [6-8] other film preparing method to explain the changes of the electrical conductivity after exposing in air.

In this section, a comparative study of AZO thin films prepared by sol-gel and RF sputtering was investigated and the mechanism of film degradation during exposing in air was also investigated by studying structural, optical and surface morphology of films.

To prepare AZO thin film by sol-gel method, doping concentration i.e., Al/(Al+Zn) atomic ratio was fixed at 1.18 at% and coating number varied between 1 and 20, according to required thickness. For Sputtered film, sputtering time was increased from 30 to 120 min and thickness was measured by surface profilometer. All of these films prepared by both methods were annealed under pure hydrogen atmosphere for 30 min.

5.2 Results

The relationship between AZO film thickness with number of coating for sol-gel and sputtering time for sputtering method is shown in Fig. 5-1(a), where, thickness was increased almost linearly with coating number or sputtering time.

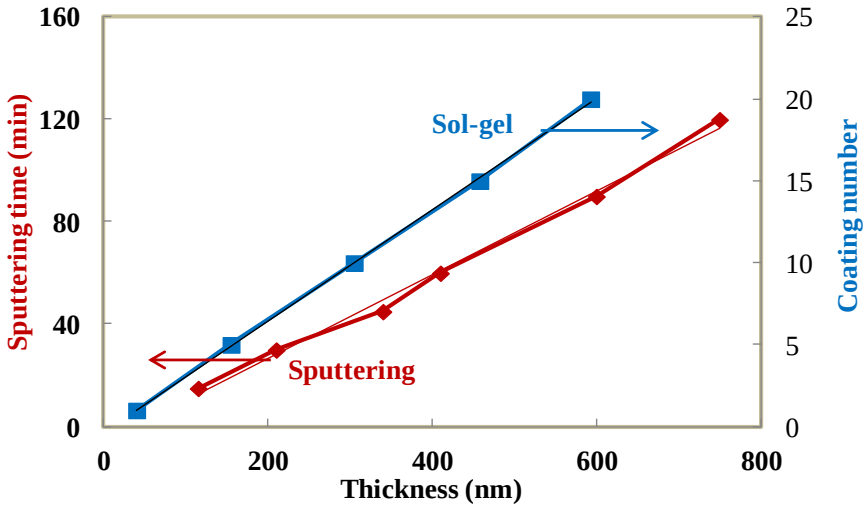

(a)

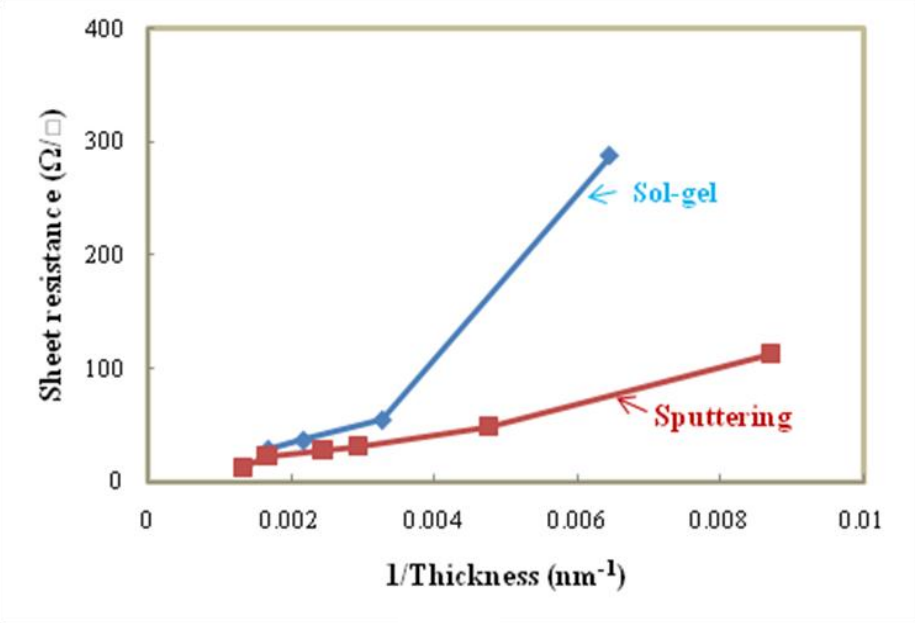

(b)

Fig. 5-1 (a) Dependence of thickness with coating number in sol-gel and sputtering time in sputtering method and **(b)** Sheet resistance vs. 1/thickness curve for sol-gel and sputtered AZO film

Fig. 5-1(b) reveals the nature of sheet resistance in terms of thickness of thin film which satisfies the theoretical tendency except that of low thickness (155 nm (1/T= 0.006)) for sol-gel method. This may be due to the formation of large amount of defects or islands in that film.

For further experiments some selected samples (sol-gel : 300 and 460 nm; Sputtering : 410 and 750 nm) were characterized in details. At first, EDX analysis was carried out to check the incorporation of doping material in the film. The result showed that Al concentration e.i. Al/(Al+Zn) atomic ratio was almost similar in films prepared by both method and that is around 3.6 at% (3.71 at% for sol-gel and 3.6 at% for sputtering). This result might be slightly overestimated due to the Al contents in the

glass substrate. Long-term stability of devices under typical environment conditions is very important which has led to recent widespread interest in damp heat treatment. In this work, comparative study of sol-gel and sputtered AZO thin films in terms of stability in ambient and damp heat condition was conducted which is shown in Fig. 5-2 (a) and (b), respectively. It reveals that sputtered film has very good stability (almost 100%) in ambient condition, whereas, sol-gel prepared films sheet resistance gradually increased after exposing in air. The same behavior was observed for harsh environment with different increasing rate. For damp heat (DH) test, AZO films were stored at 85 °C and 85% relative humidity (RH) for several days. As the films were exposed to humidity, the increased resistance indicates the possible oxygen and/or water molecule diffusion to the film that confines the number of free electrons. In addition, the energetic oxygen bombardment disturbs the grain growth, which results in an increase of the area of grain boundaries in ZnO thin film. This makes the scattering at the boundaries and decreases the carrier mobility [9-10], thus decreased the conductivity of AZO film. The decreasing trend of carrier concentration and mobility for sol-gel prepared film (300 nm) is shown in Table 5-1, where carrier concentration sharply decreased within first 12 h from 2.18 x 10^{20} to 1.92 x 10^{19} cm^{-3} and then 1.25 x 10^{19} cm^{-3} in next 12 h, where mobility decreased from 17.3 to 6.2 cm^2/Vs in first 12 h and it showed very low value of 1.9 cm^2/Vs after 24 h. On the other hand, carrier concentration and Hall mobility decreased from 4.69 x 10^{20} to 2.79 x 10^{20} cm^{-3} and 14.5 to 8.3 cm^2/Vs, respectively, after 30 days in sputtered AZO film (410 nm), which is very small compared to sol-gel prepared film.

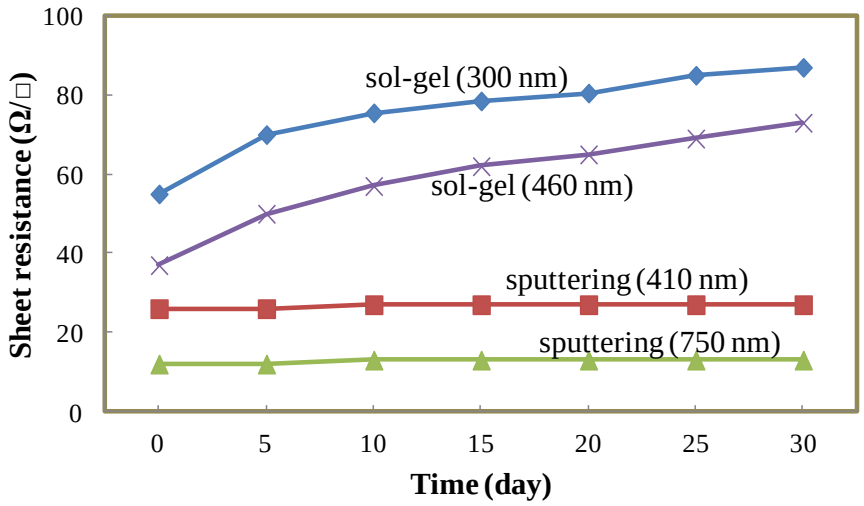

(a)

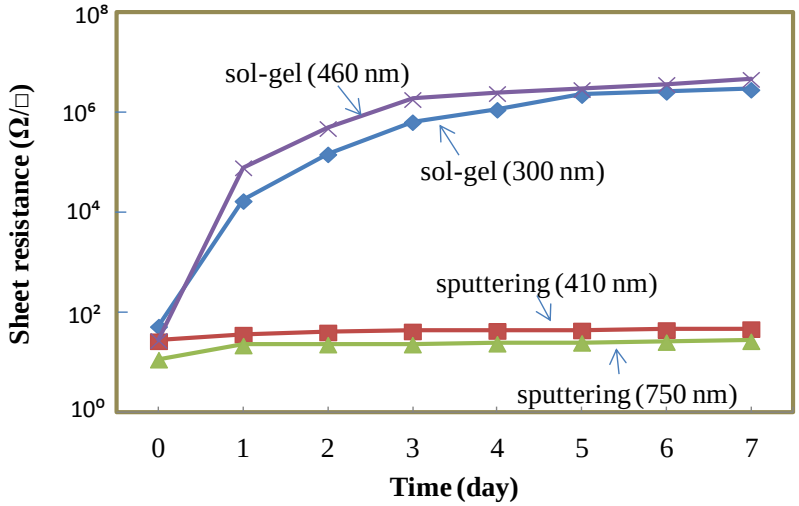

(b)

Fig. 5-2 Electrical stability of AZO thin films prepared by sol-gel and sputtering method in **(a)** ambient and **(b)** damp-heat (DH) condition

(b)

Table 5-1 Electrical properties of AZO film prepared by sol-gel and sputtering in different measuring time at DH test

Preparing method	**Thickness (nm)**	**Measuring time**	**Sheet resistance (Ω/□)**	**Carrier concentration (cm^{-3})**	**Hall mobility (cm^2/Vs)**
Sol-gel	300	As prepared	55	2.18×10^{20}	17.3
		After 12 h	1800	1.92×10^{19}	6.2
		After 24 h	8810	1.25×10^{19}	1.9
Sputtering	410	As prepared	28	4.69×10^{20}	14.5
		After 30 days	67	2.79×10^{20}	8.3

The crystalline structure and orientation of AZO films are shown in Fig. 5-3. No Al_2O_3 phase has been evidenced in the XRD pattern, which implies that Al atoms substitute Zn atoms in the hexagonal lattice and Al ions may occupy the interstitial sites of ZnO or probably Al_2O_3 segregates to the non-crystalline region in grain boundaries [11-12]. Sol-gel prepared film demonstrated a strong Bragg peak along the (002) plane indicating that the AZO films are highly oriented perpendicular (c-axis) to the substrate and two weaker peak in orientation of (100) and (101). On the other hand, for sputtered film, a transition of the growth mode from (002) vertical to (110) lateral growth is clearly observed due to the crystalline evolution during sputtering. It shows the peak intensity of (110) plane increased with increasing the thickness of film. But all peaks of sputtered AZO films are weaker compared to (002) plane of sol-gel prepared film. The

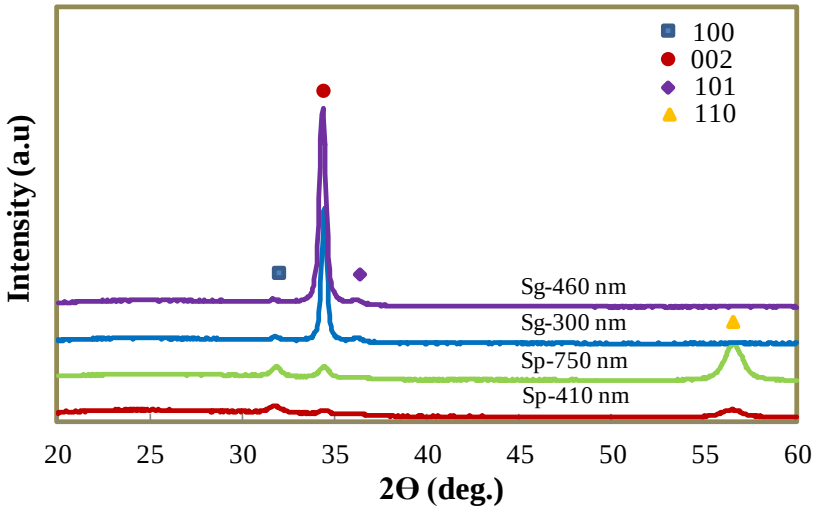

Fig. 5-3 XRD curve of AZO films. (Here, Sg and Sp indicates sol-gel and sputtering, respectively)

crystallite size was estimated from the full-width at half-maximum (FWHM) of different peaks by Scherrer's equation and the estimated crystallite size of sol-gel and sputtered AZO films are shown in Table 5-2.

Figure 5-4 depicts optical transmittance of AZO films deposited by different methods in different thickness. All of the films exhibited a good transmittance in the visible region. As the wavelength of incident light decreased to ultraviolet region, the transmittance of the AZO films decreased with a sharp fundamental absorption edge at around 380 nm of wavelength. It is also shown that the absorption edge was shifted towards shorter wavelength for sputtered AZO films. Optical band gap calculated from the transmittance data by using Tauc plot which is shown in Table 5-2.

Table 5-2 Structural and optical parameters of AZO films

Name	Plane	FWHM (deg.)	Crystallite size D (nm)	Band gap energy (eV)
Sp-410 nm	100	0.572	14	3.5
	002	0.479	17	
	110	0.857	9	
Sp-750 nm	100	0.518	16	3.6
	002	0.511	15	
	110	0.858	10	
Sg-300 nm	002	0.374	22	3.4
Sg-460 nm	002	0.405	20	3.4

It showed that the optical band gap of AZO film was increased for sputtered film compared to sol-gel prepared film. Typically the blue shift of the absorption edge or increased band gap energy of the AZO films is associated with an increase of the carrier concentration blocking the lowest states in the conduction band, well known as the Burstein-Moss effect [13-16]. We also found that an increase of carrier concentration of sputtered film in Table 5-1.

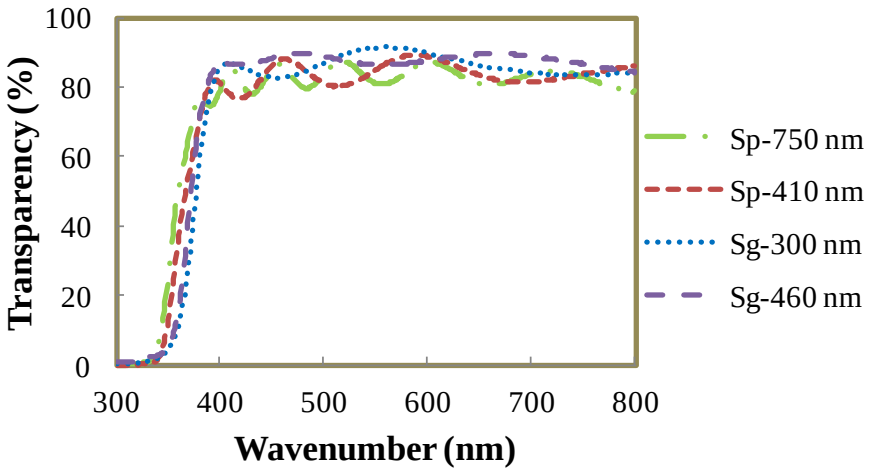

Fig. 5-4 Optical transparency of AZO films (Here, Sg and Sp indicates sol-gel and sputtering, respectively)

Fig. 5-5 shows the micrographs of the surface topography of AZO thin films grown at different methods. The morphology of the film deposited by sputtering method becomes more compact compare to sol-gel prepared film where surface was not smooth and contains many cracks or voids which can be easy path for oxygen and/or water molecule. On the other hand, the smooth surface of film prepared by sputtering was found with possibly grain coalescence. Due to this grain coalescence, an aggregate structure is formed and the films consist of a dense array of grains without discernible boundaries are observed which was also observed by A.H. Jayatissa [17]. The surface morphology was also investigated after damp heat test which is shown in Fig. 5-6. The surface was very rough in sol-gel prepared film whereas smooth surface was found in sputtered AZO film which relates to the DH stability test.

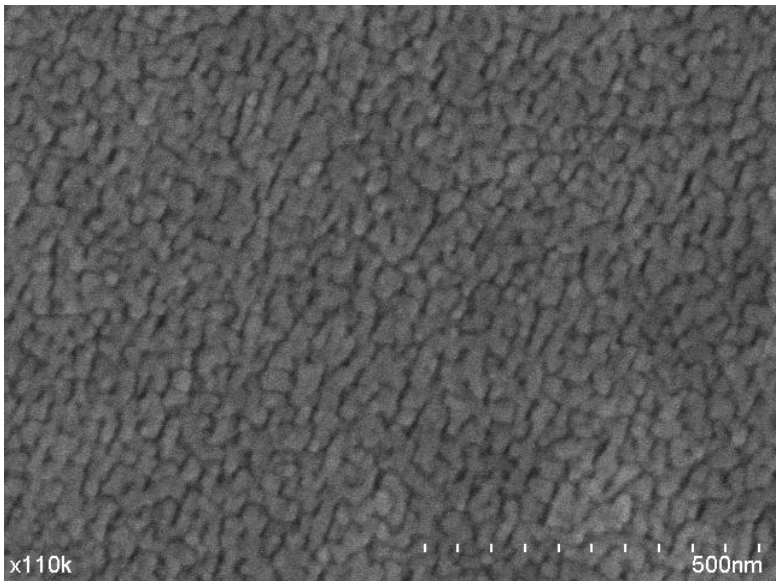

(a)

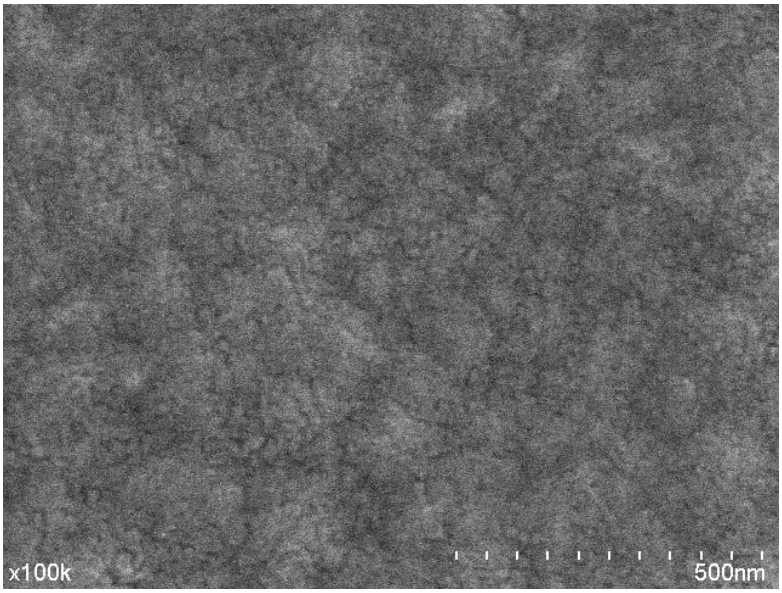

(b)

Fig. 5-5 Surface morphology of as prepared film prepared by **(a)** sol-gel (300 nm) and **(b)** sputtering (410 nm)

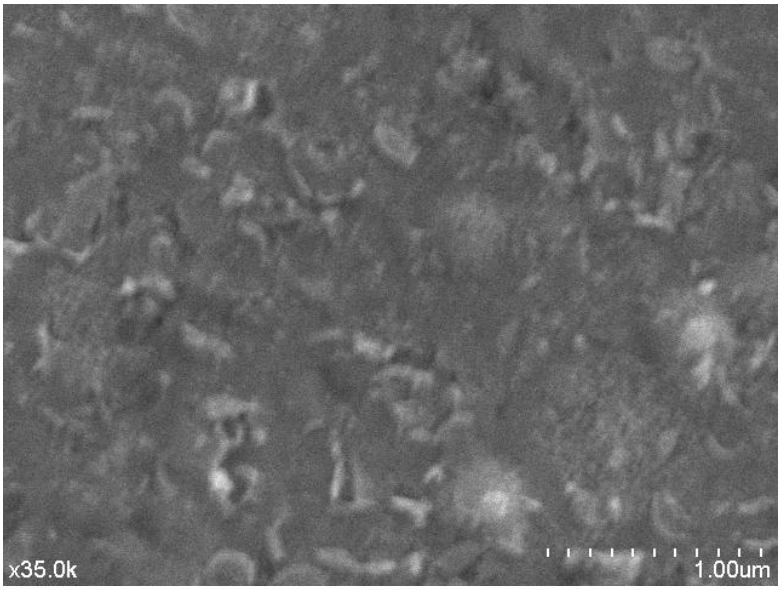

(a)

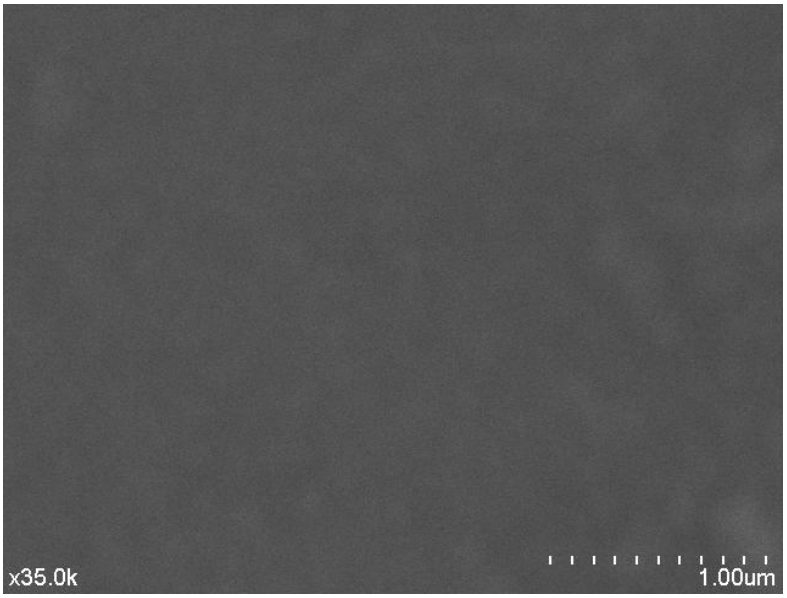

(b)

Fig. 5-6 Surface morphology of AZO film prepared by **(a)** sol-gel (300 nm) and **(b)** sputtering (410 nm) after damp heat test

5.3 Discussion

A comparative study of AZO film prepared by sol-gel and sputtering was investigated. AZO is n-type semiconductor, where free carriers are generated by the substitution of Al for Zn by doping, interstitial Zn atoms, oxygen annihilation and formation of oxygen vacancies by hydrogen annealing etc. The sheet resistance decreased in film with increased thickness. For thin layered film, stress may happen on AZO film which leads lots of defects. So, free electrons may trapped by this defects [18]. Another reason can be formation of islands of materials with lot of insulating gaps for very thin layers. This gaps can be minimized in increased thickness of film [19]. For very thin layered film, sol-gel prepared film showed higher resistance compared to sputtered film which indicates the large amount of defects or islands in that film.

It should be noted that the observed electrical stability of AZO thin films in ambient and harsh environment was strongly dependent on the deposition method used; the electrical stability of AZO thin films prepared by sol-gel was always lower than that in sputtered films. Degradation of electrical properties (resistance, carrier concentration and Hall mobility) indicate the possible oxygen and water molecule diffusion to the film that decrease the number of free electrons and reduction of the mobility by grain boundary scattering thus the resistance increases. Sputtered AZO film showed much better stability compared to sol-gel prepared film. Three possible factors are considered as the reason of large difference in electrical stability. First, it can be originated from impurity. So, adjacent to the structural, optical and morphological comparison, presence of impurity in film was also investigated by XPS. But no appreciable changes between films were observed and also no impurity was found in them which can be shown in Fig. 5-7. So impurity might not be the cause of increased sheet resistance here.

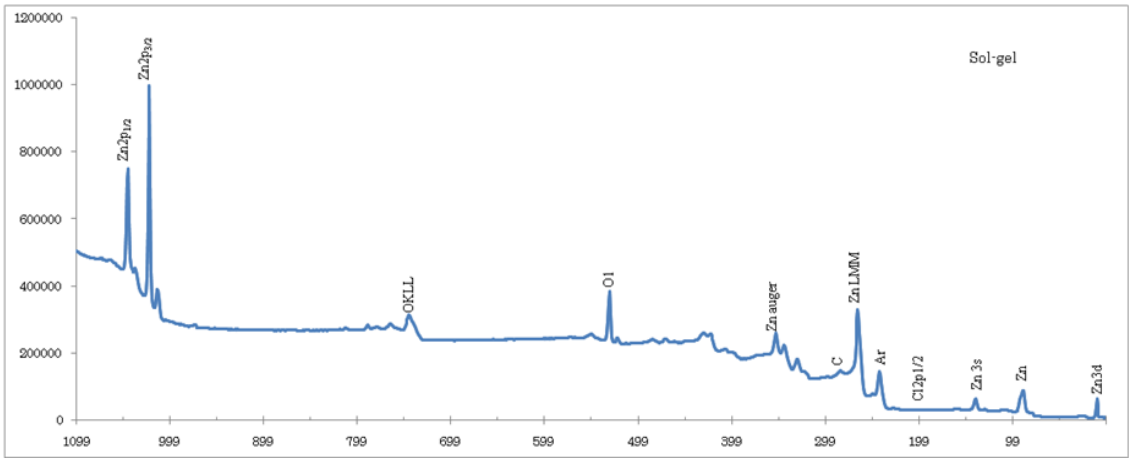

(a)

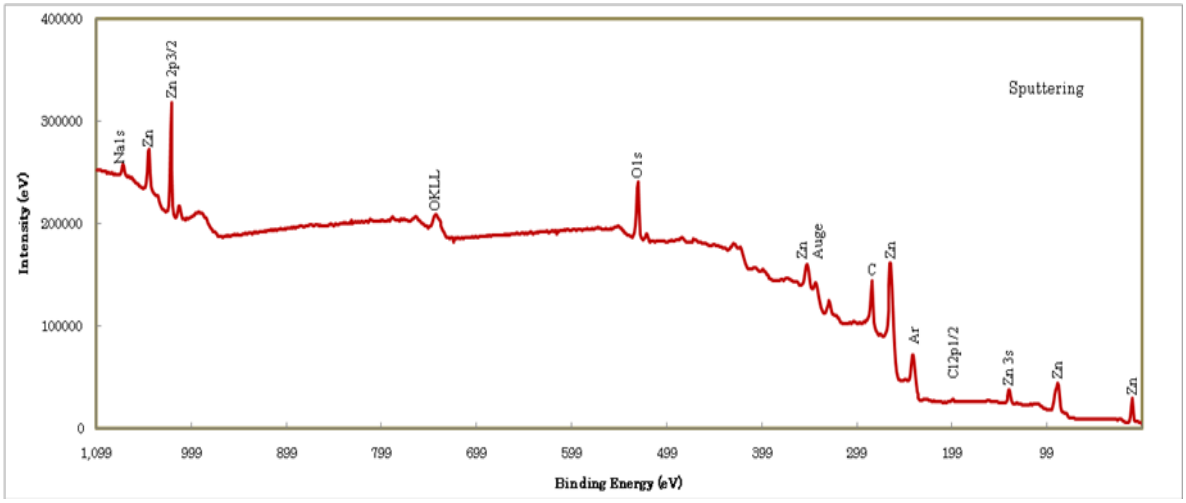

(b)

Fig. 5-7 XPS wide scan of AZO film prepared by **(a)** sol-gel (300 nm) and **(b)** sputtering (410 nm)

Second, surface structure can affect the stability of AZO film. Rough surface with many cracks or voids was found in sol-gel prepared AZO film. This voids look like the preferable diffusion path for oxygen and/or water molecule to enter the film and increase the resistance. Comparatively smooth surface with no cracks was observed in sputtered film. The tightly packed or high dense surface protects oxygen and/or water molecule to the film and make it stable. Surface of sputtered film remains smooth even after damp heat test, whereas, very rough surface was observed in sol-gel prepared film. In this manner, it can be said that, surface morphology is an important factor for improving the electrical stability. Next, the third possibility is that the high quality (110) orientation mounted in sputtered film may protest oxygen permeation into film. In our XRD curve, different preferential orientation was found from the film prepared by two different methods. Sol-gel prepared film have c-axis preferred orientation with (002) plane, whereas, sputtered film showed (110) plane as preferred orientation. Fig. 5-2 displayed the environmental stability of these films, where high degradation of electrical properties was observed in sol-gel prepared film which is highly oriented to (002) plane. On the other hand, this degradation reduces and improved stability was found for sputtered films which are highly oriented to the (110) direction. In this manner, it can be assumed that crystal orientation can lead to change of environmental stability of AZO thin film.

5.4 Summery

In summary, a comparative study was introduced between sol-gel and sputtered thin film of Al-doped ZnO. Structural, optical, electrical properties and environmental stability was the major investigated part. Environmental stability was investigated in ambient and damp heat (85 °C and 85% RH) condition. Sol-gel prepared AZO film showed very unstable electrical properties under air exposure, whereas, the degradation rate reduced significantly in sputtered film. Oxygen and water molecule diffusion to the film through the diffusion path found in sol-gel prepared film can be one of the probable reasons of this degradation, whereas, very compact and high dense surface was found in sputtered film which protects from further oxidation and improved the stability. Beside this, (110) orientation also enhanced the electrical stability in ambient and harsh environment.

References

[1] T. Minami, T. Miyata and J. Nomoto, IOP conference Series: Materials Science and Engineering, **34** (2012) 012001

[2] T.L. Chen, D.S. Ghosh, D. Krautz, S. Cheylan and V. Pruneri, Applied Physics Letters, **99** (2011) 093302

[3] T. Minami, Thin solid films, **516** (2008) 1314-1321

[4] F.J. Pem, L. Mansfield, C. DeHat, S.K. Glick, F. Yan and R. Noufi, IEEE photovoltaic specialists conference (PVSC 37), June 19-24, (2011)

[5] Z. Zhan, J. Zhang, Q. Zheng, D. Pan, J. Huang, F. Huang and Z. Lin, Crystal growth & design, **11** 1 (2011)

[6] A. Illiberi, R. Scherpenborg, M. Theelen and P. Poodt, Journal of vacuum science and technology A, **31** (2013) 061504

[7] T. Miyata, Y. Ohtani, T. Kuboi, T. Minami, Thin Solid Films, **516** (2008) 1354-1358

[8] J. Steinhausera, S. Meyera, M. Schwaba, S. Faya, C. Ballif, U. Kroll and D. Borrello, Thin Solid Films, **520** (2011) 558-562

[9] K. Wasa, I. Kanno, H. Kotera, "Handbook of Sputter Deposition Technology: Fundamentals and Applications for functional thin films, nano-materials and MEMS", 2nd edition, Elsevier, (2012) 395, ISBN: 978-1437734843

[10] H. Zhu, E. Bunte, J. Hupkes, H. Siekmann and S.M. Huang, Thin Solid Films, **517** (2009) 3161-3166

[11] H. Park et al., Thin Solid Films, **519** (2011) 6910-6915

[12] Z. Deng, C. Huang, J. Huang, M. Wang, H. He, H. Wang and Y. Cao, Journal of Materials Science: Materials in Electronics, **21** (2010) 1030-1035

[13] M. Grundmann, “The physics of semiconductors”, Springer, (2006), ISBN: 978-3-540-25370-9

[14] S. Mondal, S.R. Bhattacharyya and P. Mitra, Indian Academy of Sciences, **80** (2013) 315-326

[15] J.G. Lu, Z.Z. Ye, Y.J. Zeng, L.P. Zhu, L. Wang, J. Yuan and B.H. Zhao, Journal of Applied Physics, **100** (2006) 073714

[16] F.H. Wang, C.F. Yang, J.C. Liou and I.C. Chen, Journal of Nanmaterials, **2014** (2014) 857614

[17] A.H. Jayatissa, A.M. Soleimanppour and Y. Hao, Advanced Materials Research, **383-390** (2012) 4073 – 4078

[18] B.Z. Dong and G.J. Fang, Journal of Applied Physics, **101** (2007) 033713

[19] M.S. Shinde, P.B. Ahirrao, I.J. Patil and R.S. Patil, Indian Journal of Pune & Applied Physics, **50** (2012) 657-669

Chapter 6

Possible mechanism and related factors

6.1 Introduction

As mentioned in Chapter 5, the change of crystal orientation in AZO thin film plays a very important role for reducing the degradation of electrical properties. It revealed that high quality (110) crystal orientation formation in sputtered AZO film may one of the reasons to improve the environmental stability. To further clarify the role of crystal orientation, another method is proposed here for preparing AZO thin films combining sputtering and sol-gel method in a film. The film preparation method is divided into two sections as follows:

(1) 400 nm AZO film coated by sputtering on glass substrate

(2) 300 nm AZO film coated by sol-gel method on the sputtered film

After coating by sputtering and sol-gel, AZO film of 700 nm was annealed at 450 °C for 30 min under hydrogen atmosphere. The aim of this work is to grow a-oriented grains on the film by sputtering which will act as nuclei for the growth of the over-layered AZO film deposited by sol-gel. Role of RF power on structural, electrical and optical

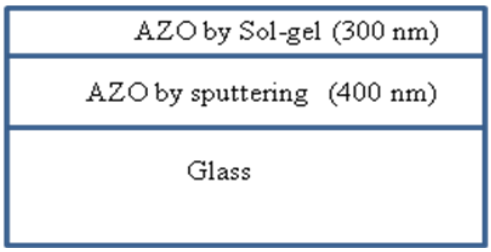

Fig. 6-1 Basic structure of AZO thin film prepared using sputtering and sol-gel method

Properties of AZO film and its environmental stability are also investigated in this chapter. Though the previous chapter showed that AZO film prepared by sputtering method is comparatively stable in humid atmosphere, it is still an unsolved problem due to low increasing rate of sheet resistance. In this point of view, improvement of environmental stability of AZO thin film prepared by sputtering is also attempted in this chapter, which will follow the mechanism of stability improvement described in previous chapters.

6.2 Results and Discussion

6.2.1 Role of crystal orientation on stability

Fig. 6-2(a) reveals the X-ray diffraction pattern of the films which have prepared using three different stages: 1) only sputtered film (without annealing) 2) sputtered + sol-gel film (without annealing) and 3) after annealing in hydrogen atmosphere of this film. The film prepared using sputtering and combination of both sputtering and sol-gel will be signified as Sp and Sp+Sg, respectively, in the following part. The resultant data of sol-gel prepared film (explained in previous chapter) which will be mentioned as Sg will also use to compare with the new film. Previous research investigations revealed that the AZO films normally are polycrystalline and have a hexagonal wurtzite crystal structure. The measured XRD pattern in Fig. 6-2 demonstrates that sputtered AZO film has weak diffraction peak intensity of (100) and (002). Comparatively strong peak of (110) is the main attention in this experiment, which should act as nuclei for further deposition of AZO film by sol-gel method. After deposing 300 nm AZO film on this sputtered film of 400 nm by sol-gel method, preferred orientation turned into (002) orientation and (110) peak was also observed with high intensity which was absent on the film prepared by only sol-gel method (Fig.

6-3(a)). The Sg film has strong (002) diffraction peak in the 2Θ region from 34.43° which showed full-width half-maximum (FWHM) of 0.374°. On the other hand, XRD pattern of Sp+Sg film ensures the presence of both orientations (002) and (110) at 2Θ of 34.451° and 56.648°. FWHM of these peaks are 0.455° and 0.879° respectively. As, Sp+Sg film has (110) plane, which is not in film Sg, it is thought that, a-plane (110) is grown by sputtering at specified condition, which acts as nuclei for the growth of the over-layered AZO film deposited by sol-gel.

Optical transmittance spectra of the Sg and Sp+Sg films in the wavelength from 300 to 800 nm are compared in Fig. 6-3(b). All of the films exhibited a good transmittance in the visible region. The damp heat test result (Fig. 6-4) shows the improved stability of Sp+Sg film under harsh condition. S. Y. Myong and K.S. Lim also found the improved stability in hydrogenated ZnO film in highly oriented to the (110) direction [1]. Improved electrical stability in the Al-doped ZnO thin film transistor was also originated in film with preferred orientation along the non-polar direction which was described by C.H. Ahn [2]. According to this point of view, it can be concluded that degradation of electrical properties can be controlled by the change of preferred crystal orientation.

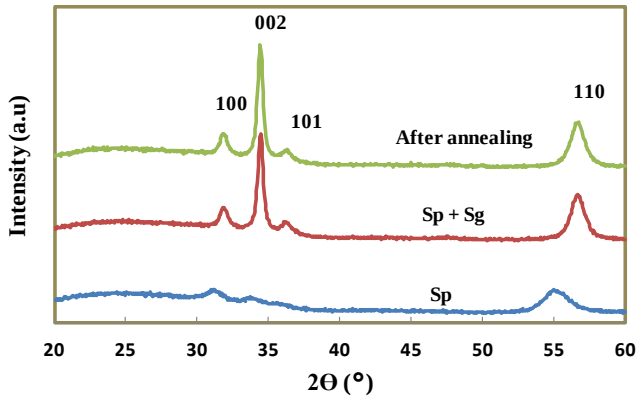

Fig. 6-2 Crystal orientation in different step of AZO film prepared by combining both sputtering and sol-gel method.

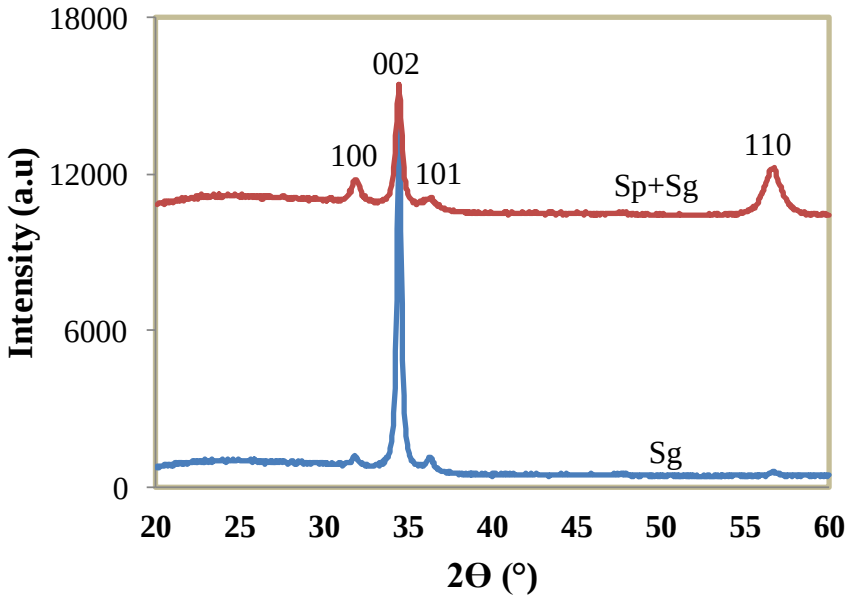

(a)

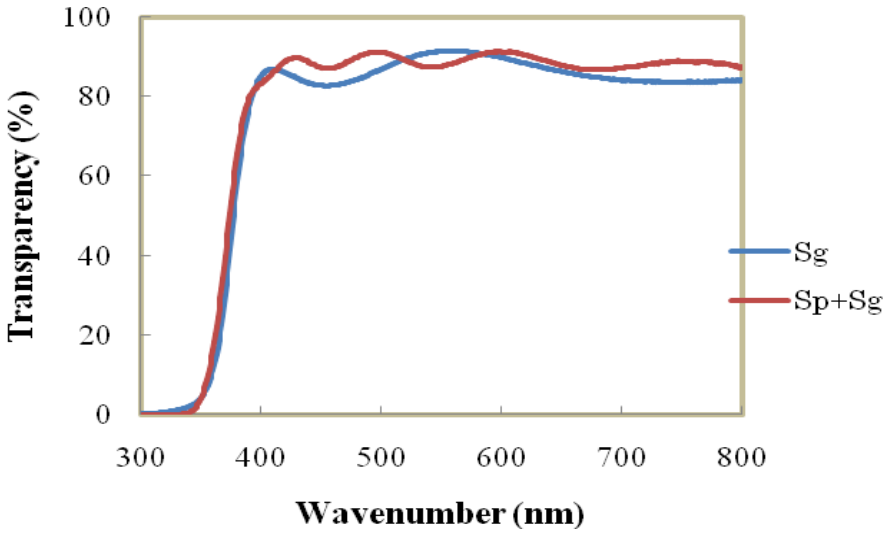

(b)

Fig. 6-3(a) Crystal orientation and **(b)** transparency of AZO film prepared by only sol-gel (Sg) and combining sputtering and sol-gel method (Sp+Sg)

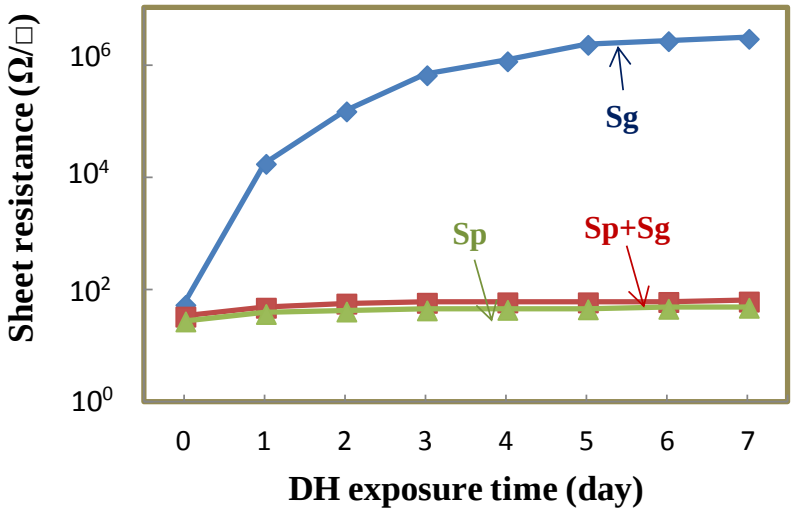

Fig. 6-4 Damp heat test result of Sg, Sp and Sp+Sg films

6.2.2 Effect of RF power on AZO film

Effect of sputtering power on AZO films structural, optical and electrical properties have been explained before in many research publications [3-5]. In this work, stability as well as different properties has investigated as function of RF power. AZO thin films were deposited by RF sputtering on soda lime glass substrate. For the deposition of AZO thin films, the vacuum chamber was first evacuated with a base pressure of 1 x 10^{-3} Pa. The glass substrates with a dimension of 48 x 28 mm were cleaned ultrasonically in acetone followed by drying in air. Argon flow (30 sccm) was used as the sputtering gas. Oxygen flow was also kept at 30 sccm. The RF input power was fixed at 100 W. The deposition was held at room temperature. The effect of the change in the RF power on the structural, optical, electrical and environmental stability on AZO thin films was investigated. The AZO films were deposited at different RF powers of 25, 50, 100 and 140 W for 1 h for each of the samples.

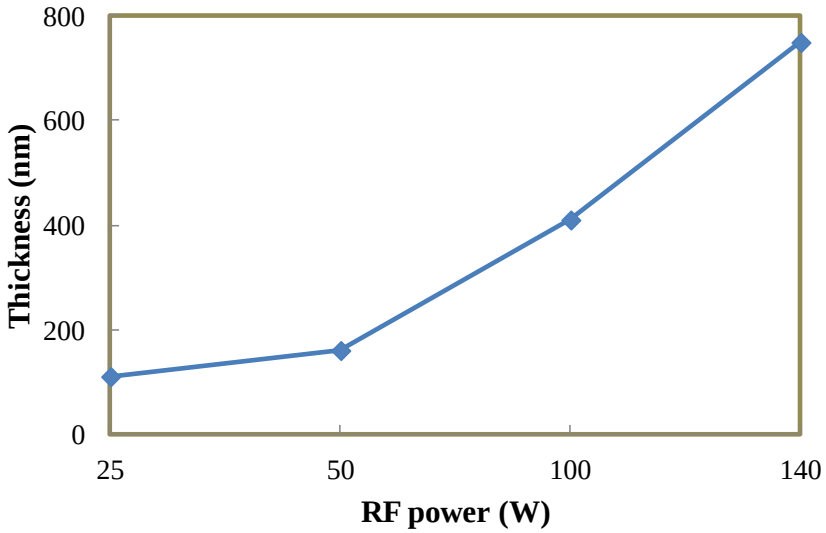

Fig. 6-5 Thickness of AZO films as a function of the RF power

Fig. 6-5 shows the increased thickness of the prepared films with the increasing RF powers, indicating the proportionality of the number of atoms sputtered from the target to the applied RF power.

Fig. 6-6 shows the XRD spectra for the prepared AZO films. All of the AZO film contains (002) diffraction peak with the crystal c-axis perpendicular to the substrate in XRD patterns. At low RF power (25 W), the peak intensity was very low which increased at 50 W. When the RF power increased to 100 W, the growth of other peaks (100) and (110) are observed. AZO films deposited at high RF power (100 W and 140 W) have the dominant (110) diffraction peak with the crystal a-axis parallel to the substrate in XRD patterns. Therefore, crystal orientation may change at different RF power. The crystallite size was measured by Scherer's equation which is shown in Table 6-1.

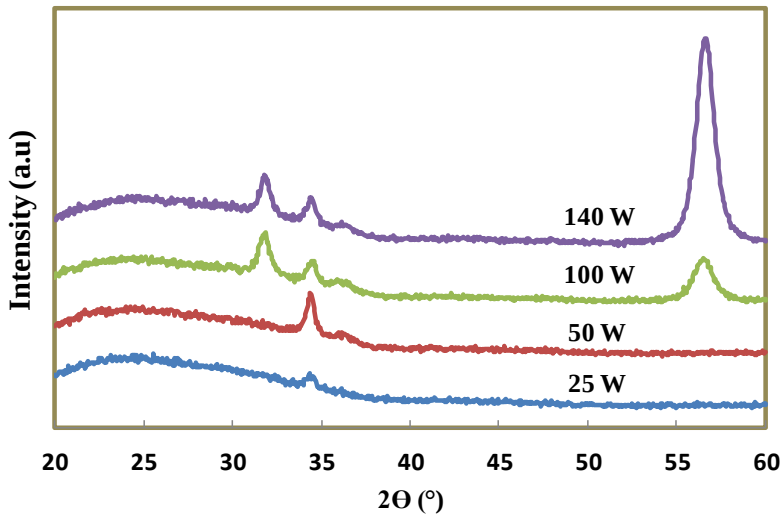

Fig. 6-6 X-ray diffraction patterns of AZO films prepared using different RF power

Table 6-1 Structural parameters of AZO films as functions of RF power

Power (W)	**Plane**	**2T (deg.)**	**FWHM (deg.)**	**Crystallite size D(nm)**
25	002	34.501	0.305	27
50	002	34.354	0.435	19
100	002	34.457	0.479	17
	110	56.452	0.857	09
140	002	34.451	0.455	18
	110	56.648	0.879	10

EDX analysis was carried out to check the concentration of Zn, O and Al in AZO films. This compositional analysis was taken by selecting only the film component. It shows that Zn/O was very low as 0.15 in the film prepared by using low power (25 W). It increases with increasing power and reached almost 1, when RF power was 140 W. Fig. 6-7 shows the energy-dispersive X-ray spectrum of AZO films. The spectrum reveals the presence of Zn, O and Al elements in the deposited films. Beside these, the silicon signal appears which comes from substrate. Trace amount of other elements were also detected in the sample. The intensity of Si signal was very high for 100 W films, which reduced with increasing power and almost negligible for film prepared using high power (140 W). This may be due to the variation of thickness of film with changing of power which is shown in previous section.

Table 6-2 EDX report of AZO films deposited using different power

Power (W)	Zn (at%)	O (at%)	Al (at%)
25	13.0	84.5	1.7
50	26.8	71.7	1.4
100	39.5	58.4	2.0
140	45.1	50.4	4.4

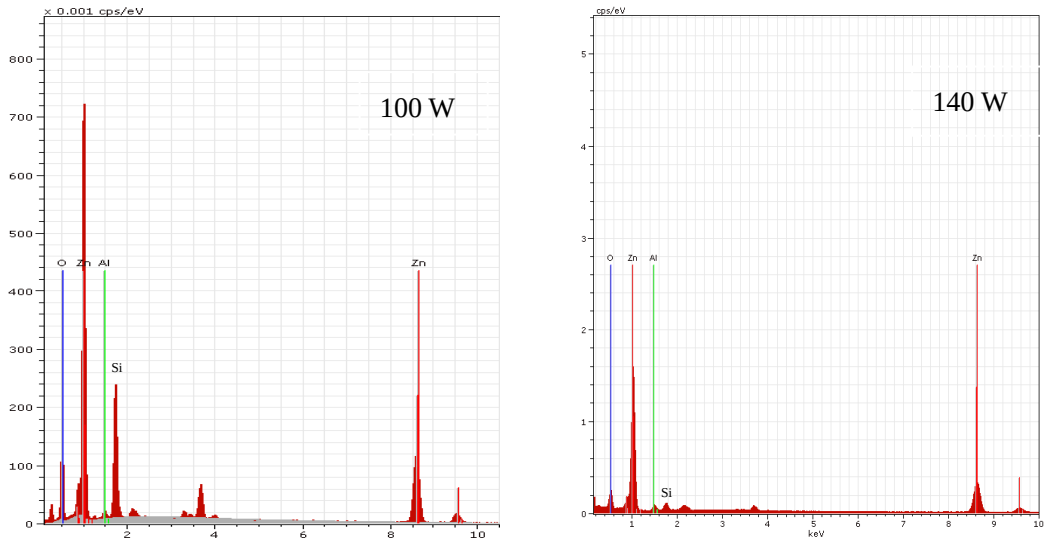

Fig. 6-7 Energy-dispersive X-ray spectrum of AZO films

Table 6-3 Electrical properties of AZO films deposited at different power

Power (W)	**Resistance (Ω/□)**	**carrier concentration (cm^{-3})**	**Hall mobility (cm^2/Vs)**
25	1700	9.4×10^{19}	3.8
50	135	2.8×10^{20}	11
100	23	4.7×10^{20}	9.5
140	15	4.7×10^{20}	9.8

Table 6-3 shows the electrical sheet resistance, the carrier concentration and the Hall mobility of AZO thin films prepared by using different RF power. The resistance of the thin film samples is seen to decrease sharply as the RF power was increased from 25 W to 50 W and reached a minimum resistance of 15 Ω/□ at around power of 140 W. The

decreasing tendency of resistance with increasing RF power was also published in previous reports [5-8]. The decrease in resistance with increasing deposition power is related to the crystallization and the grain growth of AZO thin films which is already explained in previous section. The degradation of resistance is also related to thickness of thin film. For thin layered films, stress may take place on AZO film which leads lots of defects. Therefore, free electrons may trapped by defects [9]. Another reason can be formation of islands of materials with lot of insulating gaps for very thin layers. This gaps can be minimized in the film with higher thickness [10].

Damp-heat stability was investigated for 7 days which is shown in Fig. 6-8(a). It showed that the film prepared using low RF power is very unstable compared to that of film deposited using high power. This is due to the variation of thickness as the previous result of this research has already suggested that the film with low thickness is not suitable for good stability. Beside this, it also depends on crystallinity. As 25 W and 50 W film showed very unstable resistance in DH condition and difficult to compare with other films, two films were selected for further investigation. Fig. 6-8(b) gives more clear observation for 100 W and 140 W film. The sheet resistance of both film increased in DH condition, where, no change was observed in ambient condition. According to this two figure it can say that the stability can be improved by increasing RF power as thickness and crystallinity improved in these films. But even using high power, it is still unsolved problem as resistance increased from 15 to 33 Ω/□ after 7 day under damp heat condition.

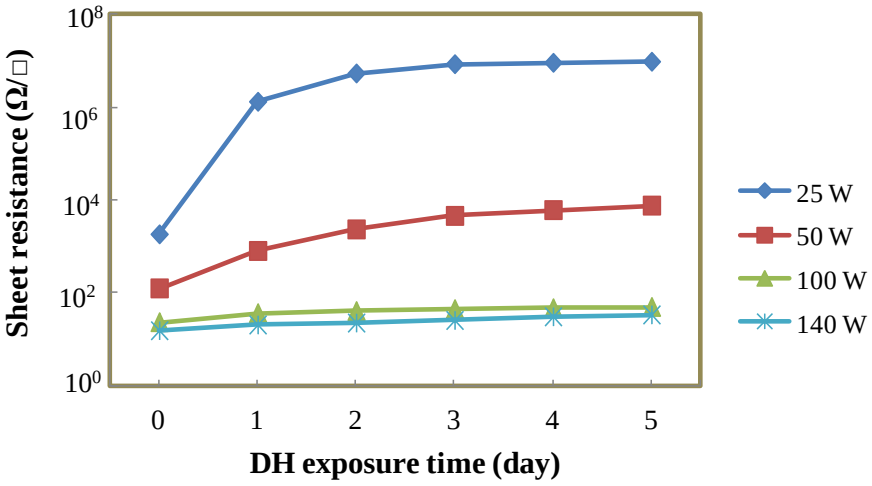

(a)

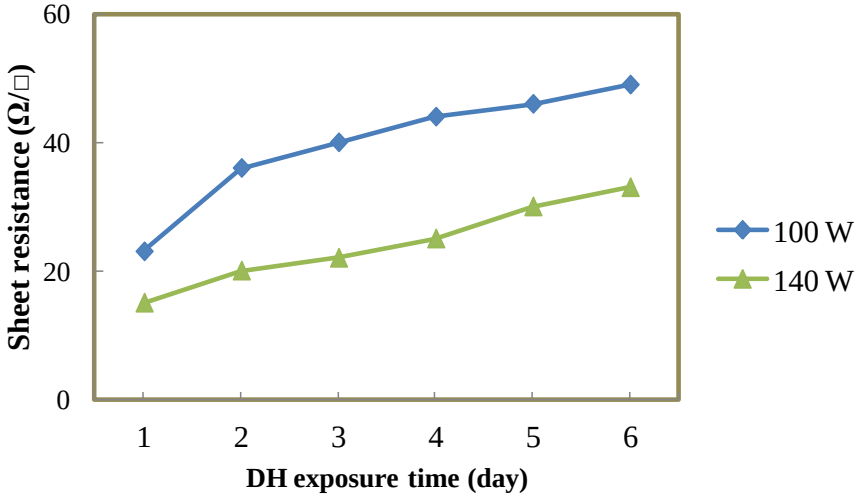

(b)

Fig. 6-8 DH stability test of AZO films using power of (a) 25, 50, 100 and 140 W (b) 100 and 140 W

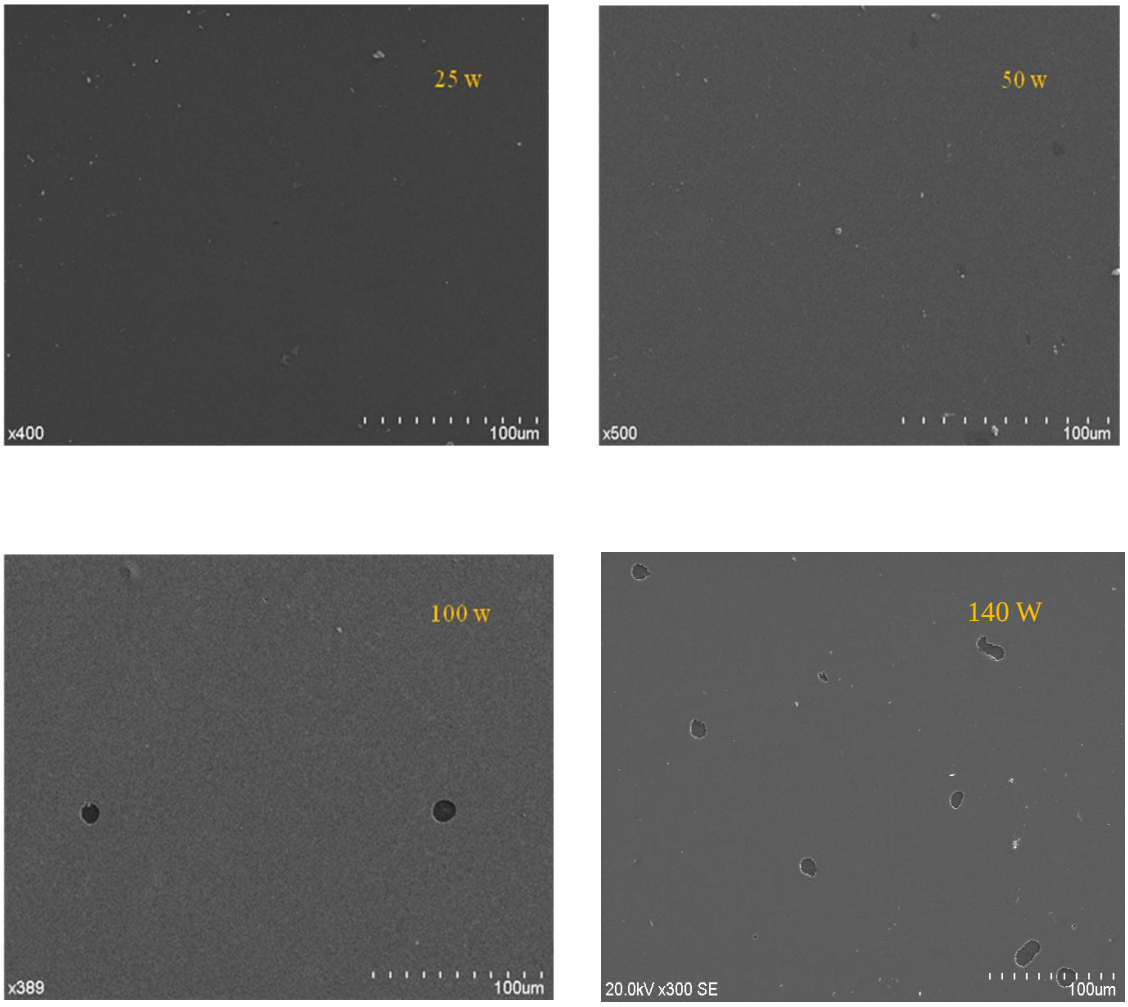

Fig. 6-9 SEM images of AZO films deposited at different RF power

Fig. 6-9 shows SEM images of AZO films deposited at different RF power. Here, the main focusing point was to investigate the micro-effects of re-sputtering due to negative ion bombardment of growing thin films. Negative ion bombardment of an evolving thin film can cause changes in the film's surface due to re-sputtering of the already deposited material [11]. In this study, surface micro-effects, i.e., changes in the surface morphology of the films at the micro scale level are dependent on the deposition powers. The film deposited using low power didn't show any hole in film which was

found in film prepared at high power. The number of hole was increased when the power increased from 100 W to 140 W. In the sputtering process, a target material is bombarded by high energy ions, causing atoms to be ejected from the material through momentum transfer. These atoms can be deposited on a substrate material, leading to the formation of a thin film. Similarly, if these atoms deposited on the substrate are bombarded by high energy particles, they can also be ejected from the substrate. This is the process normally referred to as re-sputtering [12-14]. Micro-effects of resputtering due to negative ion bombardment have also explained by D.J. Kester and R. Messier [11]. So, resputtering is a difficulty encountered in the sputtering by negative ions and reflected neutrals [15-17]

6.2.3 Improvement of environmental stability of AZO film prepared by sputtering

Chapter 5 has described a comparison study of environmental stability between sol-gel and sputtered AZO thin film. A large difference of increasing rate of sheet resistance was observed between films prepared using two methods i.e. thin film preparing method is very important for getting improved stability. To explain DH stability, logarithmic scale was used in graph as the increasing rate of sheet resistance was too high in sol-gel prepared film compared to sputtered film. In that case, sputtered film looked like almost stable. But reality is that it is still remain a problem as the sheet resistance increases under DH test but with low increasing rate compared to sol-gel prepared film.

In this dissertation, it has been suggested that some probable parameters may help to improve the environmental stability including increased thickness, improved crystallinity, preferred crystal orientation, improved surface smoothness and passivation layer on surface. It also suggests that high annealing temperature and sputtering method

can enhance the stability because of the presence of above properties on film. Therefore, combination of all of the above parameters may improve the stability. In this manner, another AZO thin film was prepared using specified condition as all of the parameters can be achieved in a single film. For preparing the film, sputtering method was chosen as the film prepared using this method have (110) preferable orientation and smooth surface also. The thickness of film was 750 nm and high temperature was applied for annealing to improve crystallinity and produce alumina layer as self passivation layer which was considered when the film annealed at high temperature. It can be noted that, the film was annealed under vacuum atmosphere as pure hydrogen is not suitable at high temperature. The films resistance was increased very sharply when AZO film was annealed in hydrogen with a temperature higher than 500 ºC. Hao Tong [18] has explained this increasing tendency by surface damage. The XRD patterns from this AZO film in Fig. 6-10 indicate a (110) preferred orientation, which suggests that the film is aligned with the a-axis oriented parallel to the substrate surface. Transparency curve confirms the high transparency of film (not shown here). The main issue was to investigate the DH stability of this film which is shown in Fig. 6-11. From this figure, it is clear that it fulfills the expected result i.e. most stable AZO film was found when all probable methods which helps to improve the stability were applied in a single film. All of these probable reasons have explained in previous chapters. But the sheet resistance was comparatively high (60 Ω/□) in this film as, it was annealed in vacuum atmosphere. Hydrogen annealed film annealed at low temperature (450 °C) have low resistance (12 Ω/□), but at a time instable in DH condition. On the other hand, though the resistance is high for film annealed at high temperature in vacuum atmosphere, it showed very high stability.

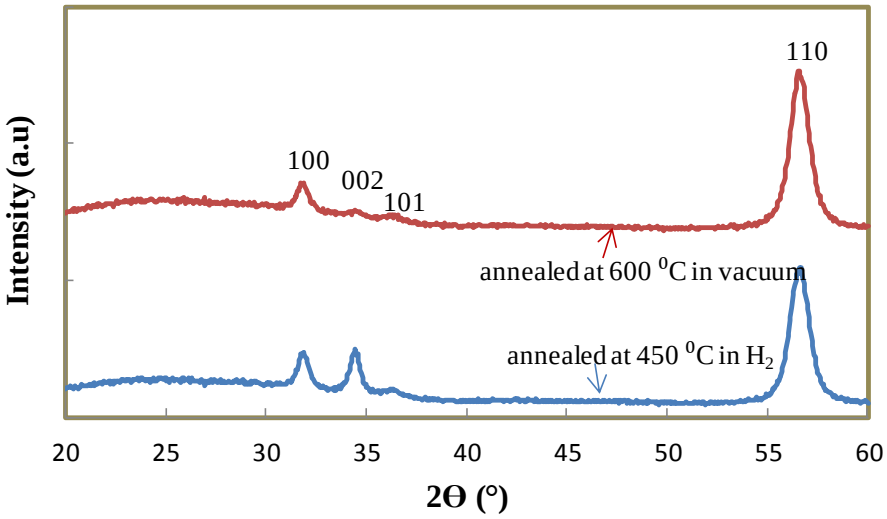

Fig. 6-10 X-ray diffraction of AZO film prepared by sputtering and annealed at 450 °C in hydrogen and 600 °C in vacuum atmosphere

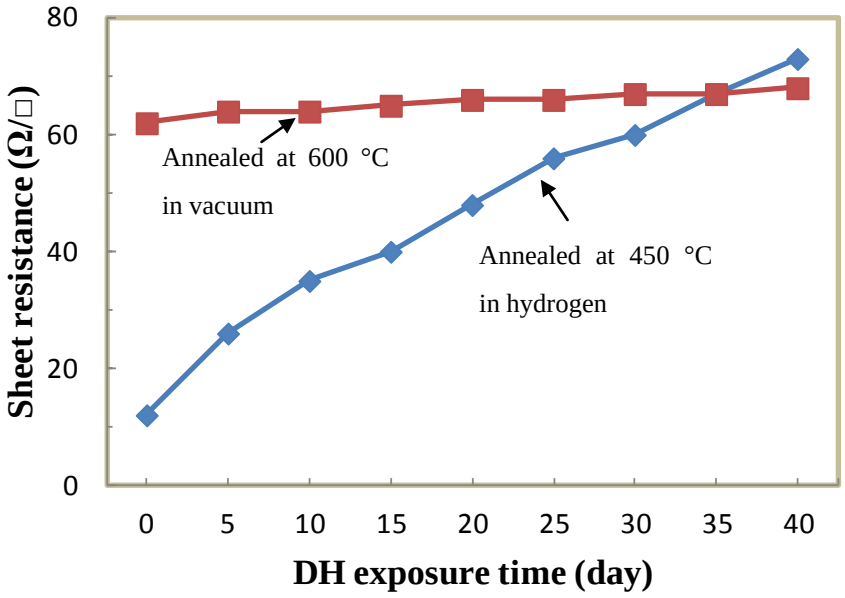

Fig. 6-11 Damp heat test of AZO film prepared by sputtering and annealed at 450 °C in hydrogen and 600 °C in vacuum atmosphere

6.3 Discussion

In this chapter, there have been a number of investigations concerning the role of crystal orientation, RF sputtering power and DH stability improvement of AZO thin film. In chapter 5, it is suggested that (110) plane can play an important role on stability which was found in sputtered film. On the other hand, sol-gel prepared film spectra are dominated by the (002) peak confirming the strong (002) textures. To clarify the role of crystal orientation, a new method was applied to form both orientations in a single film by depositing AZO film on glass by sputtering at first and then sol-gel method on the top of film. Here, a-plane (110) is grown by sputtering at specified condition, where, bottom layer provides nucleation for preferable growth of sol-gel AZO crystals through epitaxy. As the AZO film prepared by sputtering and sol-gel method which has (110) plane and showed improved stability, it is suggested that the film with high intensity of (110) plane can improve the stability. It can be due to strong bonding between Zn and O in (110) plane [19].

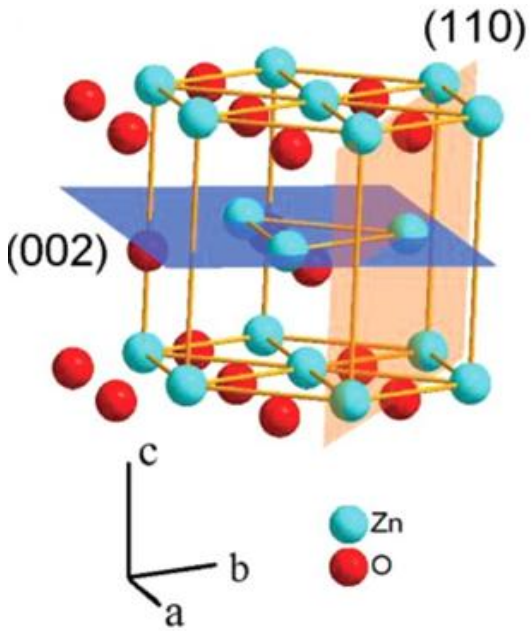

Fig. 6-12 (002) and (110) planes in ZnO thin film

In the present study, AZO thin films at various RF powers and the structural, optical and electrical properties and DH stability of the fabricated films were investigated. The AZO thin films deposited on glass substrates showed the change of preferred crystal orientation with the increase of RF power. At low power (25 W), very weak (002) peak indicates low crystallinity of the film. The dominant (110) diffraction peak was observed at high RF power of 100 W and 140 W. So, crystal orientation can be changed with the change of RF power. Here, (110) was expected orientation as it helped to improve the environmental stability of AZO film. The AZO film prepared at low power (25 W) was very unstable in damp heat condition because of low crystallinity and low thickness which was improved when the RF power was increased to 50, 100 and 140 W. Though the film showed improved stability at 140 W, where, the resistance increased from 16 to 30 Ω/□, after 7 days under damp heat condition, it is still an unsolved problem to get highly stable film under DH condition. To improve the DH stability of sputtered AZO film, the film was treated with all methods which were found as the probable reasons to improve the stability in before in this research, such as: higher thickness, sputtering method and high temperature annealing. In this case, AZO film was prepared by RF sputtering with thickness of 700 nm and annealed at 600 ºC for 1 hr under vacuum atmosphere. The result of previous experiments in this work showed that 1) sputtered film contains (110) plane and smooth surface, 2) larger thickness limits the formation of island and defects and 3) high temperature annealing improves crystallinity and form a self-passivation layer of Al_2O_3 and/or $ZnAl_2O_4$ on surface. All of these parameters may help to improve the stability. So, the new AZO film prepared using all of these parameters have very high stability in damp heat condition. But the sheet resistance of as prepared film is quite high as it annealed in vacuum atmosphere. High temperature is not suitable in hydrogen atmosphere because of surface damage though it is good for getting better electrical properties.

References

[1] S.Y. Myong and K.S. Lim, Applied Physics Letters, **82** (2003) 1718-1720

[2] C.H. Ahn, B.H. Kong, H. Kim and H.K. Cho, Journal of the electrochemical society, **158** (2011) 170-173

[3] A. Ismail, M.J. Abdullah, Journal of King Saud University-Science, **25** (2013) 209-215

[4] H. Park et al., Thin Solid Films, **519** (2011) 6910-6915

[5] J.W. Kim and H.B Kim, Journal of the Korean Physical Society, **59** (2011) 2349-2353

[6] H. Kong, P. Yang and J. Chu, Journal of physics: Conference series, **276** (2011) 012170

[7] S. Junfei et al,. Journal of Semiconductors, **34** (2013) 084003

[8] T. Chaikeeree et al., Journal of Energy Technologies and Policy, **3** 11 (2013)

[9] B.Z. Dong and G.J. Fang, Journal of Applied Physics, **101** (2007) 033713

[10] M.S. Shinde, P.B. Ahirrao, I.J. Patil and R.S. Patil, Indian Journal of Pune & Applied Physics, **50** (2012) 657-669

[11] J.H. Xu, B.M. Moon and K.V. Rao, Journal of Materials Research, **10** (2011) 798-802

[12] L.W. Rieth and P.H. Holloway, Journal of Vacuum Science & Technology A, **22** (2004) 20-29

[13] D.J. Kester and R. Messier, Journal of vacuum science & technology A: vacuum, surfaces and films, **4** 3 (1986)

[14] D.J. Kester and R. Messier, Journal of Materials Research, **8** (1993)1928

[15] S.M. Rossanagel and J.J. Cuomo, American Institute of Physics Conference

Proceedings, 165, AIP, NY, 106 (1988)

[16] T. Hada, S. Hayakawa K. Wasa, Japanese Journal of Applied Physics, **1** (1970) 1078-1084

[17] H. Tong, Z. Deng, Z. Liu, C. Huang, J. Huang, H. Lan, C. Wang and Y. Cao, Applied Surface Science, **257** (2011) 4906-4911

[18] A.S. Mohammadi, S.M. Baizaee and H. Salehi, World Applied Sciences Journal, **14** (2011) 1530-1536

Chapter 7

Conclusions and recommendations

7.1 Conclusions

In this work, structural, optical, electrical properties and environmental stability of Al-doped ZnO (AZO) thin films were investigated in ambient and damp-heat condition. As the electrical properties of AZO thin films are not stable in air, several approaches were employed to improve the stability. The results achieved in the thesis are summarized below.

In the **Chapter 3**, various characteristics and environmental stability of AZO films prepared by sol-gel method were investigated as function of annealing atmosphere (vacuum, Argon +5% hydrogen, and pure hydrogen) and doping concentration (1, 2, 3 and 4 wt%). The effect of thin metallic film (Ti or Cr) covered on AZO film was also investigated to improve the stability at low annealing temperature which is preferable for commercial applications. Pure hydrogen annealing atmosphere and 2 wt% Al doping (Al/(Al+Zn) concentration was 1.18 at%) provided the optimal electrical property. Oxygen annihilation by hydrogen annealing enhance the number of oxygen vacancy or carrier concentration. It is suggested that the increased carrier concentration and Hall mobility involved in film demonstrates the lowest resistivity of 1.65×10^{-3} Ωcm. As the films were exposed to humidity, the increased resistivity indicates the possible oxygen and water molecule diffusion to the film that confines the number of free electrons. To protect the film from oxygen diffusion, thin Ti or Cr layer was deposited by sputtering which improves the stability. Electrical stability enhancement was due to the formation

of bilayer of Cr/CrOx or Ti/TiOx on AZO. This bilayer, especially oxide layer on very top surface serves as a protective layer to prevent the penetration of oxygen and water molecule into the AZO film and reduce the degradation rate of conductivity. As the transparency decreased and found as ~70% in stable film, it seems that, it is a big challenge to get transparency and stability both in a film by using thin metallic layer on film surface.

In the **Chapter 4**, AZO thin films have been deposited by sol-gel method for optoelectronic applications as transparent electrode. Annealing treatments were carried out in various annealing temperatures (450, 500, 550 and 600 ^{0}C) and durations (30, 60 and 120 min) under vacuum atmosphere. The sheet resistance of AZO thin film is reduced from 10^5 to 10^2 Ω/□, when the film is heat treated in vacuum atmosphere, probably ascribed to intensive creation of oxygen vacancies, especially near the film surface. The electrical stability is improved, when the film was annealed at high temperature, where the structural and optical properties showed no considerable changes. The cause of improvement was explained in terms of structural and surface state. In this experiment, XPS data reveals that the surface oxygen and aluminium contents were relatively high for the stable film compared with the unstable film. This higher concentration at the topmost surface of stable film indicates the presence of ultrathin Al_2O_3 and/or $ZnAl_2O_4$ layer, though not detected by x-ray diffractometry, which would be formed during annealing at high temperature. This predicted layer of Al_2O_3 may act as a protective layer that can repel atmospheric oxygen to enter the film. On the other hand, the slight increase in the crystallite size (from 18 to 21 nm) in high temperature annealed film reduce the total path of oxygen diffusion to the film and may cause another reason of getting improved stability.

In the **Chapter 5**, a comparative study was employed between AZO films prepared by using two different methods: sol-gel and RF sputtering. Sputtered AZO film was found as very stable in ambient condition, whereas, slight degradation of sheet resistance in this film originates in DH condition. But this increasing rate of sheet resistance is much lower in sputtered film compared to sol-gel prepared film. Several approaches were employed here, in order to understand the reason of improved stability in sputtered film: 1) impurity 2) surface roughness and 3) crystal orientation. XPS results ensure that the chemicals used in sol-gel or target used in sputtering for developing thin films were highly pure, since, no other material was detected in thin film by this experiment. The surface of sol-gel prepared film contains cracks or voids which look like the preferable diffusion path for oxygen and/or water molecule and may cause the degradation of electrical properties. Comparatively smooth surface with no cracks was observed in sputtered film, which remains smooth even after damp heat test. Another possible reason was formation of high quality (110) crystal orientation on sputtered film.

In **Chapter 6**, the mechanism which relates to crystal orientation on AZO film was described. In this case, AZO film was prepared by a proposed method using a combination of sol-gel and sputtering method in a single film, which ensures the presence of (110) orientation and improves the stability. Beside this, role of RF power on AZO thin film properties also investigated in this chapter. The improvement of sputtered films stability was successfully made by using all probable methods which can raise the stability based on the result of previous chapters.

In overall summery, through an analysis of structural, optical and electrical properties, AZO films were investigated in terms of various parameters. Degradation of

these properties under ambient and harsh environment was studied and several approaches are suggested to improve the stability. With the conditions investigated, AZO films prepared by sol-gel method have polycrystalline structure and exhibits a preferred hexagonal wurtzite c-axis (002) crystal orientation. On the other hand, sputtered AZO film in designated condition contains high quality (110) plane. The average transmittance in the visible light wavelength range of 300 – 800 nm was approximately 85 – 90%, which satisfies transparent electrodes requirement. Electrical properties varied with different parameters such as annealing condition, doping concentration etc. Pure hydrogen and 1.18 at% Al confirmed lowest sheet resistance with high carrier concentration and hall mobility. Sol-gel prepared AZO film showed large degradation in ambient and damp heat condition which was improved by using high temperature (550 - 600 °C) annealing in vacuum atmosphere. Improved crystallinity and self passivation layer of Al_2O_3 on top of AZO film was explained as the probable reason of improved stability in this work. As high temperature is not preferrable for many device applications and also can not use in hydrogen atmosphere, though it is good for getting lower resistivity, thin metallic layer of Ti or Cr was deposited on AZO film to protect this from harsh environment. The stability was improved here at low annealing temperature (450 °C) but at the same time, to obtain high stability, metal film with larger thickness was needed which also reduce the transparency. AZO thin film prepared by sputtering demonstrated the result with better environmental stability. It is suggested that smooth surface and high quality (110) crystal orientation in sputtered film may improve the stability. The AZO thin film with best result in this work, which was developed by sputtering, found as sheet resistance of 12 Ω/□ (resistivity of 9.0 x 10^{-4} Ωcm), 85% transparency and very stable in an ambient

atmosphere. This films sheet resistance increased from 12 to 60 Ω/□ after 30 days under damp-heat condition, which was still increasing with time. But this also improved when sputtered film with thickness of 750 nm was annealed at 600 °C in vacuum atmosphere. This film was combination of all probable reasons which act to get improved stability such as increased thickness, improved crystallinity, improved surface morphology, preferred crystal orientation, less defect etc.

7.2 Recommendations

After the present work, there are several important issues still remain unresolved. The following recommendations are proposed in order to further research in the field of transparent conductive oxides:

It would be important to investigate further the performance, stability and reliability of AZO transparent electrodes incorporating low temperature and simple methods that are compatible with ITO in this field.

It has also been assumed in this thesis that the stability can be controlled by changing the preferred crystal orientation. It is recommended that the study be extended to develop the film on other substrates which can facilitate to change the preferred orientation in this film and improve stability.

Recently, interest in transparent flexible plastic substrates with a transparent conducting oxide (TCO) layer is becoming very popular due to the use of different applications such as flexible solar cell. For this, further investigations of AZO thin film, which has explained in this dissertation, may promote the improvement of mechanical stability to be used in flexible applications.

Appendix

Appendix A

Synthesis and environmental stability of silver, nickel and calcium co-doped AZO transparent electrode

The effects of co-doping on AZO thin films were investigated in this work. Here, AZO films were co-doped with less reactive (silver, nickel) and high reactive (calcium) material in oxygen and electrical stability was investigated in ambient condition for 30 days. Zinc acetate dihydrate was used as starting material. For co-doping with 2 wt% Al doped ZnO film, aluminum nitrate nonahydrate and silver nitrate or nickel acetate tetrahydrate or calcium nitrate was dissolved into 2 methoxyethanol, which acts as solvent. These films will assigned as AZO (only Al-doped), AgAZO (silver co-doped), NiAZO (nickel co-doped) and CaAZO (calcium co-doped). Al films exhibit the wurtzite structure with c-axis preferred orientation. High transparency observed in AZO and CaAZO film. It decreases when co-doped with Ni and Ag. But electrical stability of all films in air is not satisfactory.

Table A-1 Variation of sheet resistance for AZO, NiAZO, AgAZO and CaAZO

Annealing temperature (^{0}C)	**Annealing duration (min)**	**Annealing atmosphere**	**Sheet resistance (Ω/□)**					
			AZO	**NiAZO**		**AgAZO**		**CaAZO**
			Without co-doping	**2%-Ni**	**3%-Ni**	**2%-Ag**	**3%-Ag**	**2%-Ca**
450	60	Vacuum	290	315	273	506	553	2523

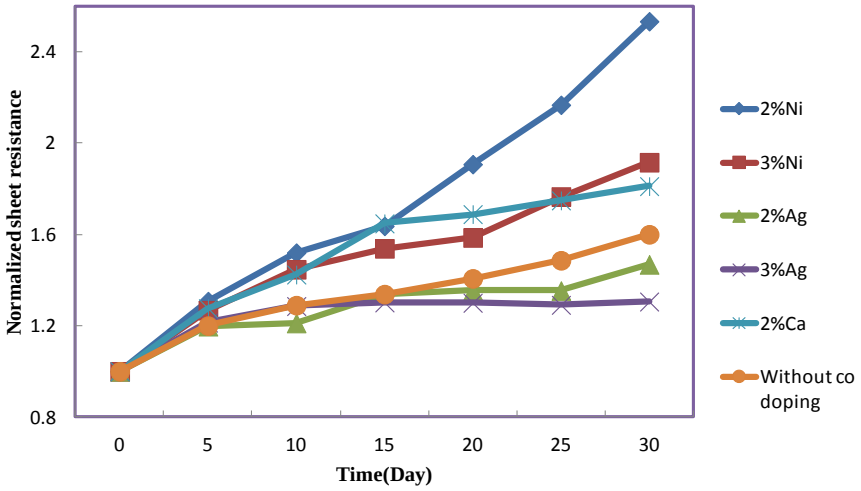

Fig. A-1 Environmental stability of AZO, NiAZO, AgAZO and CaAZO thin films in 30 days

Table A-2 Short brief of different properties of co-doped AZO thin films

Sample	Transparency (%)	Sheet resistance (Ω/□)	Sheet resistance increases after 30 days
AZO	>85	290	60%
NiAZO	75 – 85	377	250%
AgAZO	60 - 70	506	40%
CaAZO	>85	2523	180%

Appendix B

Some important resultant rechecked data are following:

Band gap energy

In chapter 4, band gap energy of two sample s-450-30 and s-600-120 was measured by using Tauc plot. The data was rechecked several times and Fig. B-1 is one of them, where, average transmittance in the visible light wavelength range of 300 – 800 nm is approximately 85 - 90% for both films. The absorption edge was shifted towards shorter wavelength at increased annealing temperature and duration. The band gap energy measured by using Tauc plot increases from 3.39 for s-450-30 to 3.46 eV for s-600-120. These data are almost similar to other one which has already described in the previous chapter.

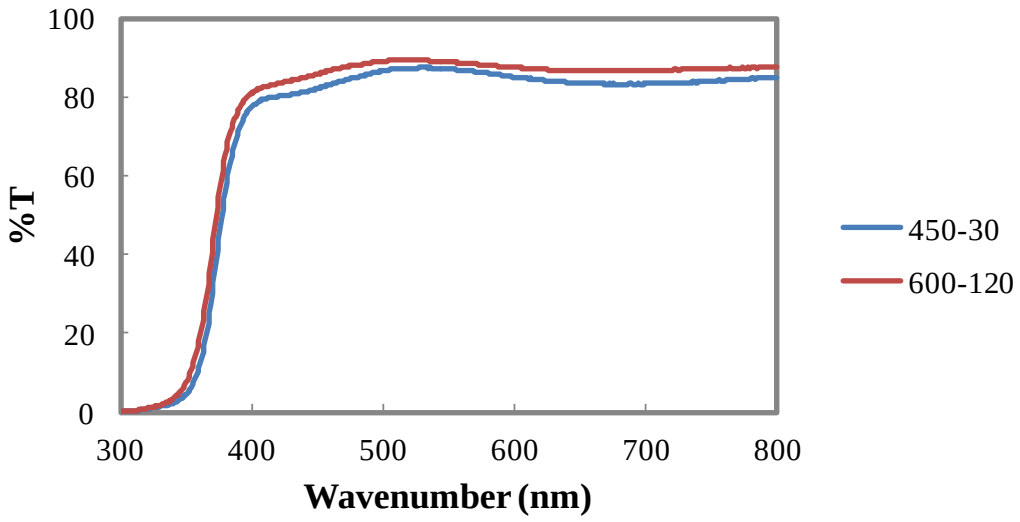

(a)

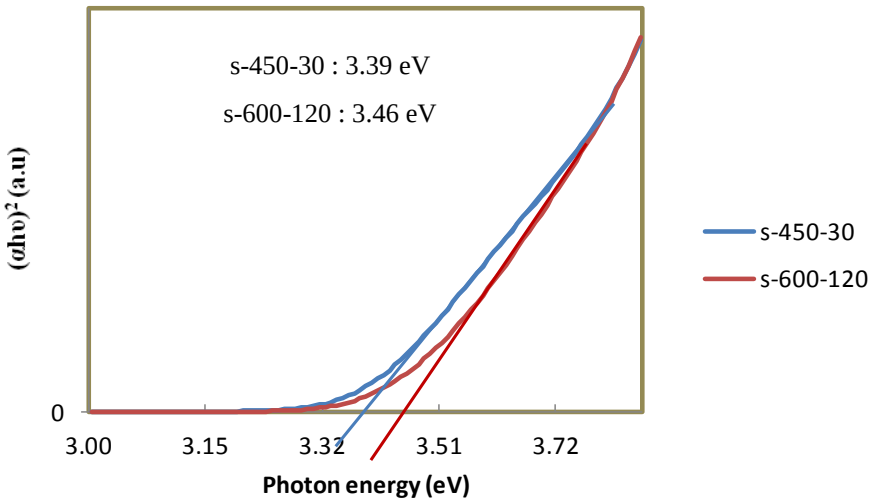

(b)

Fig. B-1 (a) Transparency curve and **(b)** Tauc plot

XPS depth profile and elemental concentration

The depth profile and elemental concretion were rechecked also and same nature was found in both films: s-450-30 and s-600-120. Here, the surface of s-600-120 also contains more O and Al, which indicates the formation of ultra thin Al_2O_3 and/or $ZnAl_2O_4$ and prevents water molecule to pass through the film.

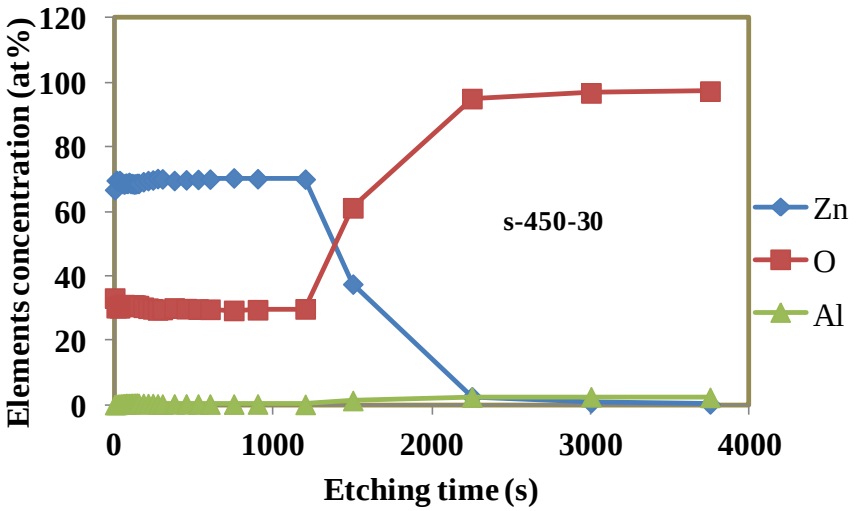

(a)

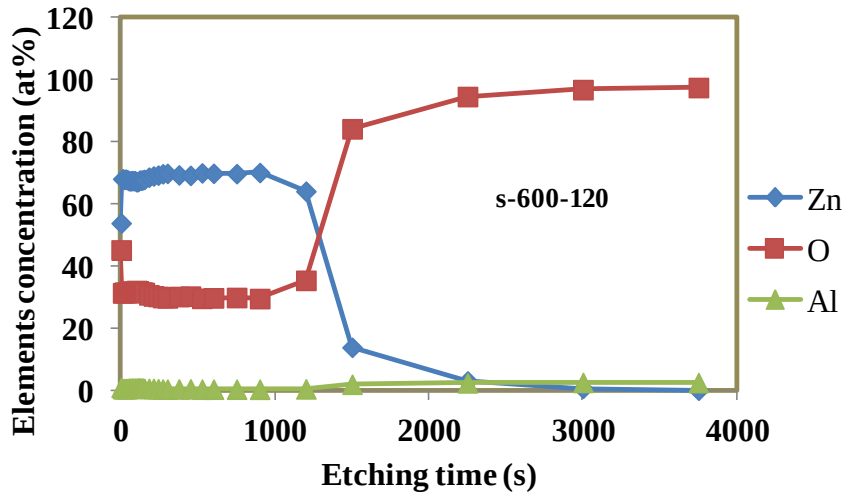

(b)

Fig. B-2 Total depth profile of **(a)** s-450-30 and **(b)** s-600-120

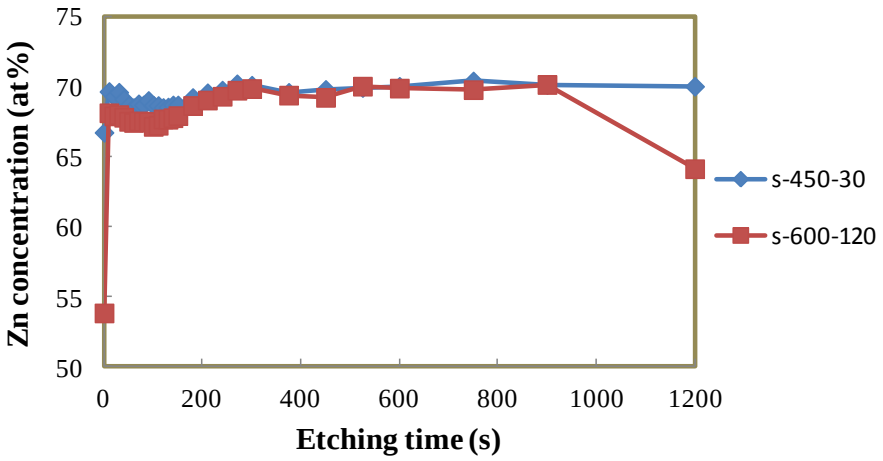

(a)

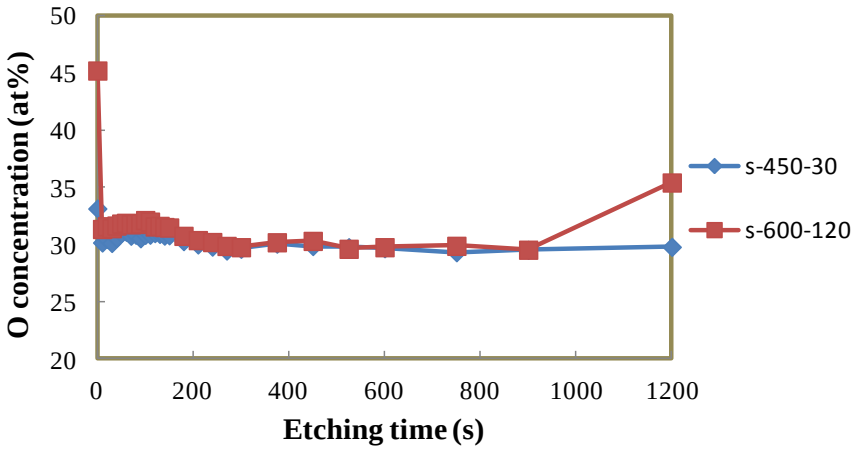

(b)

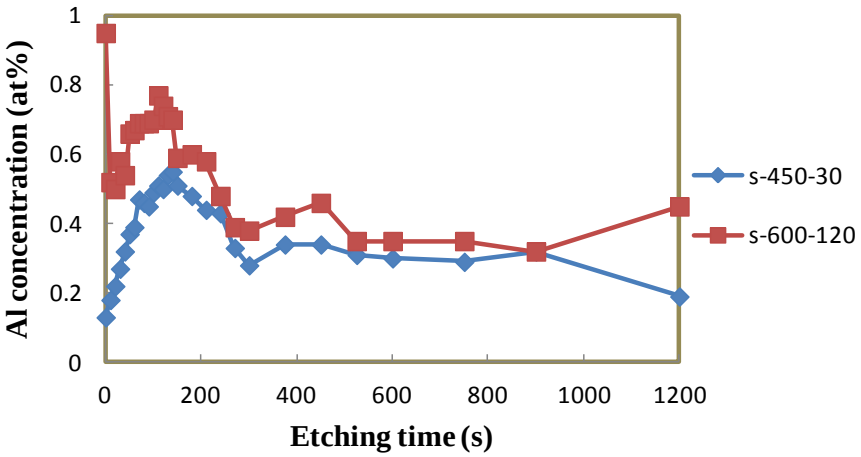

(c)

Fig. B-3 Elemental concentration of **(a)** Zn, **(b)** O and **(c)** Al

List of Publications:

[1] **Samia Tabassum**, Eiji Yamasue, Hideyuki Okumura and Keiichi N. Ishihara, Damp heat stability of AZO transparent electrode and influence of thin metal film for enhancing the stability, Journal of Materials Science: Materials in Electronics, vol. 25 (2014) 3203 - 3208

[2] **Samia Tabassum**, Eiji Yamasue, Hideyuki Okumura and Keiichi N. Ishihara, Sol-gel and rf sputtered AZO thin films: Analysis of oxidation kinetics in harsh environment, Journal of Materials Science: Materials in Electronics, vol. 25 (2014) 4883 - 4888

[3] **Samia Tabassum**, Eiji Yamasue, Hideyuki Okumura and Keiichi N. Ishihara, Improved environmental stability of Al-doped ZnO transparent electrode prepared by sol-gel method, ready for submission.

Presentation of International conference

[1] S**amia Tabassum**, Eiji Yamasue, Hideyuki Okumura and Keiichi N. Ishihara, "Effect of annealing condition on environmental stability of Al and Ga doped ZnO", Kyoto-Ajou Joint Symposium, Korea (2013)

[2] S**amia Tabassum**, Eiji Yamasue, Hideyuki Okumura and Keiichi N. Ishihara, "Effect of annealing atmosphere on electrical stability of AZO transparent electrode" 8th International Symposium on Transparent Oxide and Related Materials for Electronics and Optics, Tokyo, Japan (2013).

[3] S**amia Tabassum**, Eiji Yamasue, Hideyuki Okumura and Keiichi N. Ishihara, "Damp heat stability of AZO transparent electrode and influence of thin metal film for enhancing the stability", Kyoto-Ajou Joint Symposium, Kyoto (2013)